CHALMERS

Tissue engineering skeletal muscle on elastic fibers
– A new bioreactor system for mechanical stimulation

Master of Science Thesis in the Master Degree Programme

Biomedical engineering

PATRIC WALLIN

Department of Applied Physics
Division of Biological Physics
CHALMERS UNIVERSITY OF TECHNOLOGY
Göteborg, Sweden, 2009

Tissue engineering skeletal muscle on elastic fibers
- A new Bioreactor system for mechanical stimulation

PATRIC WALLIN

Department of Applied Physics
Chalmers University of Technology
SE-412 96 Göteborg
Sweden
Telephone + 46 (0)31-772 1000

Chalmers Reproservice
Göteborg, Sweden 1999

Abstract

Tissue engineering skeletal muscle has versatile potential applications but it is still challenging to produce large functional muscle tissues *in vitro*. Mechanical stimulation has been shown to positively influence this process. In the present thesis a bioreactor for mechanical stimulation was designed, built and evaluated. The system allows the utilization of a wide variety of scaffold materials and designs. Two potential fibrous scaffold materials were tested under static conditions. C2C12 skeletal muscle progenitor cells were cultured on aligned elastic polyurethane micro diameter fiber arrays. Fibers were obtained from Hyosung (South Korea) and composition and shape were investigated using XPS, FT-IR ATR and SEM techniques. It was shown that C-100 fibers are a potential scaffold material for fundamental reseach on the effects of stimulation on skeletal muscle cells. Cells were grown and terminally differentiated into muscle fibers on C-100 fiber arrays. Myosin heavy chain and α-actinin were used as marker proteins to confirm terminal differentiation. The developed bioreactor system together with the scaffold material allow a wide variety of potential experimental setups and can be utilized to study muscle tissue formation in response to different stimulation patterns.

Keywords: Tissue engineering, C2C12 muscle cells, cell culture, mechanical stimulation, scaffold, myogenesis, bioreactor, surface characterization

Table of Contents

List of Tables

List of Figures

Preface

At the beginning of this master thesis I want to mention some personal remarks. During my master education at Chalmers University in Gothenburg I focused my studies on tissue engineering and biomedical technology but I have a Bachelor in mechanical engineering from the Leibniz University in Hannover. This change of focus was in retrospect a great decision and I really enjoy working with animal cell cultures.

I started working on tissue engineering skeletal muscle 2007 with a literature survey for a course project. Originally I wanted to do a project on bioelectrodes but as fate wanted it was already taken by someone else and Nina encouraged me to write about skeletal muscle instead. In a second project 2008 I did my first muscle cell culture to study effects of micrometer size surface features. Both projects highly contributed to my fascination for skeletal muscle cells and the motivation to write a master thesis over this topic.

In my opinion it is incredible how complex cells are, what they are capable of doing and that tissues are formed by highly structured units spanning orders of magnitudes in size, from centimeter ranged muscle tissue, over millimeter long cellular subpopulations, to micrometer sized cells and finally nano scale proteins. Beyond that the complexity of gene transcription and activation of different gene subsets, the speed and precision with that cells can respond to a wide variety of stimuli and the possible cell-cell and cell-surface interactions are truly amazing for me. From my point of view successful tissue engineering in the future will need to rely on mimicking physiological conditions as closely as possible. The strong self organizing potential of cells should be harnessed to culture complex tissues by imitation of the environment present during embryogenesis in a single bioreactor with different cell types, physical stimuli and molecular cues. Tissue engineering will clearly change medical treatments and the possibilities to cure diseases in the next 20 to 30 years. Allowing clinical interventions that are unconceivable today. I truly hope to be able to contribute to this development.

There are many people I want to thank for their help during this thesis. Julie Gold, who was a great supervisor and examiner. She volunteered to let me work on this project despite in spite of the fact that there was neither funding nor ongoing research in this area. She gave me the freedom to design my own experiments, define the aims of the project and was always open for questions. The second person I really want to thank is Nina Tymchenko, first of all for encouraging me to start working on skeletal muscles. She taught me most of the things I know about cell culture

and was very patient when I started to work in the cell lab. Throughout the project she helped me with advice and without her this thesis would still be full of typos. Additionally I want to thank all companies that supported this thesis - without them the bioreactor could not have been built in the same way. Especially I want to thank Filip Rosengren from SKF for providing me with components and inviting me to visit SKF. Furthermore there are many people at Chalmers who helped me and where always open for questions. Special thanks to Rune Johansson and Hans Odelius who helped me with the fabrication of the bioreactor and electronics, Lars Ilver, Hanna Ingelsten and Hossein Agheli who were involved in the characterization of the fibers and the whole Biological and Chemical Physics groups as well as the people from the cell lab - it was very nice working with you. It was an amazing project that gave me the opportunity to combine my different backgrounds and work in a field I really like and I am deeply grateful for all your help and contributions.

Figure 1: Project partners from the industry that helped to realize this project

Introduction

Tissue engineering skeletal muscle, and the general cultivation of skeletal muscle cells, offer a wide variety of applications and is a steadily increasing research area. There are three main application areas: regenerative medicine, drug screening and *in vitro* meat. The first two aim at application in the medical field whereas the third one aims at food production.

Tissue engineering and regenerative medicine are terms that are used interchangeable to describe a relatively new field in medicine that aims at restoring, maintaining and enhancing tissue functions (1). It is a multidisciplinary field combining life science, material science, engineering and medicine to improve health and quality of life (1; 2).

The goal of tissue engineering skeletal muscle is to replace damaged or lost muscle tissue to maintain or restore its function. It may offer a promising treatment for muscle diseases like muscular dystrophy (3) and furthermore a possibility to deal with severe muscle lost due to trauma, tumor growth or necessary surgical interventions.(4; 5) Todays treatments for those cases are limited and are often accompanied by side effects and limited in their ability to restore muscle function. The current standard procedure for most patients is the autologous transplantation of muscle tissue which is a serious clinical intervention and remains difficult especially for severe muscle defects (6). Another possible treatment is the injection of muscle cells into the muscle area to enhance tissue regeneration, but the outcomes of this treatment are limited due to poor cell integration in the muscle tissue and cell death (4).

There are two different tissue engineering approaches: *in vitro* and *in vivo* tissue engineering.(2) For the *in vitro* approach cells are cultured on a scaffold and differentiation of the muscle cells is triggered outside the body (*in vitro*). The *in vivo* approach also uses a cell seeded scaffold but cell differentiation occurs after transplantation inside the body (*in vivo*) (6). The advantages of both approaches is that in general large amounts of muscle tissue can be produced by a small amount of initial muscle cells obtained by a minor biopsy intervention. Even though tissue engineering for skin and other tissues are becoming more and more clinical practice, complex tissues like skeletal muscle remain challenging and difficult to produce.(6) So far no clinical relevant sized skeletal muscle constructs could be produced by tissue engineering.(5)

A second application area in the field of medicine is tissue engineered skeletal muscle as a model system for drug testing. Today new drugs undergo a wide variety of tests and often a large amount of those tests are carried out in animals to investigate effects of the studied substance. This procedure has several drawbacks. First of all

is the ethical aspect of animal testing which also limits the ability to scan a wide variety of substances for potential pharmaceutical applications since animal testing requires serious considerations and motivations. Furthermore animal testing takes a long time and effects are difficult to monitor in detail. Due to limitations of animals the statistical significance is reduced for this test. Additionally the maintenance of animal facilities, housing and testing cost large amounts of money. A standardized skeletal muscle model system can help to solve and minimize some of the problems. Tissue engineering skeletal muscle tissue could in theory be produced at competitive prices and large quantities. Evaluation of effects for different drugs could be achieved at cell molecular levels with advanced analysis methods. One evaluation parameter could be the contractibility of skeletal muscle which could be easily monitored. This would result in the ability to carry out high through put scanning for potential drugs in a wide variety of substances.(7)

A third application area is in the field of food production. The demand for meat products is steadily increasing especially in countries like China. This intensifies the problem related to animal breeding like production of high amounts of greenhouse gases, limited amounts of available grazing area and animal welfare. Furthermore animal breeding can be regarded as an inefficient way to obtain meat since the animal uses much of the food derived energy for maintenance and not for generation of muscle mass.(8) Even though most parts of an animal are used today after slaughter the main purpose is still the creation of high quality skeletal muscle meat products. Due to these facts *in vitro meat* has become a considered alternative. It is realistic to distinguish between two possible *in vitro* meat products: processed meat and highly structured meat products like steak. For processed meat one approach is to culture muscle cells on microcarriers in solution which would allow the usage of large scale stirring bioreactors.(9; 10) For highly structured meat products approaches similar to tissue engineering skeletal muscle for medical applications could be used. It is important to note that it is still unclear which of the properties of "real muscle" *in vitro* meat need to have to be suitable as a substitute for conventional meat but it is clear that taste in steaks are highly depending on additional tissue like fat and blood. For processed meat this is a minor problem since the taste can be designed by adding substances to the final product, as it is already done today.(8)

The three applications areas mentioned here show the wide variety where tissue engineering skeletal muscle could be used. In order to realize and design products suitable for the market, basics principles of skeletal muscle tissue generation and function have to be understood and control mechanisms need to be identified. At the moment, it is still a long way before products might reach the commercial market.

This thesis focuses on the effects of mechanical stimulation during cell cultivation. Mechanical stimulation has been shown to play an important role during muscle formation and is regarded as an important stimulus for successful tissue engineering of skeletal muscle *in vitro*.(11; 12)

During this work, a new bioreactor system was developed and constructed that allows the stimulation of a wide variety of different scaffold shapes and materials, with stimulation frequencies up to 1 Hz. To evaluate the bioreactor, micro diameter elastic fibers were used. They offer the possibility to create 3-dimensional scaffolds

with high complexity and organization. The fiber surfaces were characterized with SEM, XPS and FT-IR ATR techniques. The used micro diameter fibers offer contact guidance, support muscle cell alignment and cell attachment. The C2C12 muscle progenitor cell line from mice was used for all cell experiments. Cell differentiation markers were identified and protocols were developed to monitor formation of muscle fibers during myogenesis.

Chapter 1

Theoretical Background

1.1 Part 1: Bioreactor system

A wide definition for bioreactors is given by the International Union of Pure and Applied Chemistry (IUPAC):

> Bioreactor: An apparatus used to carry out any kind of bioprocess; examples include fermenter or enzyme reactor. (13)

A bioreactor provides a biologically active environment that supports and facilitates the process it was designed for. A wide range of different bioreactor systems are available mainly for use with yeast, bacteria and other microorganisms.(13) In this study the term bioreactor is used in a narrower sense including only systems that are used for mammalian cell culture and tissue engineering. These systems only represent a small number of bioreactors available and most of them have been developed in the last two decades concurrent with the emergence of tissue engineering research. Most areas in tissue engineering are still fundamental research and clinical applications are often not realized yet. Thus the bioreactors used are usually specialized unique system that are optimized to study certain effects on a specific cell type. This and the comparable small market are the main reason why only a few commercially bioreactor systems for mammalian cell cultures are available and it is often necessary to design own systems.(14)

1.1.1 Bioreactor design principles

There are a some general design principles that apply to all bioreactors that are used for mammalian cell culture. The overall aim is to provide optimal culture conditions for the cells and mimic their native environment as closely as possible. Fulfilling this aim is a relatively complex engineering challenge, it includes aspects of cell biology, physiology, heat transfer, gas diffusion, mass transportation, sterility and others.(15)

Many bioreactor systems are placed inside commercial incubators which provide temperature and CO_2 control. This reduces cost and results in lean systems that can be quickly tested. On the other hand this may result in size and usability limitations.

The focus here will be on fully autonomic systems that do not require to be placed inside incubators.(14)

Temperature control and regulation

One important factor for successful culturing cells is a tight temperature control and a homogeneous heating of the cell culture media. Normally cells are cultured at 37°C mimicking native conditions. It is important to narrowly control the temperature in avoid fluctuations especially overheating is hazardous for cell survival. Proteins start to denature and lose their function at 40°C this is why even minimal overheating needs to be avoided.(16)

Another important factor is an equal heat distribution in the cell culture chamber. Strong gradients in temperature might influence the cells, resulting in migration of cells or in the worst case local overheating and cell death. Especially in systems were large volumes are used this risk should be considered. Most commonly continuous stirring of the liquid is used to achieve an equal heat distribution in those systems.

Different heating systems can be used for cell culture from direct heating elements that convert electricity into heat over systems that heat the whole enclosed atmosphere to systems that use water as a heat transfer medium. The decision for a system highly depends on the application and demands. The advantage of using water as a heat transfer medium is its high specific heat capacity which has a high damping effect on the heating system and sufficiently buffers fluctuations. Once the system is stabilized at a specific temperature it can keep this temperature even when small variations occur. On the other hand this means that several hours of pre-heating are necessary before the system is ready for operation.(17)

In most bioreactors achieving a tight temperature control is a minor problem. Utilization of a water based heating system offer a simple, suitable and cost efficient way. Combined with a sufficiently precise temperature sensor, systems can be constructed in a straightforward manner and integrated in the bioreactor setup.

Atmosphere composition control and regulation

The control of the atmosphere composition inside the bioreactor has two main tasks. First, to supply sufficient amounts of oxygen for the cells and the possibility to control the concentration of oxygen to study aerobic and anaerobic process in the cell. Second and in most bioreactors the primary task, control CO_2 concentrations which are directly related to the pH for most cell culture media compositions.(16; 18)

Commonly used cell culture media, for example Dulbecco's modified Eagle medium (DMEM), have complex buffer systems that are adjusted to be used in atmospheres with 5% CO_2. At this particular concentration the pH of the medium will be around the physiological value of 7,4.(18) If control and regulation of CO_2 is not possible a different medium needs to be used which does not have a buffer system that relies on CO_2 levels. Invitrogen offers such a cell culture medium under the brandname "CO_2-Independent medium". This media allows the cultivation of cells under normal atmosphere without CO_2 regulation.

In most systems that allow control of the atmosphere the regulation is limited to CO_2 concentrations since complete control of the composition is expensive and requires more advanced technology. Thus systems incorporating the control of other components of the atmosphere mainly oxygen are rare and mainly used in research where the influences of varying oxygen concentrations are studied. Studies have shown that oxygen levels clearly influence mammalian cell cultures and can be used as an effective design parameter.(19)

Control of the atmosphere even when limited to CO_2 levels is problematic and expensive. The major problem is that it requires a tightly sealed cell culture chamber in which the atmosphere can be controlled. Furthermore a complex infrastructure with gas supply, pressure regulators, electronic valves and sensors is needed to control the gas composition. Thus it is more convenient to use CO_2 independent media if possible or design bioreactors that can be placed inside incubators.

Mass transfer

Mass transfer is one of the main limitations in up-scaling cell cultures today and bioreactors with different approaches have been designed to solve this problem. Mass transfer describes the transport of substances to and away from the cells. In cell culture the five major substances that need to be transported are oxygen and nutrients to the cells, carbon dioxide and waste products away from the cell and secretory and signaling molecules produced by the cells.(14)

If cells are cultured on flat surfaces in monolayers or up to a few multilayers mass transfer can be achieved by simple diffusion. Simple diffusion is also sufficient in more complex scaffold systems if certain criteria are fulfilled. The cells should have access to the culture media, the formation of permanent local environments with altered liquid compositions should be avoided and the amount of media should be limited to assure adequate oxygen supply. The depth of media above the cells is directly correlated to the amount of oxygen that can diffuse to the cells. It is possible to calculate suitable values and adjust parameters to reach optimal culture conditions in simple systems, like culture well plates and to some extent even in more complex systems.(20)

For many experiments the limited amount of cells is a problem, studies might require more complex cell organizations with many cell layers or special scaffold arrangements. In most of this cases it is not sufficient to rely on diffusion alone and more advanced systems are needed.

The simplest way to achieve higher mass transfer is to use a stirring bioreactor where the media is in constant rotation. There are two main problems with this approach. First, as long as the cells are cultured on large immobile scaffolds the effects are considerably low. Second, the rotational flow results in shear forces that may trigger unwanted effects in cells.(21) Only if cells are cultured on small microcarriers that are stirred in solution this approach might be beneficial for up-scaling.(9)

To realize higher mass transfer rates for cells cultured on complex scaffolds, perfusion systems have been developed. The principle in perfusion systems is to increase mass transfer by pumping media directly to cells and use active transport instead

of only relaying on passive diffusion. There are different perfusion systems available on the market that utilize this principle for example the CellMax® Quad system (Spectrum Laboratories, USA). The CellMax® Quad system was successfully used to culture bioartificial muscles (BAMs) that reassembled *in vivo* muscle tissue more closely than comparison cultures without perfusion.(22)

Besides the mentioned systems there are several others that facilitate mass transfer. In many cases it is necessary to take all parameters like cell type, media, oxygen pressure and volumes into account to achieve sufficient mass transfer. Therefore it is important that those considerations are noted during an early stage of the design process where modifications to support mass transfer can easier be integrated into the bioreactor design.

Sterilization, cleaning and reusability

Sterility is an important factor for bioreactors and can be separated in two parts: the initial sterilization process before it is used and the maintenance of sterility during operation. Both aspects are important and should be considered during the design process.(15)

Sterilization in bioreactors is crucial since the environment created for cell culture also provides excellent conditions for transmissible agents like bacteria, yeast, fungus and others. The nutrient rich media and warm temperature will result in a fast proliferation of transmissible agents and eventually they will outgrow the mammalian cells under investigation. Application of antibiotics act as suppressors and minimize the risk of severe contaminations but are not efficient against all kinds. Additionally, it results in the problem that latent infections might not be recognized in the cell culture but may change cellular behavior and cause inconclusive cell culture results.(16)

There are different techniques that can be used for sterilization: Autoclaving, dry head, flaming, ethanol, ethylene oxide, ozone, gas plasma, gamma rays, x-rays, UV light and others. Most commonly used in research labs are autoclaving, ethanol and UV irradiation, as well as gas plasma treatments, with autoclaving being the most desired method if applicable. The sterilization methods have different effects on materials and may alter their properties. Thus it is necessary to find a suitable sterilization method for a chosen material.(23)

Sterilization is important but only provides initial sterility thus it is essential that aseptic techniques are used in the subsequent steps to retain sterility. The design of the bioreactor should facilitate simple assembly under sterile conditions or even the possibility to sterilize the whole system together. Further down the line the risk of introducing contaminations into the system during operation should be minimized. After a successful experiment the bioreactor should be easy to clean and sterilize. It should be designed in a way that most parts can be reused for further experiments and consumables are available at reasonable prices.

The design of the bioreactor can help to facilitate processes to clean and sterilize the system. Therefore it is important to consider them during early development because later adjustments often result in a compromise. Small adjustments at the beginning can have a great effect on the later system which might result in crucial

advantages of the system. The complexity to achieve and maintain sterility is depending on the overall bioreactor design and purpose. Moving parts that are connected to both the inside and the outside of the sterile culture chamber can be regarded as one of the most difficult challenges since the risk to introduce contaminations through these parts is high. In static systems sterility can be achieved more easily.

Bioreactor materials

As described before materials used in a bioreactor have to be chosen with respect to sterilization methods. Additionally the material should be inert and not influence the cells, it should not be cell toxic or elute cell toxic substances. One of the most commonly used materials is stainless steel which can be reused and sterilized by autoclaving. It can be processed and machined into diverse forms and shapes and shows no corrosion even for prolonged periods of time. Stainless steel is inert and does not interact with normal cell culture media.(23)

Many plastics have the advantage that they are comparably inexpensive, available in diverse forms and do not interact with cell culture media, but possible sterilization methods are often limited. For example, Polystyrene (PS) a commonly used transparent plastic material has the disadvantage that heat sterilization will result in deformation and thus limits the reusability. Two possible replacement polymers that do not exhibit this limitation and are often used for medical applications are polysulfon (PSU) and polymethylpenten (PMP). These two materials are inert, transparent and dimensionally stable even after autoclaving, but are more expensive than PS.(15)

There are a wide variety of other materials that are used in bioreactors and fulfill specific tasks. If specific properties are needed or parts are only available in a certain material it must be individually investigated to which extent those materials are suitable and what their limitations are.

1.1.2 Bioreactor systems for mechanical stimulation

Mechanical stimulation has been shown to influence cell fate for different cell types and different bioreactors have been designed to study these influences in cell culture. Depending on the cell type and the studied phenomena the bioreactors need different properties. Typical values for elongation reach from a few percent up to 100 percent in an even wider range of frequencies up to several Hz. A bioreactor that can operate over a wide range is highly favored because it can be used for versatile experiments and adjusted to findings during a study. There are two distinct types of bioreactors for mechanical stimulation: The first one uses membrane deformation by inflation to create mechanical stress. The second one uses linear movement to create a unidirectional elongation of the scaffold.(24)

Membrane deformation based systems

There are different bioreactor system for mechanical stimulation that use the inflation of a membrane to generate mechanical strain. The membrane seals a confined cham-

ber in the bioreactor and this chamber can be filled with a gas, and by controlling the pressure inside the chamber, the membrane can be deformed. The deformation of the membrane results in a change of surface area and cells cultured on the other side of the membrane experience mechanical strain. Membranes can be functionalized with a wide variety of coatings for example laminin, collagen or matrigel. This principle allows high frequencies but limited elongation rates. One advantage is that utilization of transparent membranes allows the live visualization of cells during mechanical stimulation. The major drawback of those systems is that cells can only be cultured on 2-dimensional surfaces which limits the possibility to culture large functional skeletal muscles constructs.(11; 25) Commercial systems that use membrane deformation are available from the company Flexcell International (USA). They offer a range of systems for different applications with different configurations and control systems.

Liao et al. use a similar approach in their bioreactor design. They use inflatable silicon tubes covert with aligned electrospun polyurethane nano fibers instead of a membrane to culture C2C12 skeletal muscle cells. The bioreactor is computer controlled using LabView and incorporates the possibility for simultaneously electric stimulation.(26)

Moving anchor point based systems

Moving anchor point based bioreactors use a varying displacement between two anchor points to deform a mounted scaffold. Thus the scaffold is directly elongated and the cells attached to the scaffold experience mechanical strain. The principle allows a wide variation of scaffolds and only requires elastic materials that can be mounted between the anchor points. Furthermore complex 3-dimensional systems can be investigated with this principle. Moving anchor point based systems normally offer a wide elongation range but might be limited in the frequency regime.

Different moving anchor point systems have been developed and used for tissue engineering. Engelmayr et al. developed a bioreactor that allows the simultaneously stimulation of 12 individual scaffolds for tissue engineering heart valves. They used a enclosed computer controlled linear actuator to generate the displacement and deform their PGA/PLLA fiber meshes. The whole bioreactor needed to be placed inside a conventional incubator during experiments to maintain physiological conditions.(15)

Webb et al. used modified T-75 flask as culture chambers in their bioreactor setup. The displacement was generated by a stepper motor coupled to a ball screw spindle and controlled by a computer system using LabView. They studied fibroblasts cultured on 3-dimensional porous polyurethane foams in their experiments.(27) Other approaches include bioreactors for the mechanical stimulation of BAMs (28) and muscle cells cultured on acellular scaffolds (12).

Control and measurement systems

Bioreactors for mechanical stimulation need at least a control and measurement systems for the cyclic deformation during experiments. Additionally control and measurement system can be used to control and measure the environmental properties

in the system to ensure physiological conditions for the cells. When the bioreactor is placed inside a commercial incubator these additional tasks are realized by the incubator. There are two main systems that can be distinguished from each other: computer based and micro controller based.

In computer based system a ordinary personal computer with a commercial data acquisition and control card is used. Digital and analog computer periphery is available from many companies. On the computer a software runs the programmed process to control the stimulation during the experiment. LabView (National Instruments, USA) is an example of such a software, it is a development environment that allows simple graphical programming and the interaction with most commercially available control hardware. The advantage of these proven control systems is the reliability and the short development time for functional systems. The market offer a wide variety of hardware components that enable the realization of most applications. The disadvantage is that a computer needs to be coupled permanently to the bioreactor to run experiments. Furthermore the required hardware is often expensive.

Micro controller based systems use controllers on individually designed circuit boards. A micro controller is a chip that incorporates all important periphery directly in one unit. It has for example integrated digital and analog inputs and outputs (I/O), communication interfaces and timers. The processor operates at comparative low speeds (4-16 MHz) this limitation is compensated by the hardware specific programming and the high code optimization potential. The ATmega micro controller platform (Atmel, USA) offers many controllers for different needs. The advantage is that the whole system can be customized on the hardware level and no computer must be permanently coupled to the bioreactor. Micro controllers and additional electric components are inexpensive and enable the realization of small optimized systems at low cost. The disadvantage is that systems need to be self designed and are often error-prone. Furthermore the support is limited to individual components and does not cover the whole setup.(29)

1.2 Part 2: Selection and characterization of a scaffold material

1.2.1 Scaffold materials and properties

Scaffolds are normally necessary to study cells because most mammalian tissue forming cells are adherent and need a surface to attach to for survival. In medical applications scaffolds are further commonly needed to support cells and keep them in a defined area after transplantation. Scaffolds can have a wide range of forms and properties from a simple flat surface to gels to a complex 3-dimensional shape with functionalized surfaces.

Scaffold materials have to be chosen with respect to the application because different applications require different properties and have diverse limitations. Scaffolds and materials meant for transplantations have much stricter regulations and have to be approved for each product individually. In laboratory cell culture systems every

material can be tested but later applications and the suitability of the material should be kept in mind when choosing a material. Besides specific properties there are some common rules that have to be fulfilled for all scaffolds that are used with cells.

The most important property is that the material is biocompatible, it should not be directly cell toxic or elute cell toxic products. Furthermore it should support cell attachment - as mentioned previously, most cells are contact dependent and will eventually die if they cannot attach to a scaffold. For medical applications and transplantations the material should elicit none or only little inflammatory response in the host. It should be noted that the definition for a biocompatible material is under permanent discussion in the field and is mainly used for materials used in medicine and not in such a wide definition including cell culture surfaces and scaffolds as done here.(30; 31; 32)

Besides the biological aspects of the material, manufacturing and economical limitations have also be taken into account. It has to be possible to manufacture the desired material in the requested form and shape. Additionally material and manufacturing cost have to be reasonable in order to create a successful product.(33)

For functional tissue engineering it is important that the scaffold have similar properties compared to the native tissue where it is going to be implanted. This includes matching mechanical properties like elasticity and strength as well as surface topography with defined nano and micro structures. An elastic modulus E of around 12 kPa is reported for native skeletal muscle tissue.(34) Mimicking the native environment has been shown to support and influence cell proliferation, differentiation and organizing into functional tissue. Cells are able to sense their environment and response to it in specific ways. Tailoring the scaffold exactly to the specific needs and match the native properties can help engineer complex tissue constructs *in vitro*.(35) Furthermore bioresorbable scaffold materials that completely degrade over time are preferred for tissue engineered implants. Those materials enable the development of system that have a scaffold material for initial cell growth that disappears over time to allow the formation of native like tissue. This limits the risk of host rejection, infection and fibrous encapsulation often associated with permanent implants.(23)

1.2.2 Scaffolds for Tissue Engineering skeletal muscle

Skeletal muscle cells are contact dependent and therefore need a scaffold material to attach to. There have been many different approaches to culture skeletal muscle cells which can be classified into the following groups: 2-dimensional surfaces (36), $2\frac{1}{2}$-dimensional surfaces with defined topography (37), electrospun fiber meshes (38), aligned micro diameter fibers (39), microcarriers (10), 3-dimensional porous materials (40) and hydrogels (41). Additionally muscle constructs without an integrated scaffold, termed bioartifical muscle (BAM), were developed.(42; 43)

In a broader sense scaffolds can be separated into virtual 2-dimensional systems where dimension in x and y direction widely exceed the hight in z-direction and true 3-dimensional systems in which cells can grow in all directions without severe limitations in z-direction. These more complex 3-dimensional systems mimic the native environment more closely and are promising to produce skeletal muscles that

have similar properties to native muscular tissue.(5) One problem in those systems is the limited supply of nutrients and oxygen as mentioned in 1.1.1. It is not sufficient to rely on diffusion alone for those constructs and more advanced systems need to be integrated to solve the problem, for example, perfusion systems.

In order to produce complex defined 3-dimensional scaffolds solid free-form fabrication is a promising technique. It allows tight control of pore size, interconnectivity, micro and macro structure, variable integration of substances and is highly reproducible.(44)

$2\frac{1}{2}$-dimensional surfaces with defined topography have been produced in different materials, commonly used are polydimethylsiloxane (PDMS) and oxidized silicon wafers. Defined topographical features are used to study cell contact guidance, cell alignment and the influence of feature size on muscle fiber formation. Parallel surface features in the right size can support myoblast alignment and myogenesis. Lam et al. studied the effect of different sizes of continuous wavy micropatterns on silicon substrates. Their results show that a wavelength of 6 μm for the wavy patterns result in the highest degree of cell alignment.(37) Our group did some experiments using grooves and ridges in PDMS as well as on silicon wafers to study the effect of cell alignment and myotube formation which also showed contact guidance for cells, data not published.

Electrospun fiber meshes can be seen as a similar approach since they normally do not exhibit large heights, commonly only up to a few hundred micrometers. The spacing between fibers and fiber diameters can be regarded as features which can stimulate cells in a similar as topography features on surfaces. Riboldi et al. observed cell alignment on aligned, non random, electrospun DegraPol fiber meshes. DegraPol is a polyurethane polymer and a known tissue engineering scaffold material.(38; 45)

In contrast to electrospun fiber meshes individual micro diameter fibers can be used to produce a different kind of scaffolds. The most distinct difference is that fibers are separated from each other and can be combined and aligned individually which allows highly controlled scaffold organization, fiber spacing and scaffold shape. The effects of different fiber spacings between fibers was studied by Neumann et al. They observed fiber bridging and formation of complete cell sheets for spacings up to 50 μm.(39) Shah et al. studied phosphate glass fiber meshes and showed their suitability for muscle cell culture. Phosphate glass is a promising biomaterial because it is biodegradable without dilution of any cell toxic substances. Additionally degradation rates are linear and can be tailored to specific needs by slight modifications of the material.(46)

1.2.3 Scaffolds for mechanical stimulation of skeletal muscle cells

Scaffolds for mechanical stimulation need to fulfill the additional requirement of being elastic. They must allow repeated elastic deformation without material failure and large permanent deformation. They should return to their original length and form after deformation when the force is released. This considerable lowers the number of

suitable materials. Different materials have been used in the past most of them can be grouped into 2-dimensional membrane systems, 3-dimensional porous scaffolds or BAMs.

2-dimensional membrane systems have the advantage to allow in situ visualization of the cells and real time studies on effects of mechanical stimulation. This is one of the drawbacks using more complex 3-dimensional systems since it is difficult to observe effects in real time. Commonly used for this studies is the BioFlex platform from Flexcell (Hillsborough, USA). The silastic membranes used for this system are normally coated with collagen or growth factor reduced Matrigel.(36; 47; 48; 11; 49)

The BAM systems offer an additional way to study effects of mechanical stimulation of skeletal muscle cells *in vitro*. BAMs are produced by culturing cells in collagen suspension on a flat surface with two anchor points at opposite positions in the dish. The anchor points mimic tendons in native muscle tissue, stainless steel and silk have been used as materials.(50) Eventually the cells will roll-up and form a tissue construct between those two anchor points. They then can be transfered and attached to a bioreactor system for mechanical stimulation. Those system have shown the most promising results and created the largest viable muscle constructs so far. Contraction forces for *in vitro* BAMs reach up to 10% of those measured in *in vivo* muscles when values are normalized according to size.(12; 28; 7; 51; 42; 43)

To our knowledge mechanical stimulation on individually micro diameter elastic fibers has not been investigated yet. It offers a possible alternative to create 3-dimensional scaffolds with high complexity and organization. Furthermore micro diameter fibers offer contact guidance and support myoblast alignment as well as defined fiber spacing can be realized to facilitate muscle cell mass increase.

1.2.4 Polyurethane elastic fiber properties and production

Polyurethane elastic fibers are known under different brand names for example Spandex, Lycra and Elastane. They normally show elastic elongation rates between 400-800% and quickly return to their original length once the stress is released. They exhibit only minimal permanent deformations even after prolonged repeated stretching. Furthermore polyurethane can be spun into small diameter fibers and the chemical composition of the polymer can be tailored to meet specific needs. A wide varity of polyurethane elastic fibers are available with different diameters, functions, elongation rates, surface modifications and resistances.(52) Polyurethane fibers could also be modified to be bioresorbable which would be an important property for later applications. The polymer can be modified which different segments to fine tune the degradation time and behavior.(38)

Polyurethane polymers consist of two segments, hard and soft, which have glass transition temperatures above and below room temperature, respectively. The short, rigid, hard segments give the fiber stability and strength whereas the long, amorphous, soft segments enable large elongation rates. During elongation the coiled soft segments are straightened and bonds between hard segments are temporarily broken, after release of the stress the soft segments recoil and the fiber returns to its original state.(53)

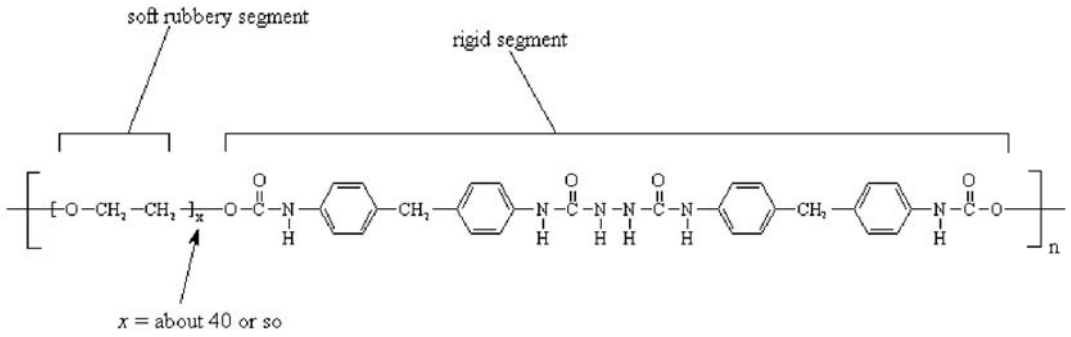

Figure 1.1: Chemical structure of Spandex® fiber polymers indicated soft and hard segments. The number of units can vary depending on the desired properties of the fiber. (55)

Polyurethane fibers can be produced by four different spinning methods: melt extrusion, reaction spinning, solution dry spinning and solution wet spinning. The most common production method is dry spinning which accounts for around 90% of the total fiber production.(52)

During spinning two pre-polymers react to form the final elastic polymer and this process is facilitated by chain extenders added during spinning. The first pre-polymer is a long macroglycol which forms the soft segment. This pre-polymer can be polyester, polyether, polycarbonate, polycaprolactone or combinations. A long, flexible back bone chain in this pre-polymers gives the end product its elasticity. The second pre-polymer forms the hard segments and is often a polymeric dissocyanate. FIGURE 1.1 shows the typical structure of spandex. The two pre-polymers are connected through urea and urethane linkages, N-C-N and N-C-O respectively.(52; 54)

Stabilizers are often added during polymer production to enhance its resistance against UV-light, heat and other influences. The chemicals used as stabilizers are manifold and are normally handled confidentially by the companies. After spinning, fibers are often treated with finishing agents, such as PDMS, magnesium stearate or other polymers depending on the application area for the fibers. The finishing agents prevent fibers from sticking to each other and thus facilitate and simplify their processing in large textile machines.(52)

1.2.5 Characterization of polymer scaffold materials

In general it is difficult to receive information about exact production procedures, chemical compositions and treatments from companies that produce fibers for textile industry. Normally that information is confidential and only marketing information is available. This makes it necessary to use different techniques to analyze the polymers in order to gain as much information about the fibers as possible. Techniques used in this thesis include FT-IR ATR spectroscopy for bulk chemistry analysis, XPS for surface chemical composition and SEM imaging for topographical and size information.(56; 54; 52)

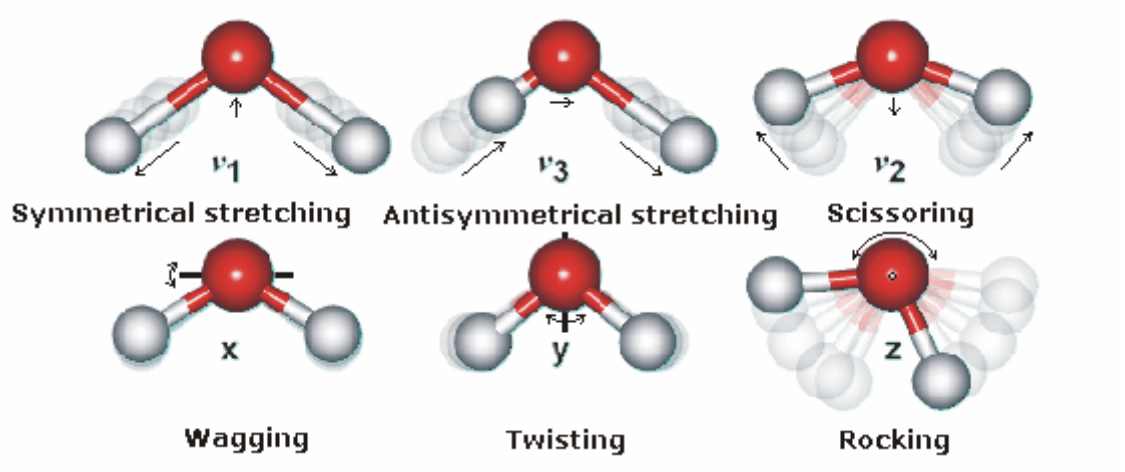

Figure 1.2: Overview of the six fundamental vibration modes for a water molecule excited with infrared radiation.(58)

Fourier transform infrared spectroscopy

Fourier transform infrared (FT-IR) spectroscopy is regularly used to identify the chemical composition of substances and polymers. It is a special form of infrared spectroscopy which utilizes the interference of beams to quickly measure absorbance spectra in the IR region. The main element is a Michelson interferometer (schematically shown in FIGURE 1.3), a continuously moving mirror that generates a difference in the optical path length of two beams. Recombination of both beams results in interference. The wavelength of the interference changes in accordance with the continuously changed path length and a Fourier transform of the spectra is obtained directly.(57)

The physical principle of infrared spectroscopy relies on molecular vibrations and the resulting absorbance of specific wavelengths for different chemical groups. Mid-infrared radiation ranging from 4000 to 400 cm^{-1} excites fundamental and rotational structure vibrations. Bonding energies and discrete energy levels of atoms result in different resonant frequencies at which a molecule absorbs radiation. The number of possible vibration frequencies increases with the number of atoms forming a group or molecule. For example a water molecule has six different vibration modes, see FIGURE 1.2.(57)

FT-IR ATR (Attenuated total reflection) spectroscopy is a special configuration for measuring FT-IR spectra, a schematic is shown in FIGURE 1.3. The excitation beam is coupled into a prism, where it is internally reflected at least once before it is coupled out again and travels to the detector. The total internal reflection creates a evanescent field which propagates several micrometers into the sample. The propagation depth depends on the wavelength, the coupling angle and the prism material, but normally does not exceed 10 μm. For this reason samples are pressed against the crystal with a force clamp to enhance the contact and avoid disruptions at the interface. FT-IR ATR allows fast spectra recording without complicated sample preparation and allows the measurement of a wide variation of samples including

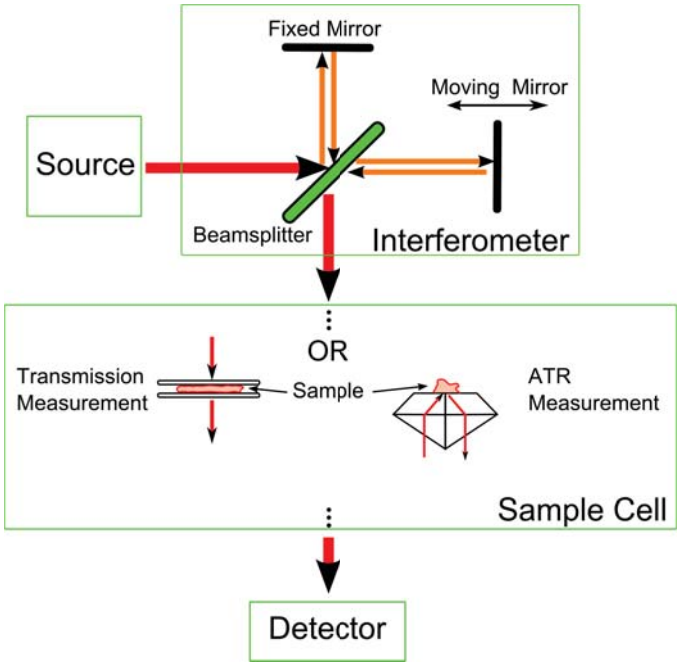

Figure 1.3: Schematic of a FT-IR spectrometer with a Michelson interferometer. Both measurement configurations, transmission and ATR, are indicated in the figure.

solids, powders, fibers and liquids.(57)

The main challenge in FT-IR spectroscopy is not the measurement but the interpretation of the obtained spectrum. Highly pure substances are fairly simple to identify especially if information about the expected composition are available. More complex and mixed substances are much more difficult to analyze, due to the fact that vibration modes are often overlaying and influencing each other. Without knowledge about the anticipated compositions identification of substances and their chemical structure are often impossible. One feasible way is to use FT-IR spectroscopy for the comparison of complex substances since differences can be more easily identified and corresponding chemical groups can be assigned.

X-ray photoelectron spectroscopy

X-ray photoelectron spectroscopy (XPS) is a technique to study surface chemical composition of materials. It gives information about the atomic composition, electron configuration and state of atoms on a surface. The penetration depth is limited to a few layers of atoms, the maximum is between 1-10 nm. The detection area depends on the beam size and can vary from a few micrometers up to one millimeter. The detection limit is in the range of parts per thousand for normal scans, for lower detection limit longer high resolution scans are necessary.

XPS uses a focused x-ray beam to irradiate the sample surface which results in the removal of electrons from atoms at the surface, the principle is shown in FIGURE 1.4. The photo emitted electrons are collected in an electron energy analyzer which measures the number of electrons and their corresponding kinetic energy. From the

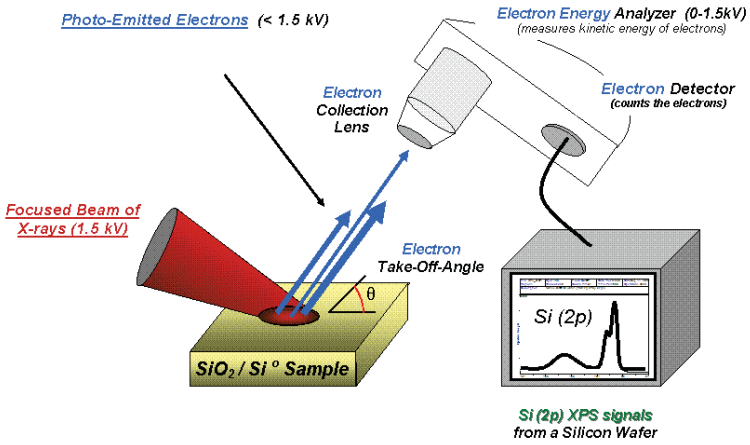

Figure 1.4: Schematic of the XPS principle with the different elements indicated in the figure.(58)

kinetic energy of emitted photoelectrons and the excitation energy of the x-ray beam, the binding energy of electrons in the material can be calculated. Data is than presented as the number of electrons detected as a function of binding energy of the electrons.(59)

Each element has a characteristic binding energy of its electrons, because different electron configurations are possible each element shows a set of peaks, corresponding to the 1s, 2s, 2p, 3s, ... electron configurations.

The advantage of the XPS is the possibility to directly determine the atomic composition of the sample surface from the spectrum. The reason is that peaks can be clearly assigned to elements and the intensity of the peak is proportional to the amount of the element, after correction by a sensitivity factor for each element. This observations can be obtained by a fast wide scan over a large range of binding energy (0-1400 eV). If more detailed information about specific peaks are needed high resolution spectra can be obtained to investigate the shape of the peaks more closely.(59)

One disadvantages of the technique is that ultra high vacuum is needed to measure spectra which requires time consuming evacuation of the chamber after sample loading. Additionally XPS cannot detected elements that have a lower atomic number than lithium, so no information about the hydrogen and helium content can be obtained.(59)

Overall XPS offers a efficient way to study surface chemistry and determine the surface composition of unknown samples. Surface chemistry is important in many application, for example in cell biology where those parameters are highly influencial on molecular interactions at surfaces, and thereafter cell-surface interactions, cell survival and cell fate.(60)

Scanning electron microscopy

Scanning electron microscopy (SEM) is an imaging technique that allows resolutions down to one nanometer. It images the sample surface by scanning an electron beam

in a raster pattern over the surface. Due to the large depth of field SEM images appear 3-dimensional and allow a detailed analysis of surface topography and shape.

An electron beam with an energy between 100 eV to 40 keV is focused to a small spot for imaging, the spot size is directly related to the resolution. The beam is then deflected in x and y direction to raster scan the whole sample. The beam interacts with the sample and generates three emissions that can be measured to create an image: reflection of high-energy electrons, emission of secondary electrons and emission of electromagnetic radiation. For each type special sensors are required, most commonly used to generate SEM images is to measure the emission of secondary electrons.(61)

One of the main limitations of SEM is the fact that samples need to be electrically conductive. This means that most biological samples as well as polymers need to be coated with conducting materials like gold or palladium. Sputter coating allows the homogeneous deposition of thin films of those materials on the sample surface. For biological samples another important limitation is that the samples need to fixed and dried and are therefore subjected to shrinkage artifacts before they can be coated and imaged.(61)

In summary SEM offers high resolution imaging with some limitations for biological samples. The increased resolution and the pseudo 3-dimensional images allows more detailed studies of fiber structure and topography than light microscopy for micro diameter polymer fibers.

1.3 Part 3: Skeletal muscle cells

1.3.1 Anatomy of skeletal muscles

Skeletal muscle tissue can be distinguished from smooth and cardiac muscle tissues, by the ability to be controlled voluntarily. The skeletal muscle is attached to bones and move the skeleton which gives rise to the name.

Skeletal muscles have three functions: Generating body movement, stabilizing body position and producing heat. Generating body movements is normally a voluntary decision whereas stabilizing body position and producing heat is involuntary controlled by the brain. Each skeletal muscle is an individual organ composed of muscle fibers, connective tissue, nerve fibers and blood vessels. In order to understand the function of skeletal muscle one has to take a closer look at the composition and organization.(62)

FIGURE 1.5 depicts schematically the organization of a skeletal muscle. The muscle is attached to the bone via a tendon, a dense connective tissue with parallel collagen fibers. The tendon is an extension of the epimysium which surrounds the whole muscle. The muscle is organized in fascicles enclosed by a different type of connective tissue called perimysium. Each fascicle is composed of up to several hundred muscle fibers and each muscle fiber is surrounded by epimysium, a third type of connective tissue. One individual muscle fiber cell can reach dimensions up to 3 cm long and 100 μm in diameter.(63)

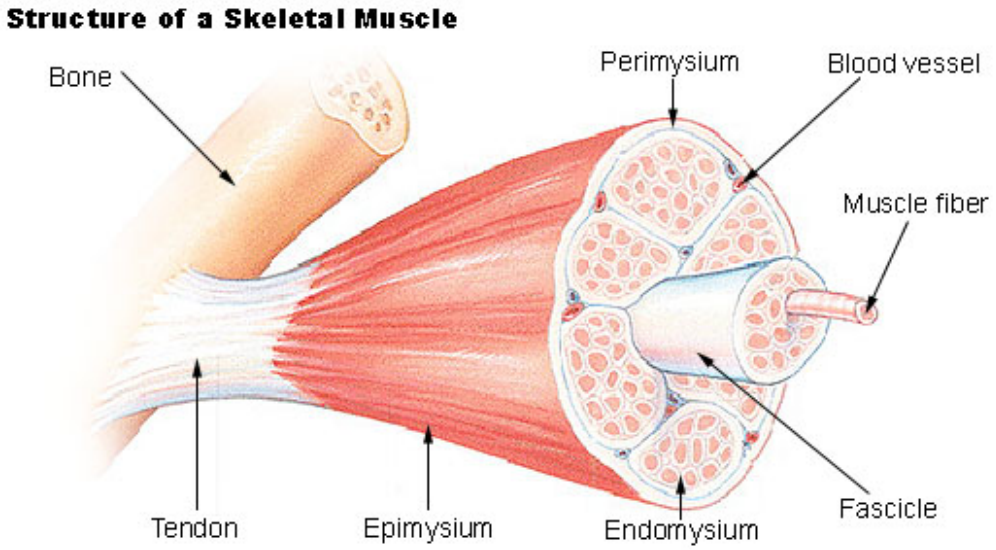

Figure 1.5: Schematic of the structure of a skeletal muscle with indicated names.(62)

Blood vessels and nerve fibers are embedded in the connective tissue and connected to the muscle fibers. Skeletal muscles have a high density blood capillary system to supply them with the amounts of oxygen and nutrients required for muscular function. Inside muscle cells oxygen transport is facilitated by myoglobin, a molecule similar to hemoglobin in blood, that can bind and transport oxygen. Furthermore nerve fibers need to penetrated each muscle fiber at multiple points to generate nerve impulses that trigger muscle contraction. For this purpose many axon terminals, which are directly connected to the muscle fibers, are formed at the end of the nerve fiber.(62)

Besides muscle fibers there is an additional muscle cell type called satellite cells. Satellite cells are myoblast progenitor cells which retain the ability to proliferate. Under normal conditions those cells remain quiescent in the tissue but can be activated by different stimuli. The exact activation pathways are still unclear but it has been shown that satellite cells are activated by muscle injury and are able to repair damaged muscles. However the repair potential is limited and not sufficient in muscular diseases or to heal severe trauma.(64; 65; 66) Tatsumie et al. identified hepatocyte growth factor (HGF) as a substance involved in satellite cell activation in response to mechanical stimulation. HGF levels increase during mechanical stimulation and bind to c-met receptors of satellite cells which are subsequently activated and initiate proliferation but the pathway and its importance is still unclear.(48)

1.3.2 Inner structure of muscle fibers

A muscle fiber is a single multinucleated cell formed by cell fusion, as described in section 1.3.3. Looking in more detail at a single muscle fiber, complex organized structures can be observed which are necessary to generate movement. A single muscle fiber can have up to 1000 nuclei, located at the periphery of the cell to allow myofibrils to form in the center. In each cell many myofibrils are aligned in parallel and

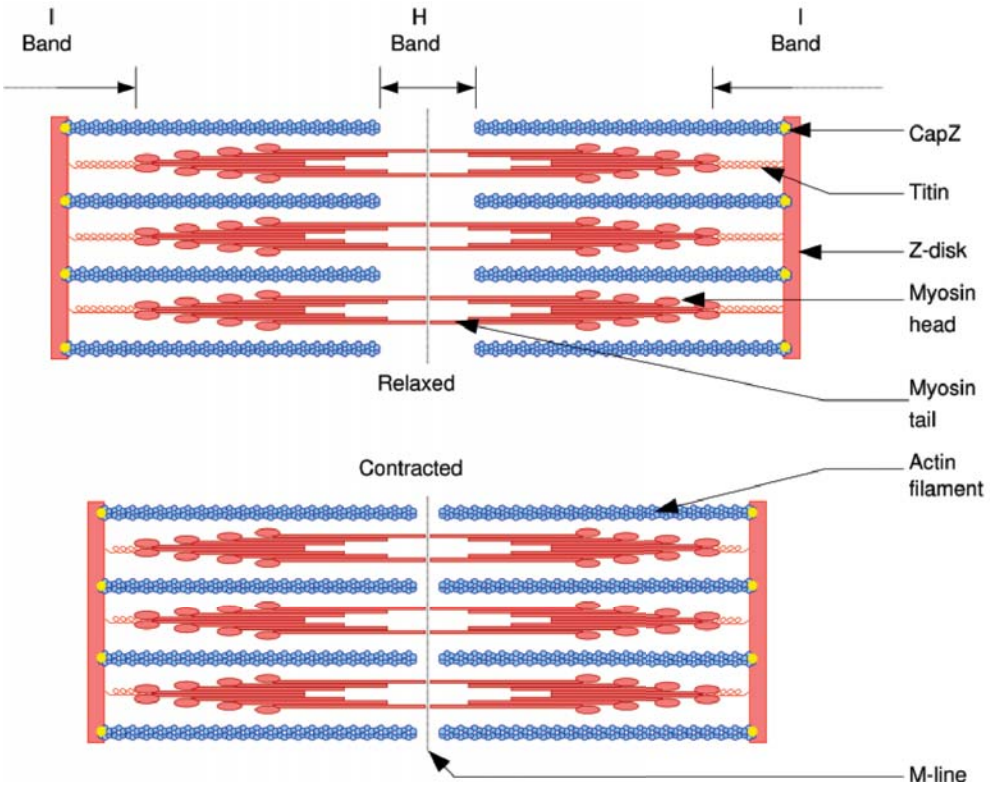

Figure 1.6: Schematic of the myofibril organization with indicated names of the different structures.(58)

span the whole length of the cell. Furthermore muscle fibers contain large numbers of mitochondria to produce the high amounts of ATP required during contraction.(62)

The myofibril is the part in the muscle where the movement is generated, it consists of thin and thick filaments as shown in FIGURE 1.6. Thin and thick filaments are overlapping each other and form distinct units called sarcomeres. Repetition of this units gives skeletal muscle fibers a characteristic striation pattern.(67; 68; 69)

The total number of muscle fibers in adult humans is nearly constant and the observed muscle growth in response to exercise is mainly an effect of increasing the number of myofibrils per cell. Depending on the intensity and duration of exercise, different effects can be observed.(62)

Movement is generated by a sequence of events where thin and thick filaments interact with each other, this processes is called the sliding-filament mechanism see FIGURE 1.7. In a first step the myosin heads from the thick filaments get activated by ATP hydrolysis. The next step is binding of myosin heads to the actin in the thin filaments. Followed by a rotation of the myosin heads which moves the thin filaments, this is called the power stroke, where the movement is generated. The last step is the release of the myosin heads from the actin by ATP binding. This process is repeated as long as the Ca^{2+} ion concentration is high and ATP is available. The Ca^{2+} ion concentration is controlled by processes in the sarcoplasmic reticulum in response to nerve signals. The simultaneous displacement of thin and thick filaments along the

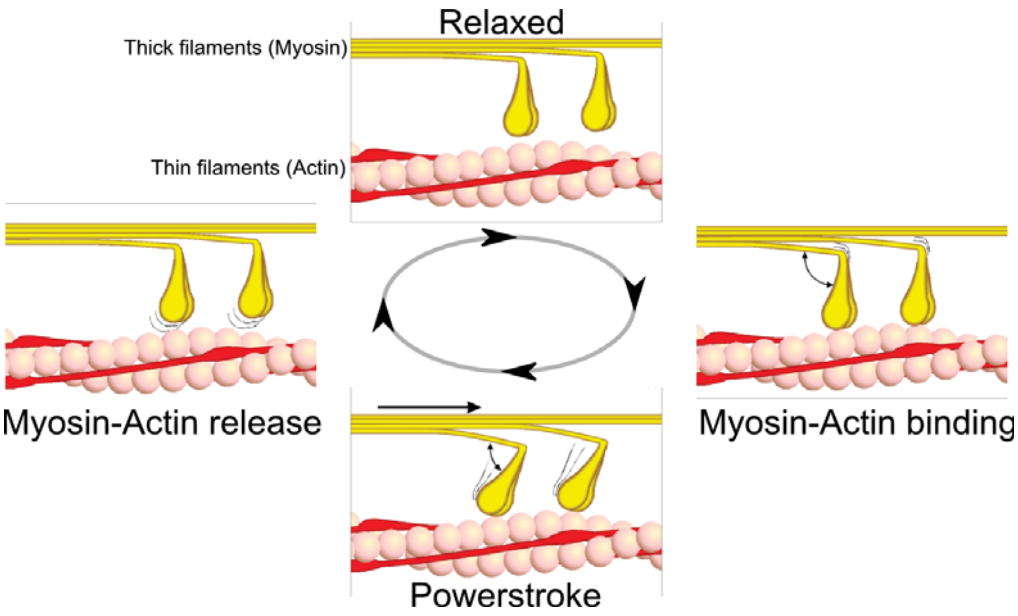

Figure 1.7: Schematic showing the 4 stages of the sliding filament mechanism that generate forces in muscle fibers. Modified from (58)

myofibril generates the macroscopic movement that moves the connected bone via the tendons and is visible as body movement.(67; 62)

Nerve signals from neurons are transmitted to muscle fibers in neuromuscular junctions. For stimulation, neurons release acetylcholine which binds to nicotinic acetylcholine receptors located in the muscle fiber plasma membrane. This process results in the opening of channels and an influx of sodium into the muscle fibers. The inner cellular Ca^{2+} ion concentration is further increased by the release of ions stored in the sarcoplasmic reticulum that surrounds myofibrils. The high Ca^{2+} ion concentration in the myofibrils then triggers contraction of the muscle fibers.(70; 62)

In skeletal muscle cells the thick filaments are formed by myosin type II, which consists of two myosin heavy chains (MHC) and four myosin light chains (MLC). The heads that bind to actin during contraction are located at the N-terminal of the heavy chains.(71) The actin in the thin filaments is attached to the z-disks via α-actinin.(72) There are different protein isoforms known that define the properties of muscle fibers. It can be distinguished between slow and fast muscles that express different subsets of proteins isoforms for example fast and slow myosin. Slow muscle fibers rely on aerobic metabolism and are able to generate repetitive forces for prolonged time periods whereas fast muscle fibers use an anaerobic metabolism to generate larger forces over short time periods.(73; 74) It has been shown that native skeletal muscles are highly plastic and can change their phenotype between fast and slow in response to exercise.(75)

1.3.3 Forming of skeletal muscles - Myogensis

Skeletal muscles are formed simultaneously with bones during embryogenesis, this process of muscle formation is called myogenesis.(76) Muscles originate from myotome, a special form of somites that are the root of all mesoderm tissue in vertebrates.(62) Once a cell is committed to become muscle tissue it cannot change its fate. These cells are called myoblasts and are the precursor cells of muscle fibers.(63)

Skeletal muscle formation can be described in three stages.(63) The first stage is myoblast proliferation where cell numbers highly increase. This process is stimulated, among others, by high concentrations of fibroblast or hepatocyte growth factor (FGF or HGF). In a second step the condition of myoblasts is changed significantly and cells undergo strong changes in gene expression. Gene expression is changed towards muscle specific proteins which start the differentiation process. Once a myoblast starts to differentiate it can no longer divide. In this stage cells start to fuse and form multinucleated cells, up to 10 nuclei, termed myotubes.(77) Myoblast fusion into myotubes normally occurs as end-to-end fusion and is steered by cell-cell interactions. The transition from myoblast proliferation to myotube formation is mediated by several factors, including low growth factor concentrations and mechanical stress. Furthermore fusion is controlled by a positive feedback loop, once cells start to fuse they secrete signaling molecules and recruit other cells to initiate differentiation. The last stage is muscle fiber formation. In this stage myotubes continue to fuse and form muscle fibers with up to several hundred nuclei. This fusion process occurs as end-to-end fusion as well as lateral fusion. At the end of the whole process are fully mature muscle fibers that have functional myofibrils and are able to contract. This last stage does not always occur in *in vitro* cell cultures and it was reported that muscle fibers formed *in vitro* are normally smaller than those found *in vivo*.(78; 28)

There are several gene transcription factors that play an important role during myogenesis called myogenic regulatory factors (MRFs). Important MRFs are: MyoD (79; 80), Myf5 (81), myogenin (82) and MRF4 (83). Those factors control gene expression during myogenesis at different time points and mediate final differentiation.(84) The complex interplay of these MRFs has been widely studied.(85; 86; 87; 88) Additionally the process is influenced by the proteinase m-calpain which increases shortly before myoblast fusion starts(89) and C6ORF32 protein was identified to play a role in the cytoskeletal rearrangement during myotube formation.(90)

1.3.4 The C2C12 cell line as a model system for skeletal muscles

The C2C12 cell line is a commonly used model system to study processes and mechanism in skeletal muscles. C2C12 cells are immortalized mice myoblast-like cells and can be differentiated into skeletal muscle fibers. The C2C12 cell line was established 1977 by D. Yaffe and O. Saxel.(91) It has been shown that C2C12 are still contact inhibited and are thus not cancer like cells.(92)

The advantage of using a cell line model instead of primary cells is that people at different laboratories, at different time points, can work with nearly identical cells,

which allows simpler comparison of results.(16) The C2C12 cell line shows rapid proliferation, a high degree of myotube formation and formation of fully differentiated muscle fibers expressing skeletal muscle specific proteins. Differentiation of C2C12 cells can be initiated by changing serum concentration and composition. The most common way is to use 10% fetal bovine serum (FBS) for proliferation and 2% horse serum (HS) for differentiation. The lower amount of growth factors in 2% HS triggers the differentiation process in the cells.(93; 94; 95; 96) The maintenance of these cells requires passage prior to reaching confluency and culture in 10% FBS in order to avoid differentiation and loss of proliferative potential. Due to the described properties which allow simple control of the differentiation processes and the easy maintaince compared to primary cells, the C2C12 cell line is such a well studied cell model.

One factor in skeletal muscle cell cultures that is often not taken into account are oxygen levels. Without oxygen control, levels are normally around 20% in *in vitro* cultures which is contradictory to levels observed *in vivo* where oxygen levels are between 1-10% for muscle tissue.(97) Mimicking the environment more closely with 3% oxygen results in incresased cell proliferation and the formation of larger myotubes and muscle fibers.(19)

However it is important to note that it is still a model system and has several drawbacks.(98) Dennis et al. reported that C2C12 cells are less excitable and contractible than primary cells. They suggested that this might be due to the lack of normal metabolism, phenotype or growth regulation. Furthermore they observed differences in cellular organization and chemomechanical coupling of C2C12 cells compared to primary cells. They concluded that C2C12 cells are less suitable to engineer functional muscle than primary cells.(50)

Considering both the advantages and disadvantages, the C2C12 cell line offers a convenient way to study elementary processes occurring during myogenesis and can help to understand the principles of skeletal muscle formation and function; results which can later be used to design tissue engineering applications with more relevant primary cells.

1.3.5 Mechanical stimulation of muscle cells

Cells are able to sense mechanical stress with a variety of different mechanisms but the associated cellular pathways are still not fully understood. It is likely that the cellular response to stress is highly dependent on pre-existing forces and conditions. This pre-stress might be the reason why similar stimulations can have different effects on cells depending on their situation prior to the stimulation.(24)

The cells repertoire of mechanical sensing elements include integrins and mechanically gated ion channels. Integrins located in the focal adhesion points play an important role in mechanotransduction, they are connected to the substrate and are changed in response to deformation. This results in the recruitment of additional focal adhesion proteins to strengthen the contact to the substrate.(99) Additionally integrins mediate whole signaling cascades that result in altered gene expression and cellular reorganization for example by changing cyclic adenosine monophosphate (cAMP) levels.(100) Mechanical gated ion channels open and close in response to

mechanical stress and thus influence ion concentrations in the cell.(101)

In vitro mechanical stimulation of muscle cells can be divided in two general groups: passive continuous elongation and active cyclic stretching. This can be related to the native process occurring in vertebrates like bone elongation during embryogenesis and muscular training, respectively. A typical value for bone elongation in humans is 2 mm/week during embryogenesis (102; 103). For cyclic stretching in native tissue, peak-to-peak values of up to 26% deformation between contraction and relaxation have been reported.(104).

The underlying processes for the two stimulation types is different. During passive continuous elongation myoblasts align along the stretching direction, myotube formation and final differentiation into muscle fibers take place.(11) Whereas cyclic stretching influences the protein composition of muscle fibers and results in increasing muscle fiber diameter.(28) Furthermore it can, to some extent, activate satellite cells which then proliferate and eventually laterally fuse with the existing muscle fibers.(48)

For cyclic stretching of muscle cells *in vitro*, different stimulation patterns have been used. Commonly a period of stimulation (5-60 minutes) is followed by a longer period of resting. Normally deformation rates between 10 and 30% are used with frequencies between 0.1 and 2 Hz.(12; 48; 49; 28; 47)

Otis et al. studied the influences of mechanical stimulation on myoblast proliferation. They showed that cycloxygenase COX2 is involved in the sensing pathway of mechanical stress and showed that mechanical stimulation increases myoblast proliferation.(49) Several groups have shown that protein isoforms in muscle fibers can be changed in accordance to cyclic stretching. It is possible to transform fast muscles into slow muscles by prolonged cyclic stretching.(105; 106) Febbraio et al. showed furthermore that heat shock protein (HSP) 72 levels increases during prolonged exercise to prevent cell damage. HSP72 acts as a chaperone to ensure correct protein folding and protects cells against protein aggregation. HSPs have been shown to mediate cell responses to different stress factors in many organisms.(107)

The effects of different stimulation patterns are widely discussed in the field and are still under investigation. To summarize the different findings, it can be said that it is likely that cyclic mechanical stimulation of myoblasts results in an enhanced proliferation whereas the same stimulation on myotubes will result in higher numbers of thicker and more functional muscle fibers.

1.3.6 Immunocytochemistry as an analysis method

Immunocytochemistry is a method to study cells, investigate cellular fate, protein expression, cell number, cell morphology and further aspects. In contrast to immunohistochemistry, were complete tissue slices with different cells and matrix are used , immunocytochemistry samples are normally free of matrix. Often fluorophores are used in immunocytochemistry to visualize the proteins and structures of interest in the cell. There are different ways of visualization: direct and indirect antibody methods as well as chemical specific reactions. (See Figure 1.8)

Both antibody methods rely on highly specific binding of primary antibodies

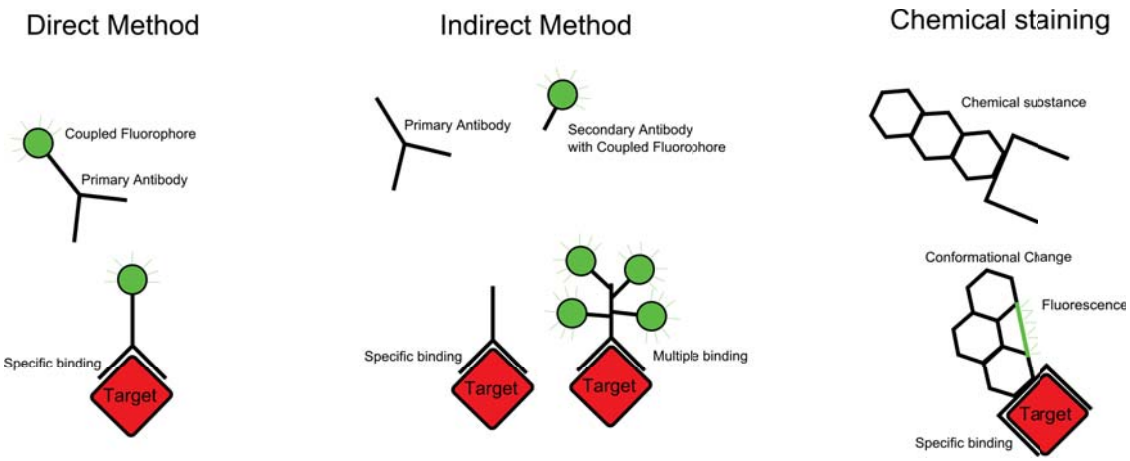

Figure 1.8: Schematic of the three most common staining methods: Direct and indirect antibody staining and chemical staining.

against the protein of interest. Primary antibodies are available for a wide range of proteins and species. Sigma-Aldrich Corp. currently offers around 8000 primary antibodies. Thus it is possible to obtain them for all common applications, furthermore it is possible to get individually designed primary antibodies against special proteins from GenScript Corp. for example. In order to visualize the specific primary antibody the direct and indirect method differ. For the direct method a fluorophore is directly coupled to the primary antibody. Thus it is a one step method were results can directly be obtained after the specific binding. In the indirect method a secondary antibody with a coupled fluorophore is used to show the protein of interest. This secondary antibody binds normally to a whole group of primary antibodies with a specific immunoglobulin class for example IgG. Since the binding is much less specific the number of secondary antibodies is considerably less and similar secondary antibodies can be used for many primary antibodies. In addition several secondary antibodies can bind to a single primary antibody which result in an amplification of the signal and the ability to study low protein concentrations.(108; 109)

Another method relies not on antibody binding but on chemical binding and structural modifications. It uses chemicals that bind with a high affinity to the structure of interest in the cell. The chemical is either directly fluorescent or can be coupled to a fluorophore. Two typical substances that use this method are DAPI (4',6-diamidino-2-phenylindole) and phalloidin. DAPI binds strongly to DNA and when bound, changes its chemical properties and results in blue fluorescence with an emission maximum at 461nm for an excitation around 358nm. Phalloidin is a toxin that binds specifically to actin filaments in cells. Phalloidin can be coupled to a fluorophore to visualize actin filaments, it is commercially available as rhodamine/phalloidin for example.(109; 63)

In general immunocytochemistry is a powerful method to study cells and shows low detection limits. The wide range of proteins and cell structures that can be visualized allow detailed cell studies. One of the drawbacks is that most immunocytochemistry stainings need dead and fixated cell samples. Cell membrane permeabilization agents

such as Triton-X-100 are necessary to allow the staining substances access into the cells. Thus only distinct time points can be measured for the most immunocytochemistry stainigs. The repertoire of available live cell labels is considerably lower than conventional stains and often the genetical modification of the protein of interest is the only way for live cell studies. By coupling DNA encoding a fluorescent protein to the protein of interest it is possible to tag and visualize it. Often green fluorescent protein (GFP) or one of its derivatives is used for co-expression. Immunocytochemistry in general is one of the most commonly used and powerful techniques in cell biology.

1.3.7 Fluorescence microscopy

Samples that are labeled with immunocytochemistry and use fluorophores need fluorescences microscopy to obtain images. Fluorescences microscopy differs from normal brightfield microscopy in the way the sample is illuminated. In brightfield microscopy the sample is illuminated with white light at any given time point with wavelengths reaching over the whole visible spectrum. In contrast fluorescences microscopy uses filter cubes allowing only specific excitations and emission wavelengths to pass through. This defined illumination together with the particular properties of the fluorophores are the foundation to obtain high quality specific cell images.

A fluorophore is a molecule that has the ability to absorb light at a specific wavelength and emit light at a longer wavelength. Absorption of a high energy photon excites the fluorophore and a electron is transfered to a higher energy state. During relaxation the electron does not fall back directly to the ground state but first to an intermediate state by transferring energy into heat or vibration. In a second step the electron falls back to the ground state which result in emission of a photon with a longer wavelength, less energetic. The difference between excitation and emission wavelength is called Stokes shift. Commercially available filter cubes are optimized for specific fluorophores and Stokes shifts. Individual images are normally taken successively with a black and white camera for each filter cube, called channel. All channels are combined to a false color image by assigning colors to the the channels, normally colors similar to the emission color are used.(109; 110)

Another important property of fluorophores is the quantum yield and photo stability. Quantum yield gives information about how much light is emitted from a fluorophore. It is defined as the ratio between emitted and absorbed photons, quantum yields around 0,1-0,2 are considered well fluorescent. Photo stability gives information about how long a fluorophore can be excited. A fluorophore gets less and less excitable with exposure time and eventually gets destroyed losing the ability to emit light, referred to as bleaching.(109)

Commercially available fluorophores have been improved over the last decades resulting in high quantum yields and strong photo stability over prolonged exposure times. Furthermore a wide range of colors are available today. Molecular probes (Invitrogen) offers 19 colors in their Alexa Fluor dye series. Figure 1.9 shows the emission wavelength of those dyes. Even though a wide range of colors is available it is important to have in mind that simultaneously visualization of more than three or

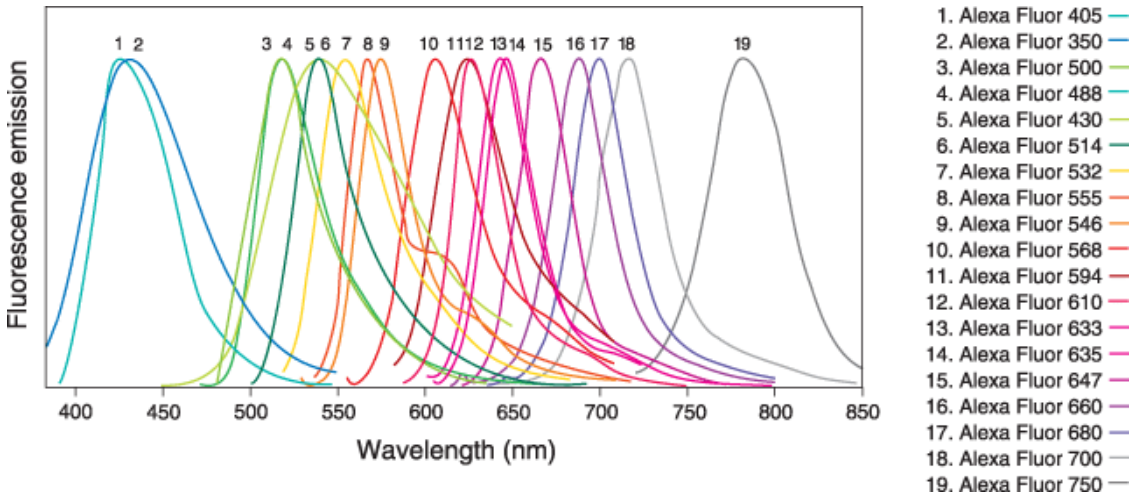

Figure 1.9: Overview of 19 different fluorophores from the Alexa Fluor series with the according emission spectra.(110)

four dyes in one image is difficult since the exication and emission wavelengths might overlap. Due to this reason normally wavelengths far apart from each other are used, red, green and blue are the most commonly ones.(110)

Fluorescent microscopy has enabled researches to study processes and mechanisms ongoing in cells in great detail. Improvements in the dyes have simplified the technique and made it one of the standard methods in cell biology. One drawback when using epifluorescence microscopy is the fact that overlaying structures are difficult to distinguish from each other and images might occur blurry. This is due to a fairly deep focus resulting in a decreased resolution in the z-direction. More advanced illumination and image techniques such as laser scanning confocal microscopy (LSCM) overcome this problem by focusing the light at a narrow position in the sample. This highly increases the z-resolution and minimizes the blurring effect, giving rise to sharp detailed images.(109)

Chapter 2

Materials and Methods

2.1 Bioreactor

2.1.1 Bioreactor design

The whole bioreactor was designed using the academic version of the 3-dimensional modeling environment Solid Edge V17 (UGS Siemens, Germany). The different parts of the bioreactor were designed in the *Part environment* and assembled in the *Assembly environment*. 2-dimensional drafts for machining the elements were generated in the *Draft environment*. The advantage of having a complete 3-dimensional model of the system is that it is possible to investigate functionality and consistency directly during the design process. In this way it is possible to identify problems at an early stage and easily modify the design to account those problems. FIGURE 2.1 shows a rendered image of the complete assembled 3-dimensional bioreactor model. The drafts for the different parts can be found in the Appendix A.

The bioreactor consists of four main parts as depicted in FIGURE 2.2: A culture chamber, a mechanical motor unit, a heating system and a electronic control unit.

The culture chamber is designed to support sterile working techniques and simplify sterilization processes. Therefore all metal parts of the culture chamber are produced in stainless steel, in order for it to autoclave them prior to use. Polystyrene is used for the plastics parts of the system, and can be sterilized with ethanol. 9 individual culture wells are integrated into the culture chamber to allow the cultivation of 9 samples simultaneously. Each culture well is 70 mm long, 16 mm wide and 15 mm high and should be filled with approximately 12 ml culture media.

A channel is integrated into the underside of the culture chamber. Warm water flowing through this channel is used to heat the culture wells to 37°C. The channel is wound around the individual culture wells to achieve a homogeneous heat transfer. The liquid in the channel is not in direct contact with the upper culture side of the culture chamber and is therefore not a risk of contamination. To seal the channel at the rear side several approaches were tried, and in the end the most efficient method was to glue a plastic plate on to the bottom. The heating characteristic and elements of the system are described in 3.1.2.

Metal shafts couple the mechanical motor unit and the scaffold holder inside the

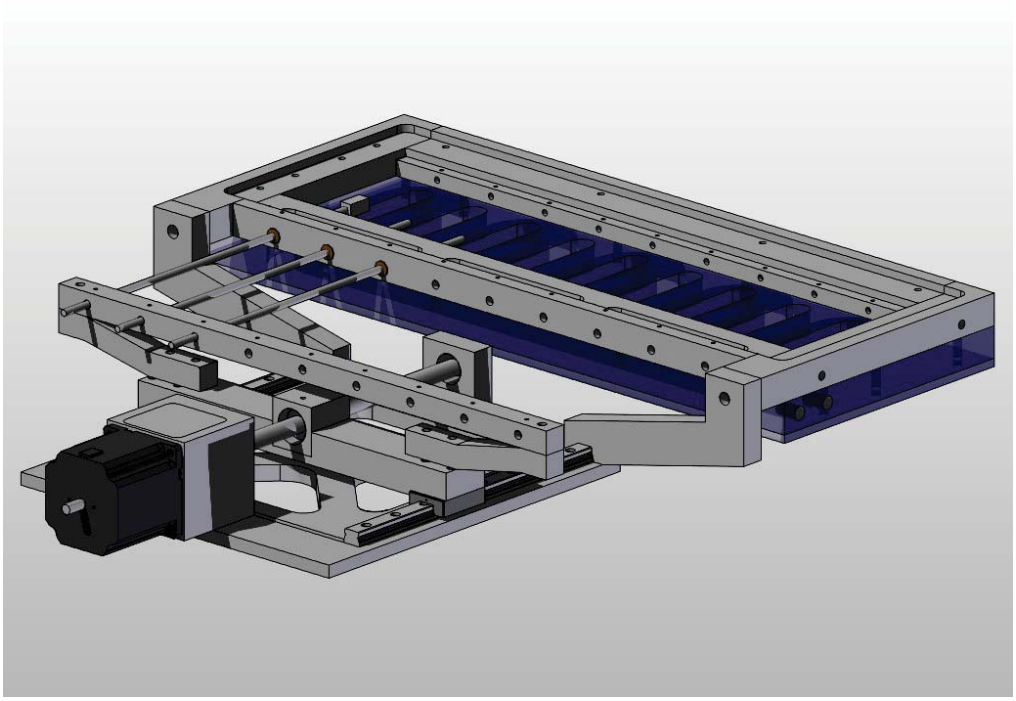

Figure 2.1: Rendered view of the 3-D computer model of the bioreactor.

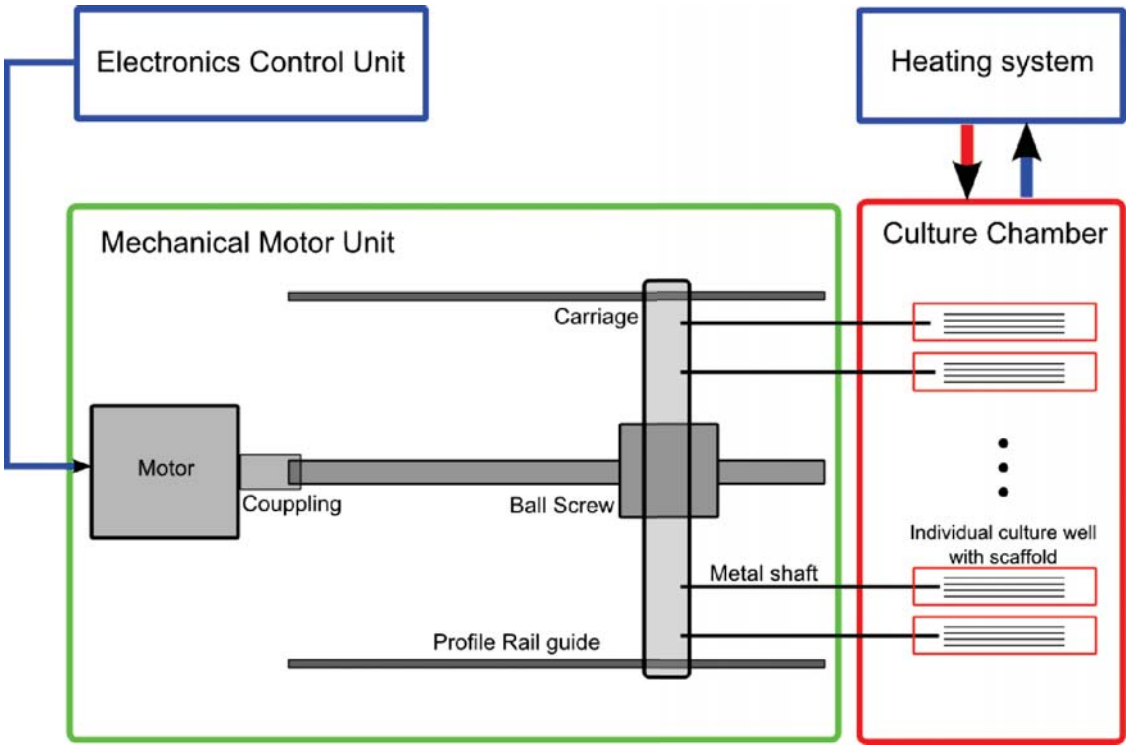

Figure 2.2: Schematic overview of the bioreactor system showing the main parts of the system.

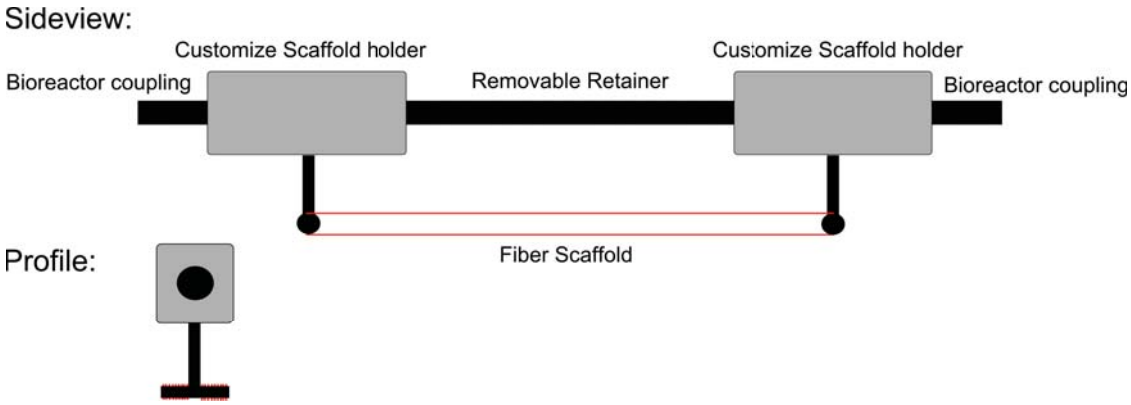

Figure 2.3: Customized scaffold holder for the bioreactor system. The design can be altered to fit different materials. The retainer in the middle simplifies the placement of a scaffold into the bioreactor and is removed after mounting in the reactor.

culture wells and allow the displacement for mechanical stimulation. Each scaffold holder can be coupled individually which allows a free selection of samples that undergo mechanical stimulation. The customized scaffold holder with the attached retainer is shown in FIGURE 2.3. The metal shafts are also one of the major risk factors of contamination during cell culture experiments, since those shafts are constantly changing position from inside the culture chamber to the outside during stimulation. The original plan was to minimize this risk by integration of a chamber containing ethanol which the shafts have to pass through before coming into the culture chamber. The problem is to find suitable seals to avoid ethanol from entering the culture chamber. Due to this reason the ethanol chamber is currently not used. The metal shafts are support by friction bearings, iglidur A500 (A500FM-0405-04 Igus, Germany). The advantage of the iglidur A500 bearing is that it can withstand high temperatures and can stay in place during autoclaving, furthermore it is approved by the FDA for the use in food production machinery.

Elements of the mechanical motor unit are manufactured in aluminum to reduce the weight of the system. A stepper motor (ST5709-K1V05435 Nanotec, Germany) is used to generate a rotational movement. The advantage of a stepper motor is that an external measurement system is not necessary to get information about the position. Since the motor operates in discrete steps it is possible to count the steps and calculate the distance. The selected motor has a a small step angle ($0,9°$) and a high torque (1,91 Nm) to generate movement.

The rotational motion of the the motor is converted into a translational displacement of a carriage using a ball screw spindle. The ball screw spindle (SDS 10x2R 205/240 G9 S-L SKF, Sweden) is connected to the motor via a Controlflex®coupling (CPS 15,1/6/6,36 Schmidt-Kupplungen Gmbh, Germany) and supported by two ball bearings (626-2RSL SKF, Sweden). Two profile rail guides with carriages (LLMHS 12 1 TA T0-200 SKF, Sweden) are positioned on each side of the spindle, in this way the risk of unbalanced movement is minimized. When the motor turns, the carriages are moved and the connected metal shafts transfer the movement into the culture

chamber to stimulate the cells on the deforming scaffold.

2.1.2 Bioreactor electronics and control systems

The bioreactor uses a specially developed electronic control unit. It was decided to use a home-built system with a micro controller instead of using a commercial solution that is coupled to a computer. The advantage is that the system can be customized on the hardware level to allow optimization for specific task and that no permanent connection to a computer is required. Once the programmed code is loaded onto the micro controller it can operate independently and does not require a connection to a computer.(29)

It was decided to use a ATmega32 (Atmel, USA) micro controller because it has a well-proven programming environment and it is possible to use the programming language C instead of assembler code. The program is loaded on to the controller with a AVRISP mkII device (Atmel, USA) via the serial programming interface (SPI). The source code for the current program can be found in the appendix C. The ATmega32 is a low power 8-bit RISC controller that can operate at speeds up to 16 MhHz, at the moment it operates at 8 MHz. Due to the RISC architecture, that means that 8 million operations can be performed per second which is more than sufficient for the current program tasks. The controller has most of the necessary periphery directly integrated on the chip, including timer, counters, analog digital converter, comparators and interfaces. It also provides 32 free programmable digital input/output (I/O) lines.

Figure 2.4 shows a flow chart of the signals and elements of the whole electric circuit. The voltage for the system is provided by a dual tracking DC power supply (6302A, Topward, USA) and a LF7805 and LF33 voltage controller (STMicroelectronics, USA) are used to regulate the voltage for the micro controller. Besides the interfaces directly supported by the controller a RS232 interface is integrated in the circuit via a MAX232 controller chip (Maxim Dallas Semiconductors, USA). This interface can be used to couple the controller to a computer and allows online interactions with the program. The interface for MMC/SD memory cards is integrated but currently not in use. Most of the I/O ports are available as multipoint connectors in groups of 8 ports. The circuit design is based on the reference design from the RoboterNetz internet portal (www.robtornetz.de).

A second circuit board is use for the stepper control because high voltages (30 V) and currents (4 A) are used in this part which otherwise could interfere with the signals on the micro controller board. The L297 stepper driver (STMicroelectronics, USA) modulates the signal required by the stepper motor. It gets three digital input signals from the micro controller: enable for the motor power, direction of rotation and a step signal. Each time a step signal is sent the chip generates a signal to turn the motor. Two L298 dual full-bridge driver (STMicroelectronics, USA) are used to convert the modulated low power signal into a high power signal that can drive the stepper motor. High speed diodes (BYV27-200, Vishay, USA) are used to allow a fast decline of currents and high step frequencies. A current control feedback system is integrated in the system that should permit the application of high voltages

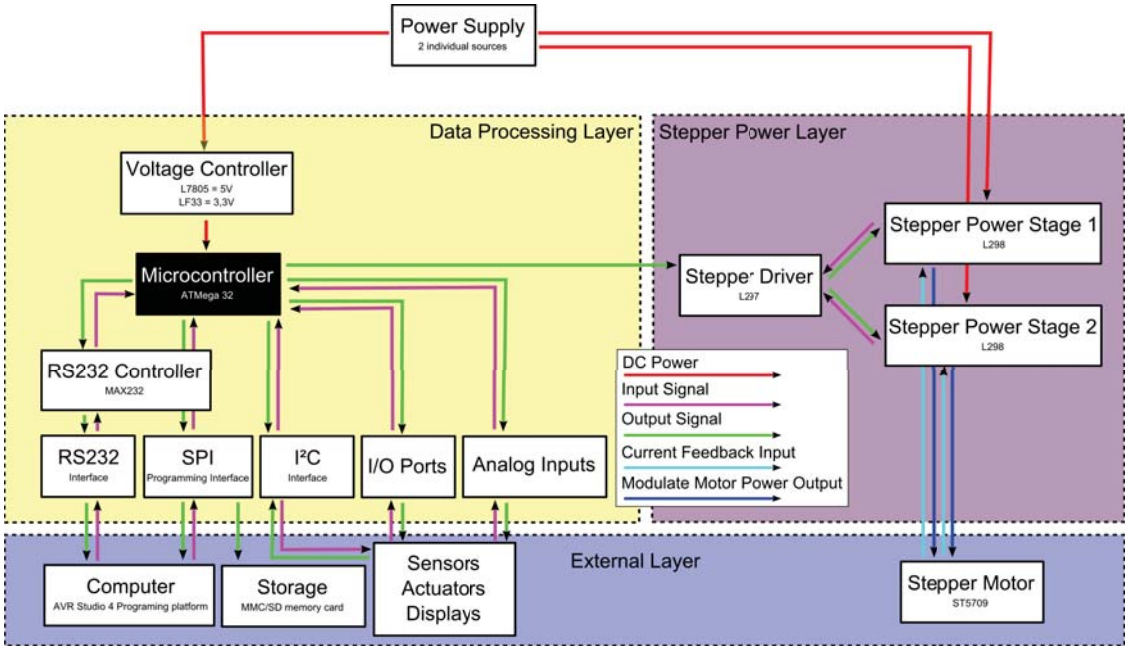

Figure 2.4: Flow chart showing the different parts of the electronic control circuit.

without overloading the motor. By using high voltages it is possible to increase the step frequency without severely decreasing the torque. Currently this system is not operational and the error could not be identified after several control measurements. The electronic design is based on the reference design described in the application notes for the two chips provided by STMicroelectronics.

All electronic parts were obtained from ELFA (Sweden). The electronic circuits and printed circuit board (PCB) layouts can be found in the Appendix B. The electronics were designed and mapped in Eagle 5.3.0 (CadSoft Computer Gmbh, Germany). The PCBs were produced with a special milling machine by Hans Odelius, Department of Applied Physics, Chalmers University of Technology.

Figure 2.5 shows a flow chart diagram of the current micro controller program. The program is written in C using the free AVR development environment AVR Studio 4 (Atmel, USA). In a first step all required parameters and variables are defined and initialized. Afterwards a timer is started and the main program runs in an infinite loop.

The main program has three parts: a clock to measure the time, a generator for the motor steps and a part where the experimental setup is defined. The clock is used to count the time between stimulations and could later also be used for the longterm program control. Individual counters are programmed for seconds, minutes and hours. The generator for the motor steps has a variable that defines the frequency with which steps are generated. Additionally it counts the steps and half turns of the motor. A step is generated by setting the digital output PD3 to low. The experimental setup part controls the direction of movement, the number of executed turns and thus the elongation distance and the stimulation duration. This part needs to be adjusted for

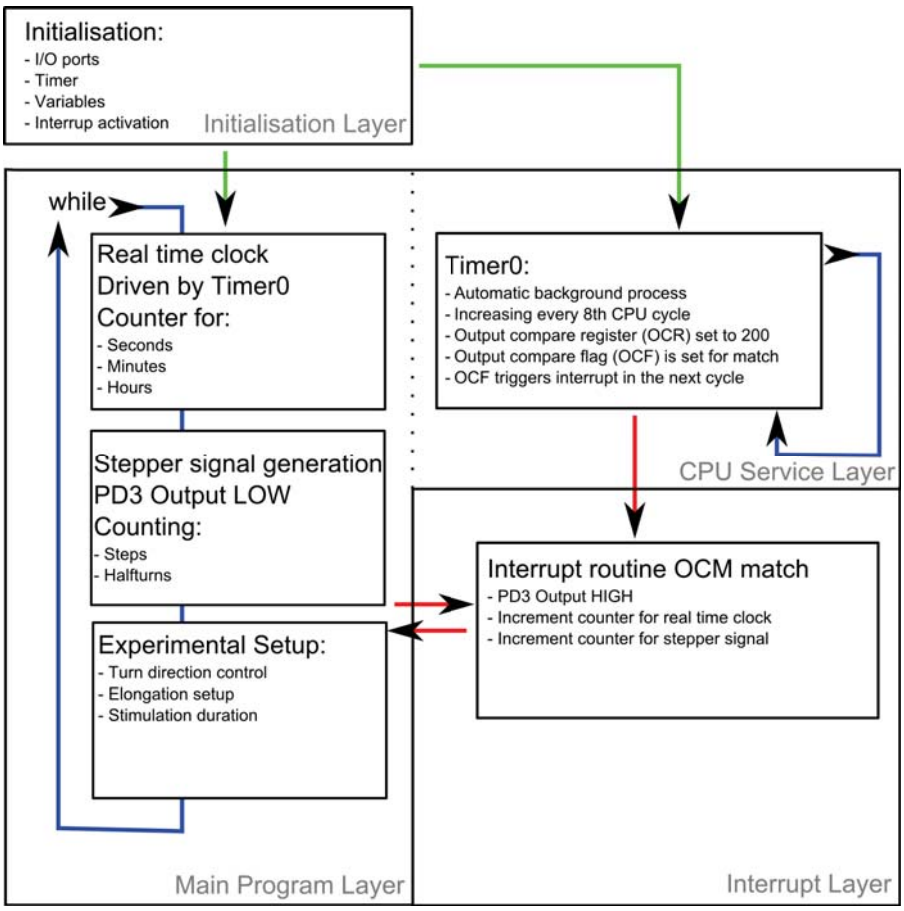

Figure 2.5: Flow chart showing the general operation of the program that controls the bioreactor.

individual experiments.

The timer is set to be incremented at every eighth CPU cycle and compared constantly against the value in the compare register (currently 200). If both values are equal the output compare flag is set which triggers an interrupt in the next cycle and the timer is set to 0. This process is repeated constantly. The interrupt frequency with the current settings (8 Mhz, every 8th cycle and compare register set to 200) is 5000 Hz. In the interrupt routine the step signal is reset to high (deactivation) and the counter for the clock is incremented.

2.2 Bioreactor characterization

2.2.1 Precision measurement

The precision measurement for deflection of the motor-controlled rods was performed using a light microscope (DM4000M, Leica, Germany) to image the position of the end of the rod at different time points in the cycle. For the measurements, the culture well was detached from the bioreactor and the stainless steel frame was placed on the

sample table of the microscope. The motor unit was leveled to the desired height to connect it to the frame. One of the metal shafts was used to monitor movement and position. By utilizing the front edge of the metal, it was possible to achieve high accuracy for the measurement. Four different measurements were performed, three to measure the repeat accuracy and one to measure the step width. All measurements were repeated three times to gain statistical certainty.

Repeat accuracy was measured by cyclic movement, 5 motor turns in one direction, direction change and 5 motor turns back to the original position. When the direction was changed the motor paused for 5 seconds to take an image, images were always taken at the first position. The displacement of 5 motor turns (400 steps) equals approximately 10 mm. Acceleration and deceleration ramps as well as number of cycles were varied during the three experiments.

For the first experiment the number of cycles was set to 4 and the acceleration ramp in the program was parameterized to increase from a step frequency of 14 to 140 steps per second. The frequency was increased non-linearly after each step according to this formula: $f = \frac{1000}{n}$ where n is increased by one after each step. Images were taken at the beginning and after each cycle, 5 images in total.

In the second experiment similar acceleration ramps were used but the number of cycles was increased. The system was run for 5 minutes, images were taken before starting, after the first cycle and at the end, 3 images in total.

The third experiment investigated the influence of the acceleration ramps, the parameters were changed to increase from 10 to 140 steps per second. Otherwise the experiment was similar to the first one.

Step width was measured and compared to the theoretically calculated value. To measure the step width one image was taken at the start position, then the motor turned 100 steps and a second image was taken. From the distance between both positions the step width was calculated. The step frequency was fixed at 1 step/second.

Images were processed with imageJ 1.41 O (NIH, USA), distances were measured in pixels and converted into micrometers using the objective calibration data stored in the microscope software. Statistical calculations were performed with SigmaPlot 10.0 (Systat Software Inc., USA).

2.2.2 Temperature control and stability

Measurements for the bioreactor heating system were conducted to get information about the heating characteristics and temperature stability. The culture chamber was placed on styrofoam for the measurements and the motor unit was not connected to the chamber. The whole experiment was performed under a running laminar flow hood (LaminAIRn safety class 2 S2010 1.5, Holten, Denmark) to simulate conditions for later application. The heating system of the culture chamber was connected to a submersible water pump (Biltema, Art. 25-980, Sweden), which was placed in a glass beaker filled with 1,9 l tap water sitting on a hot plate (RCT basic, IKA Werke Gmbh, Germany). The water was preheated to 40°C before the measurement was started, the reservoir water temperature was controlled with the internal feedback loop integrated to the hot plate. Therefore the associated temperature probe was

placed into the beaker.

Heating characteristics and temperature stability were measured by filling the culture wells in the chamber with water (10ml/well) and placing a temperature probe in one well. As a temperature measurement system, an DMM M-3890D USB digital multimeter (Voltcraft, Germany) with an attached Pt100 resistor thermometer (Voltcraft, Germany) was used. The water pump was operating at 5V creating a consistent flow. The combined volume of water in the tubing and the chamber was 300ml.

For the first 20 minutes the temperature was measured every minute. Afterwards the interval was decreased to 10 minutes. After 60 minutes the temperature was only measured hourly until the experiment was stopped after 3 hours. At all time points the temperature in the culture well and the water reservoir temperature was noted.

In an second experiment the hotplate temperature was increased step-wise. The temperature was measured at the beginning and after one hour when the system had reached equilibrium. The different hotplate temperature were 42, 44, 46 and 50°C.

2.3 Fiber characterization

The two different fibers used in this study are Creora® H-100 and Creora® C-100 (Hyosung Corporation, South Korea). The fibers were supplied on large bobbins.

2.3.1 Light microscope images

Light microscopy images of the fibers were taken to investigate fiber diameter and micrometer size surface topology. The samples were prepared by twisting dry fibers around rectangular glass coverslips. The fibers were slightly stretched during the process to keep them straight on the glass but stretching was minimized as much as possible.

Images were taken using the Leica microscope in differential interference contrast (DIC) mode. The magnification was varied, 10x, 20x, 50x and 100x, to study different feature sizes. For each fiber type images were taken at several separate spots.

2.3.2 Scanning electron microscope images

Samples were fixated on a sample holder but neither aligned nor stretched. The samples were sputter coated with a 10 nm layer of gold to enhance the conductivity. The magnification and voltage were adjusted individually and are indicated in the images. The images were taken with a JSM (Jeol Ltd., Japan) SEM system by Hossein Agheli, Department of Applied Physics, Chalmers University of Technology.

2.3.3 Fourier transform infrared spectroscopy

FT-IR spectra were measured in ATR mode using a FTS 6000 spectrometer (Bio-Rad, USA) with a horizontal ATR module (PIKE Technologies, USA). Different ATR

crystals were tested, namely ZnSe, Ge and Silicon, but for the final measurements a ZnSe crystal was used. Spectra were recorded from 4000 cm^{-1} to 700 cm^{-1}, using a liquid nitrogen cooled mercury cadmium telluride (MCT) quantum detector. A background spectrum was recorded prior to sample measurements.

Samples were measured as bundles of fibers placed parallel on top of the crystal and clamped down with the integrated clamp. This was necessary to enhance the contact between the material and the crystal. Each spectrum is the result of 20 accumulated scans. The crystal surface was cleaned with ethanol between samples.

The data was analyzed with Win-IR Pro 2.6 (Bio-Rad, USA) using manual baseline correction, Boxcar smoothing with averaging over 13 data points and manual peak assignment.

2.3.4 X-ray photoelectron spectroscopy

The fiber samples were twisted around a metallic sample holder and placed inside the vaccum chamber. The chamber was evacuated over night until ultra high vacuum was reached. A monochromatic x-ray beam with a photon energy of 1486 eV was used for excitation. The area of excitation was approximately 1mm in diameter. In a first measurement a complete spectrum with binding energies ranging from 0 to -1300 eV at a resolution of 0,8 eV was recorded for each fiber type. Additionally high resolution spectra (0,125 eV) were recorded for the valence electron band (0 to -35 eV). The polymer fiber samples were charging during analysis. To compensate for the charge, an electron gun was used to neutralize the charging until the start of the valence band was positioned at 0 eV. The system used for XPS measurements was a PHI5000 (Physical Electronics, USA). Analysis of the spectra and the calculation of atomic ratios were performed directly in the PHI software. The XPS spectra were obtained by Lars Ilver, Department of Applied Physics, Chalmers University of Technology.

2.4 Cell experiments

Water was deionized and purified using a MilliQ plus (Millipore, USA) system. Phosphate-buffered saline (PBS) was prepared by dissolving one tablet (P4417-100TAB, Sigma-Aldrich, USA) per 200ml milliQ water. PBS was sterilized by autoclaving and stored at 4°C.

2.4.1 Media composition

Different media compositions were used as indicated. Media was stored at 4°C and preheated in a water bath to 37°C before application.

Growth Medium (GM): Dulbecco's Modified Eagle's Medium high glucose 4,5 g/l with Sodium Pyruvate without L-Glutamine (PAA Laboratories, Austria) + 1% L-Glutamine (Invitrogen Corporation, USA) + 1% Penicillin/Streptomycin (Invitrogen Corporation, USA) + 10% Fetal Bovine Serum (FBS)(PAA Labratories, Austria)

Differentiation Medium (DM2%): Dulbecco's modified eagle medium high glucose

4,5 g/l with Sodium Pyruvate without L-Glutamine (PAA Laboratories, Austria) + 1% L-Glutamine (PAA Laboratories, Austria) + 1% Penicillin/Streptomycin (Invitrogen Corporation, USA) + 2% Horse Serum (Invitrogen Corporation, USA)

Growth Medium CO_2 independent (GM CO2): CO_2-Independent Medium (Invitrogen Corporation, USA) + 1% L-Glutamine (PAA Laboratories, Austria) + 1% Penicillin/Streptomycin (Invitrogen Corporation, USA) + 10% Fetal Bovine Serum (PAA Labratories, Austria)

2.4.2 Cell maintenance

All cell experiments were performed under sterile conditions using aseptic techniques in a dedicated cell laboratory. Cells were cultured at 37°C with 5% CO_2 unless stated otherwise. C2C12 (European Collection of Cell Cultures, ECACC, 91031101, United Kingdom) cells were used at different passage numbers (17-40), cells were maintained over the whole time of experiments (5 months) and were always passaged prior to reaching confluence. They were cultured in T-75 flasks (LAB) with 10ml GM, at a seeding density of approximately 100.000 cells/flask. One T-75 flask gave rise to around 8-10 million cells after 5 days.

For harvesting, cells were rinsed with warm PBS first and then incubated with 2 ml 0,25 % Trypsin-EDTA (Invitrogen Corporation, USA) at 37°C for 4 minutes. Trypsin was inactivated by adding 2 ml FBS. To dilute the cells 2 ml GM was added, resulting in a total volumen of 6 ml cell suspension. If cells were seeded for experiments they were counted using a hemocytometer (LAB). In the case cells were only passaged, cell concentration was estimated.

2.4.3 Fixation

Samples were washed with cold PBS once. Cold fixative, 4% Formaldehyde (LAB), in an adequate volume was applied to completely cover the sample. Samples were incubated for 15 minutes at 4°C. Afterwards the fixative was removed and the sample was rinsed three times with cold PBS. Samples were kept in PBS at 4°C and checked regulary to avoid drying until they were stained.

2.4.4 Static cell culture on flat surfaces

Cells were cultured on flat surfaces to study C2C12 cell proliferation and differentiation on an unmodified reference surface. Furthermore those samples were used to optimize staining protocols.

Cells were cultured on glass coverslips or directly on tissue culture polystyrene (TCPS), depending on later use and culture duration. Glass coverslips, 25 mm in diameter, were placed in culture dishes and 3 ml of GM was applied. Cells were seeded at two different densities, 20.000 cells/dish and 100.000 cells/dish. The calculated amount of cell solution was added into the dishes, which was gently shaken for 30 seconds to reach equal cell distribution. Three samples for each density were prepared. The media was switched to DM2% after 48 hours and cells were feeded every third

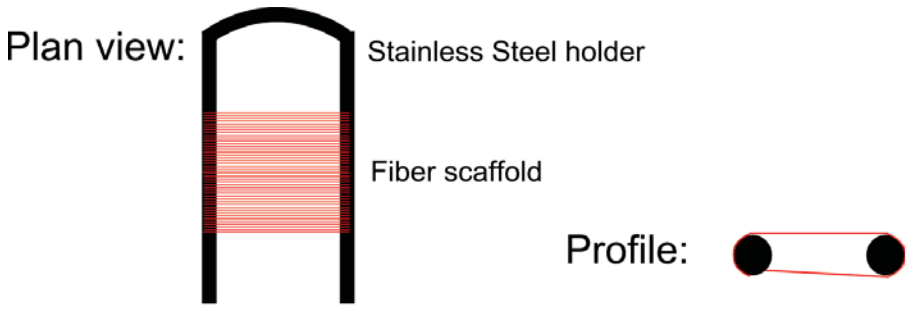

Figure 2.6: Scaffold holder for static cell culture on elastic fibers. Only the cells on the free-hanging fibers on the upper side were used for studies.

day. Samples were fixed after 48h, 96h and 7 days and stained with DAPI and Rhodamin/Phalloidin, according to standard fixation and staining protocol.

To study muscle cell differentiation and muscle fiber formation cells were cultured directly on TCPS to avoid early detachment of cells. Cells were cultured in 6-well plates (TPP, Switzerland), the surface area (9 cm^2) of an individual well is similar to the one of the culture dishes used for the glass coverslips. Since the wells are deeper 4 ml of GM was used. Cells were seeded at a high density, 100.000 cells/well by adding the calculated amount of cell solution into the wells. Again, slight movements were used to ensure an equal cell distribution. The media was switched to DM2% after 48h, cells were fed on day 5, 8, 10 and 12. Samples were fixed and stained after 14 days according to protocol.

2.4.5 Cell culture on fibers under static conditions

Creora®fibers were twisted around a U-shaped stainless steel wire, wire diameter was 1 mm. The design of the holder is shown in FIGURE 2.6. The distance between the two arms of the U was approximately 20 mm. For each sample around 1-2 m fiber material was used. The fibers were slightly stretched during the process to ensure that they would stay in place on the wire. The assembled sample was autoclaved for sterilization.

Cell culture was performed in 6-well plates (TPP, Switzerland), samples were placed in individual wells. 5ml media per well was used to ensure complete coverage of the samples.

Samples were seeded at a density of 100.000 cells/well. First 5 ml GM were applied, afterwards the calculated amount of cell solution was added in the middle of the fiber sample. Light movement was used to ensure an equal distribution of cells and break small air bubbles formed around the fibers.

Samples were switched to DM2% after 4 days and fed every other day. Samples were taken on day 4, 6, 8, 11 and 14. For fixation the samples were transfered in a new well of an additional 6-well plate, thereafter fixation was carried out accordning to protocol. During the process care was taken not to rotate the samples. Staining was performed corresponding to protocol.

C-100 and H-100 were handled identically throughout the whole process.

2.4.6 Bioreactor cell cultures

The first experiment using the bioreactor was designed to test the general usability, cell growth, the mechanical stimulation unit and identify any problems. Three fiber samples in individual wells and six glass coverslips, 9 mm in diameter, placed in one extra well were used. The whole experiment was performed under a laminar flow hood.

The C-100 fiber scaffolds were produced by twisting roughly 1 m fibers around the two scaffold holders separated by the retainer. The distance between the two holders was approximately 30 mm, again the fibers were slightly stretched to make sure that they would stay in place. The complete constructs were autoclaved for sterilization. All surfaces in the culture chamber were wiped with ethanol for sterilization, the culture wells were filled with ethanol for 15min and rinsed with sterile milliQ water. The metal parts and glass coverslips were autoclaved for sterilization.

The whole bioreactor was assembled inside the laminar flow hood and contamination risks were minimized. The heating system was started 2 hours prior to the start of cell experiments to reach steady state conditions. The water reservoir temperature was set to 40°C, resulting in a temperature of 36°C in the culture wells, and the pump was operating at 5 V. Styrofoam was placed under the culture chamber to minimize heat losses. The upper lid of the chamber was closed but not tightly sealed to allow sufficient gas exchange.

The first four wells were used for cell culture and the five remaining wells were filled with sterile milliQ water to achieve high humidity levels in the culture chamber. The fiber scaffolds were attached to the bioreactor and the retainer between the two holders was removed. 12,5 ml GM was preheated in each of the 4 cell wells to 36°C before starting the experiments.

Cell solution was carried from the cell laboratory in a falcon tube and mixed gently before seeding. The seeding density was 450.000 cells/well and the calculated amount of cell solution was added above the scaffold to the media with a syringe. Due to sever liquid evaporation, wells were filled to their original 12,5ml with sterile filtered milliQ water daily.

The first glass coverslip sample was taken after 4 hours and imaged directly with the Leica light microscope using dark field microscopy to control initial cell attachment and survival. Further glass coverslip samples were taken after 24, 48 and 72 hours, those samples were fixed according to protocol.

Mechanical stimulation was tested after 24 hours with one fiber sample. The displacement was set to +6 mm which correspondents to 20% elongation. Due to a software problem the sample was over strechted, displacements went up to +18 mm (60%). Afterwards the sample was detached from the bioreactor and the two scaffold holders were spaced at the initial 30 mm by placing the retainer between them. The other two fiber samples were not stimulated and culturing was stopped simultaneously after 72 hours. Sample two was detached from the bioreactor similar to the first sample, this process involves light stretching (around 10%). Sample three was detached from the bioreactor without placing the retainer between the two holders. In this case the fibers were never streched after cell seeding, the fibers were detached from

the holders afterwards and immersed in PBS. All fiber samples were fixed according to protocol.

2.5 Cell experiment analysis and evaluation

2.5.1 Immunostaining

Immunostaining procedures were carried out similarly for the different samples, the only difference was the selection of antibodies and the amount of solution was adjusted for each sample. Cell membranes were permeabilized with 0,1% Triton-X100 (Sigma-Aldrich, USA) added to the staining soultion.

Cell nuclei were stained with DAPI (1:1000,LAB) diluted in PBS. Actin filaments were stained with Rhodamin/Phalloidin (1:400,LAB) diluted in PBS. Normally both were carried out simultaneously using DAPI(1:1000), Rhodamin/Phalloidin (1:400) and 0,1% Triton-X100 in a combined PBS solution. The samples were taken out of the refridgeerator and the PBS, they were stored in, was aspirated. A suitable amount of staining solution was added to the samples to completely cover them. The samples were incubated at room temperature for 30min and rinsed three times with PBS afterwards. Glass coverslips were mounted on microscope slides using mounting media (Dako A/S, Denmark), other samples were stored in PBS. Samples were stored at 4°C and kept from light.

Myosin heavy chains and α actinin were stained using a two stage antibody staining. Monoclonal Anti-Myosin MY-32 (1:1000, M4276 Sigma-Aldrich, USA) and monoclonal Anti-α-Actinin EA-53 (1:1000, A7811 Sigma-Aldrich, USA), both antibodies produced in mouse, were used. The appropriate amount of antibody was diluted in solution with 3% skimmed milk (Scharlau microbiology, Spain) and 0,1% Triton-X100 in PBS. Fluorescent secondary antibody against mouse (1:2000 Alexa594, Invitrogen, USA) or (1:2000 Alexa488, Invitrogen, USA), diluted in PBS with 3% skimmed milk were used for visualization.

Samples were incubated for 1,5 hours at room temperature with primary antibodies. Rinsed three times with 3% skimmed milk PBS solution to block the samples and then incubated 1 hour at room temperature with secondary antibody. Afterwards samples were rinsed three times with PBS. In the case both, myosin heavy chains and α actinin, were stained in the same sample the procedure was repeated for the second set of antibodies. DAPI and Rhodamin/Phalloidin staining was carried out after antibody staining.

2.5.2 Fluorescent microscopy imaging

Fluorescence microscopy images were taken with an upright fluorescent microscope (Axioplan 2, Zeiss, Germany) with a black and white digital camera module (AxioCam, Zeiss, Germany). Image acquisition and microscope control was carried out with AxioVision software 4.2 (Zeiss, Germany). Depending on the sample modalities one of the following objectives was used: Plan Neofluar 10x/0,30, Plan Neofluar

20x/0,50, Plan Neofluar 40x/0,50, Epiplan 50x/0,80, Achroplan 40x/0,80 and Achroplan 100x/1,00. The two Achroplan objectives are water immersion objectives which were used for samples kept in PBS.

Three different fluorescent filter cubes were used. Filter set 1 DAPI (488001-0000, Zeiss, Germany), Filter set 10 Alexa488 (488010-0000, Zeiss, Germany) and Filter set 20 Rhodamin and Alexa546 (488020-0000, Zeiss, Germany). The excitation time for the different channels was optimized for each sample individually to achieve high contrasts and image quality without bleaching the sample. After image acquisition the channel specific histogram was adjusted, using the integrated functions in AxioVision, to improve image quality further. Images were saved in their native *.zvi format and exported as *.png images for later use. The image spots on the samples were chosen manually.

Chapter 3

Results

3.1 Bioreactor

3.1.1 Precision testing

Positioning precision and repeat accuracy of the bioreactor system were measured to evaluate the potential of the system and test the interplay of the mechanical and electric components.

FIGURE 3.1 shows a representative series of images from the first experiment to explain the general measurement setup. Distance X was measured for all five positions, marked A-E. The first position was excluded from the measurement because there was an initial offset due to the programming. This offset does not represent an error in the precision of the system and could be avoided by software modifications.

The results from the first repeat accuracy measurement are shown in TABLE 3.1(top). The maximum calculated standard error is 31 μm, for a total moving distance of 10 mm. Decreasing the speed of acceleration and deceleration in the third experiment resulted in a decrease of the standard error, data shown in TABLE 3.1 (bottom). Furthermore the error is more consistent through all three repetitions of the experiment. The maximum standard error for these parameters is 13 μm.

The second experiment to measure the error for a higher amount of cycles (5 minutes) failed due to software problems. After several cycles the system stopped changing the direction at the end of a cycle. This error was not reproducible and occurred randomly.

The fourth experiment was designed to measure the displacement per single step

Sample Nr.:	1	2	3
Std.Err Exp. 1 [μm]:	10	29	31
Std.Err Exp. 3 [μm]:	13	13	13

Table 3.1: Standard Error for repeat accuracy measurements. Fast acceleration ramps in experiment 1 increase the error compared to slower ramps in experiment 3. The first cycle was excluded from the calculation.

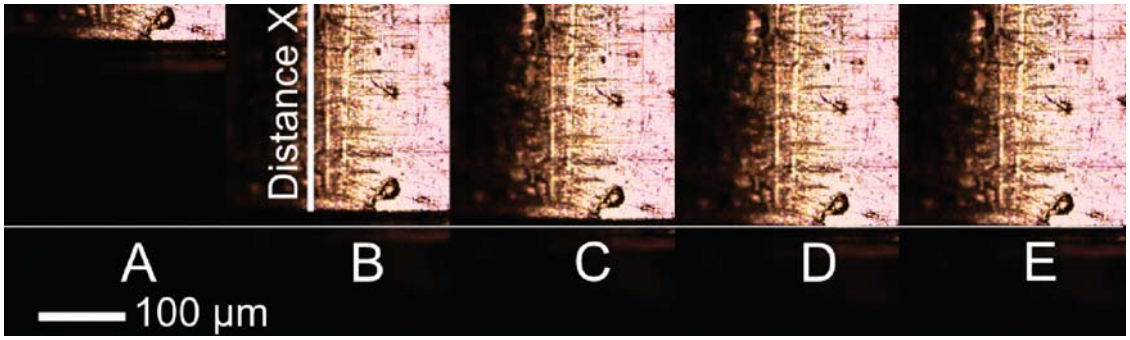

Figure 3.1: Repeat positioning accuracy measurements, combined image with images taken after each cycle as indicated with an unchanged field of view. A large offset between image 1 and 2 is visible which is not considered for later calculations, the offset in the other images is considerably smaller.

of the motor. The mean value is 489 μm with a standard error of 7 μm for 100 steps. The experimental step width was calculated according to Equation 3.1 resulting in an experimental mean step width of 4,89 μm. The theoretical value is defined by the ball screw pitch and can be calculated according to Equation 3.2. The difference between the theoretical and experimental value is 0,11 μm per step.

$$\text{Step width} = \frac{\text{Distance}}{\text{Number of steps}} = \frac{X\mu m}{100} \tag{3.1}$$

$$\text{Step width} = \frac{\text{Ball screw pitch per turn}}{\text{Number of steps per turn}} = \frac{2000\mu m}{400} = 5 \tag{3.2}$$

3.1.2 Temperature control and stability

The temperature stability and heating characteristics of the bioreactor were measured to gain information about their suitability for cell culture. Temperature stability is essential for cell culture where small temperature variations in particular to higher temperatures can rapidly kill cells by denaturing proteins.

Figure 3.2 shows the heating characteristic of the bioreactor. It displays temperature over time for both the liquid in the culture well and the water reservoir. The water in the reservoir was preheated to 40°C and dropped initially to 37°C when the pump was started due to heat losses. The internal feedback loop of the hotplate stabilized the temperature in the water reservoir and heats it up again to 40°C over time.

The bioreactor was at room temperature (23°C) at the beginning of the measurement. The warm water pumped through the reactor heated it up. It took approximately 50 minutes till the liquid temperature in the well reached a steady-state at 35°C. The measurement showed that the temperature is stable and does not change anymore. The measurement was stopped after 3 hours.

The offset between the water reservoir and well temperature was 5°C which is due to heat losses in the system. A second measurement, data not shown, measured

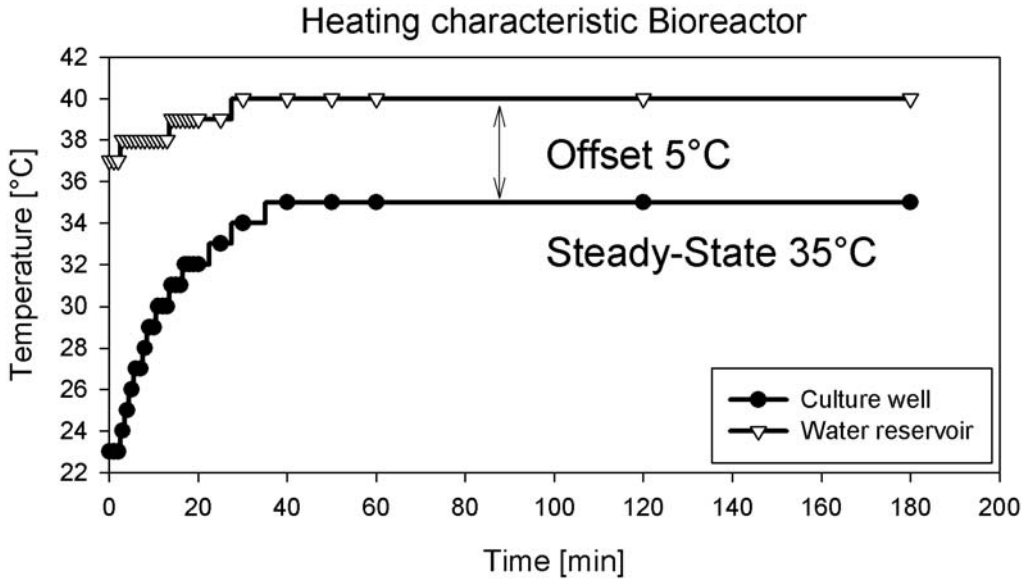

Figure 3.2: The graph shows the heating characteristic of the culture chamber in the bioreactor. The temperature of the water reservoir drops at the beginning since heat was transfered to the chamber. The system needs around 50 minutes until it reaches a steady state. The offset between the culture well and the water reservoir is 5°C and is due to heat losses in the system.

the offset at increasing water reservoir temperature. The offset increases with higher temperatures, up to 11°C for a water reservoir temperature of 50°C.

For cell culture application the water bath should be set to 42°Cwhich correspondents to a temperature of 37°Cin the culture well. The systems needs around one hour to reach the temperature and is stabilized.

3.1.3 Sterilization procedure

Sterility is essential for the bioreactor system to get reliable data from cell experiments. The results presented here only show a starting point to investigate sterility issues of the bioreactor system and are not suitable for final assumptions. It might be necessary to further optimize sterilization methods and the bioreactor assembly process.

The stainless steel mainframe from the culture chamber can be autoclaved without complications. The friction bearings can stay in place and are not affected by autoclaving. The plexiglass parts were cleaned with 70% ethanol which should be sufficent for removal of many contaminats but not all. Ethanol was used instead of autoclaving because the heat might result in deformation of the plexiglass, furthermore it is not clear how the glue between the plates would withstand the heat. Other elements that come in contact with the culture chamber, the metal shafts and scaffold holders are manufactored in stainless steel and were autoclaved.

Another high risk of contamination is the assembly process. Working under a laminar flow hood decreased but may not eliminated the risk. The problem was that

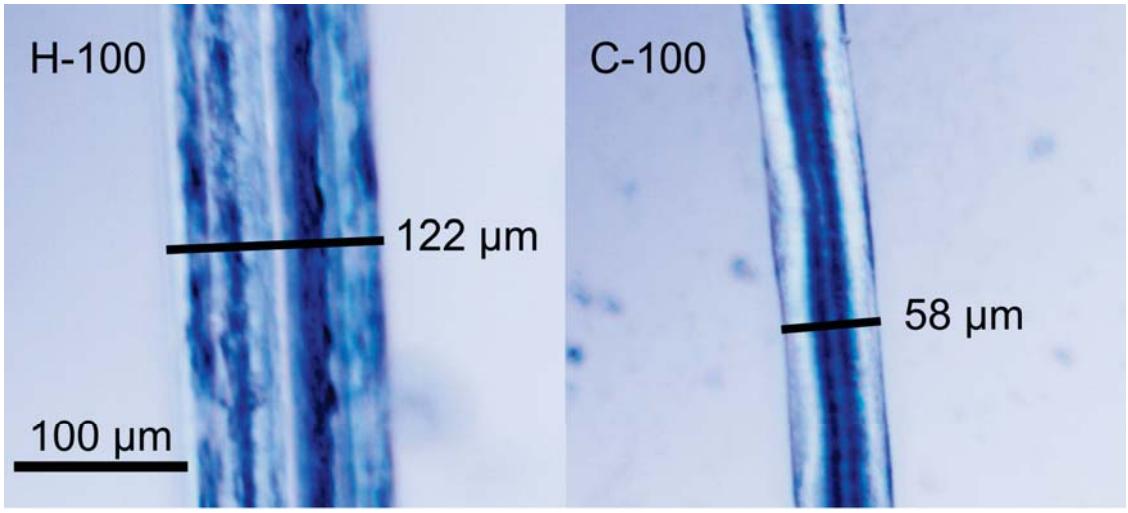

Figure 3.3: Comparison of fiber diameter for H-100 and C-100 fibers. Bright field images at 10x magnification. Both fibers clearly differ in diameter with H-100 being around 120-150 μm and C-100 being around 50-60 μm.

the different parts needed to be placed to the correct positions and most of them needed to be screwed together. By touching and the usage of tools potential sources of contaminants were introduced to the system.

The first cell experiments with the bioreactor did not show obvious signs of infections after 72 hours. It has to be noted however that possible contaminations might be suppressed by the presence of antibiotics in the culture media and that no thorough analysis for infections were performed.

3.2 Fiber characterization

3.2.1 Fiber shape and topography

In a first examination the shape and topography of the C-100 and H-100 Creora®fibers were compared with each other.

Figure 3.3 shows a bright field image at 10x magnification for each fiber type. The fiber diameter is indicated in the images, C-100 fibers are approximately 60 μm and H-100 fibers 120 μm in diameter. This observation was confirmed at higher magnifications, images not shown here. That means that H-100 are around twice as thick as C-100 fibers. Besides the fiber diameter, it is not possible to conclude anything about fiber shape and topography from the light microscope images.

Therefore scanning electron microscope (SEM) images were taken for both fiber types. Figure 3.4 shows images of the fibers at different magnifications. It can be observed that individual C-100 fibers have circular cross-sections and tend to twist around each other. The twisting might be a result of the sample preparation since the fibers were not wrapped around a slide to achieve fiber alignment. The fibers were not attached to each other and could be separated again. It should be noted

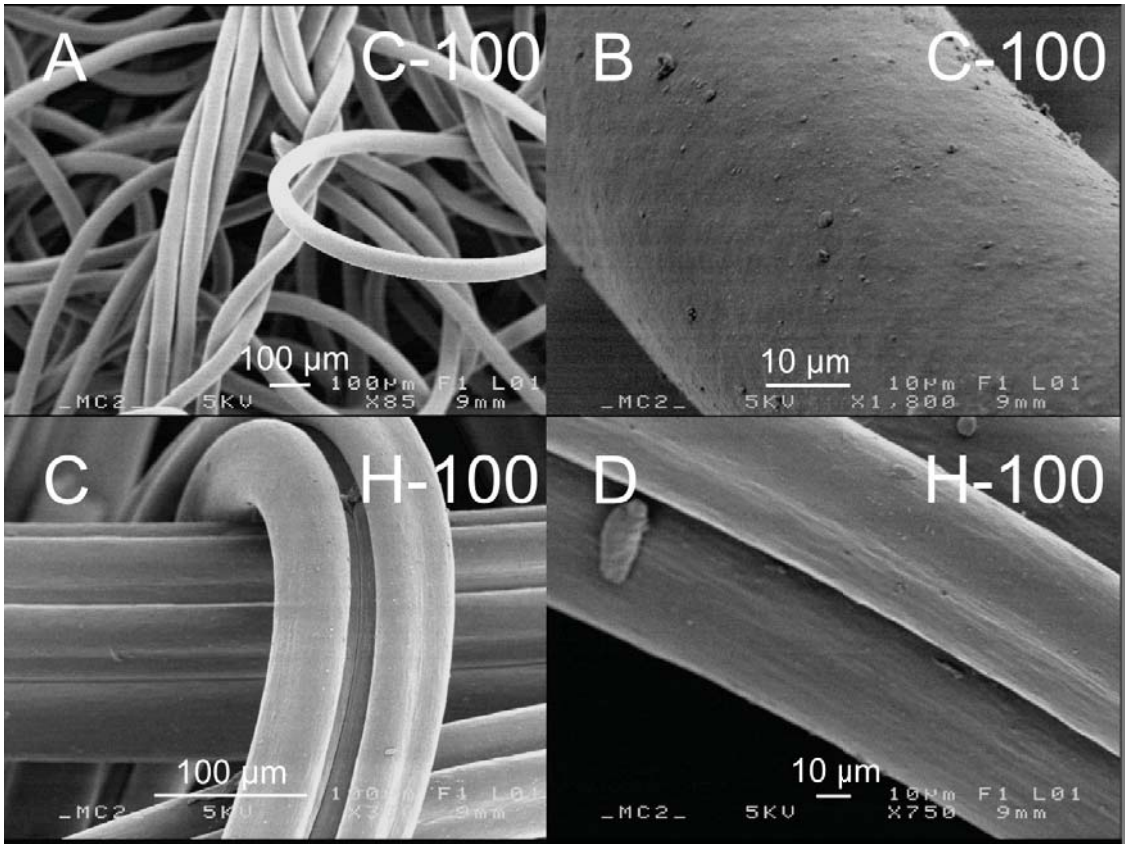

Figure 3.4: Comparison of fiber surface topology and form. SEM images at different magnifications. A) C-100 fibers are twisted around each other but single fibers have a circular round shape. B) Surface defects on C-100 fibers. C) H-100 fibers show a distinct 3-dimensional profile and seem to be composed of several fibers. D) Surface defects on H-100 fibers.

that twisted fibers were not seen in samples where the fibers are aligned and slightly stretched which reflects the way they are used during cell culture. Furthermore small defects are visible on the fiber surface at higher magnification. The defects are 1 μm or less, with a wide size distribution and random positioned on the surface.

The topography and shape of the H-100 fibers differs distinctively from C-100 fibers. It seems that one H-100 fiber is combined from 3 to 5 fibers resulting in a cross-section that is not circular shaped. The shape of the H-100 fibers are much more complex having grooves and ridges. From the available SEM images it is difficult to definitely define the exact shape of the cross-section. Beyond the differences in cross-section shape, H-100 fibers also differ slightly in surface topography. Similar defects in the surface as for the C-100 fibers are visible but there are also larger defects present on H-100 fibers ranging up to several μm.

3.2.2 Fourier transform infrared spectroscopy

FT-IR spectra were measured in ATR mode and used to analyze the chemical composition of the fibers. Figure 3.5 and 3.6 shows the whole recorded spectrum (4000-700

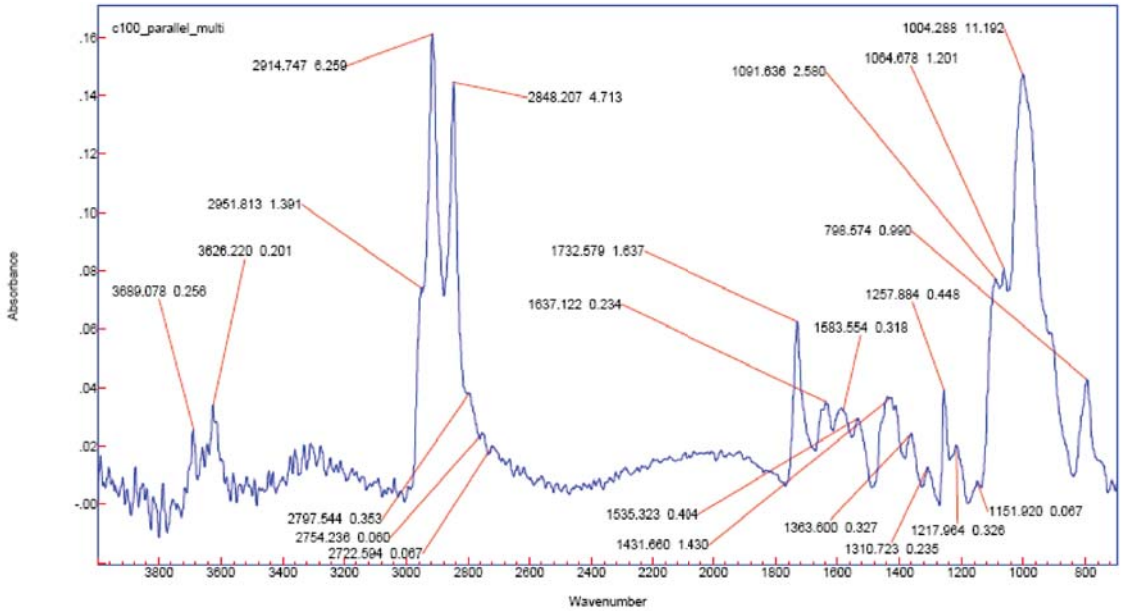

Figure 3.5: FT-IR spectrum (4000-700 cm^{-1}) from C-100 fibers recorded in ATR mode. Position and area are indicated for the major peaks in the spectrum

cm^{-1}) with indicated peak positions for C-100 and H-100 fibers, respectively. Peak position and associated chemical groups are summarized in TABLE 3.2 for both fibers. The two areas with the strongest peaks (2800-3000 cm^{-1} and 850-1150 cm^{-1}) are corresponding to hydrocarbon groups and silicon oxide groups, respectively. This indicates high concentrations for those two chemical groups in the fibers. Furthermore peaks for esters (≈1730 / 1258 cm^{-1}) are visible in the spectra for both fiber types.

The overall shape and peak positions are similar for the two different fibers but small differences can be identified. FIGURE 3.7 shows an overview of both overlaid spectra for the whole spectrum and magnifications of three regions were distinct differences are visible. FIGURE 3.7 b shows the region between 1280 and 1170 cm^{-1} where there are clear differences in peak ratio between the two peaks whereas peak position is not changed. This indicates a variation of the amount of C-C and C-O groups between the two fibers. FIGURE 3.7 c shows the region between 3000 and 2720 cm^{-1} which is associated with CH_2 and CH_3 groups. The differences in peak shape and ratio are less distinct as in the first region but differences are visible. FIGURE 3.7 d shows the region between 1180 and 840 cm^{-1} representing Si-O-Si groups. Peak ratio differs clearly whereas peak position is again unchanged, suggesting differences in the composition of the Si-O-Si containing surface.

3.2.3 X-ray photoelectron spectroscopy

X-ray photoelectron spectroscopy was used to get more information about the surface chemical composition of the fibers.

FIGURE 3.8 shows the complete spectrum and the calculated composition of the major elements in atomic percent for both fiber types. The small nitrogen peak in the

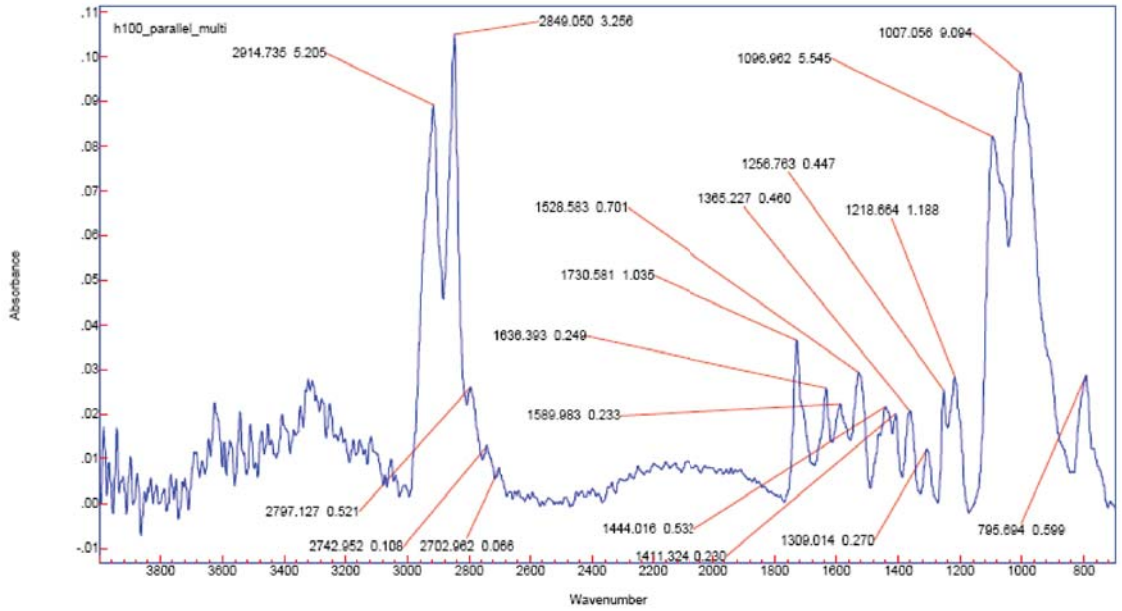

Figure 3.6: FT-IR spectrum (4000-700 cm^{-1}) from H-100 fibers recorded in ATR mode. Position and area are indicated for the major peaks in the spectrum

C-100:	Peak		H-100:	Peak	
	2915	CH2		2915	CH2
	2848	CH2		2849	CH2
	1733	Esters C=O		1731	Esters C=O
	1535	NH (Amide II)		1529	NH (Amide II)
	1364	CH2 def.		1365	CH2 def.
	1258	Ethers / PDMS		1257	Ethers / PDMS
	1218	C-C /C-O		1219	C-C / C-O
	1092	Si-O-Si		1097	Si-O-Si
	1004	Si-O-Si		1007	Si-O-Si
	799	Si-C		796	Si-C

Table 3.2: Position for major peaks of C-100 and H-100 fiber FT-IR spectra and the corresponding chemical groups.

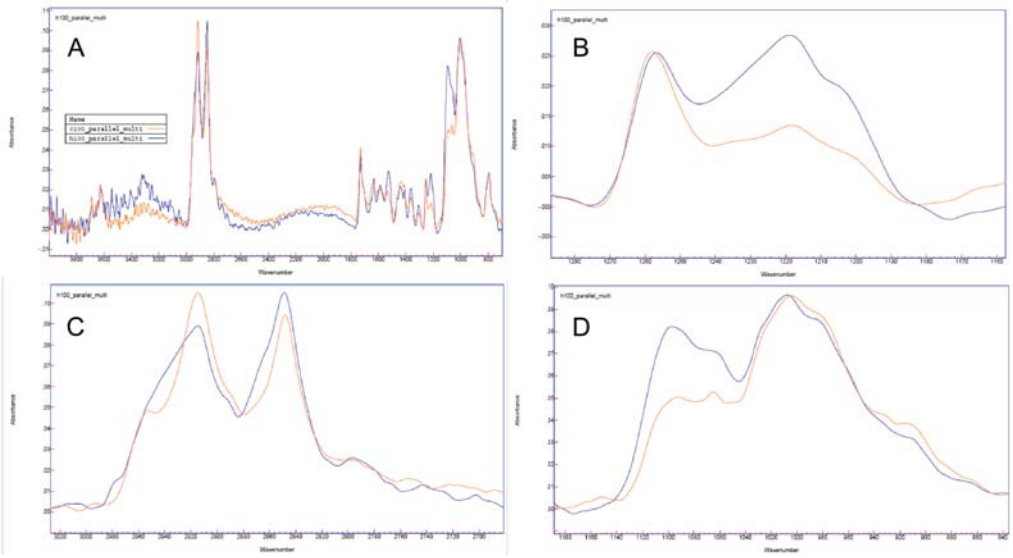

Figure 3.7: Comparison of FT-IR spectra from C-100(orange) and H-100 (blue) fibers. There are several differences in the spectra indicating slightly different chemical composition of the two fiber types. A) Overview of the whole spectral range 4000-700 cm^{-1}. B) Magnification 1280-1170 cm^{-1} (C-C / C-O stretching) the peak position for both fiber types is similar but the peak ratio for the peaks at 1256 cm^{-1} and 1218 cm^{-1} differs. C) Magnification 3000-2720 cm^{-1} (CH_2 / CH_3) the peak shape vary between the two fiber types. D) Magnification 1180-840 cm^{-1} (Si-O-Si) the peak ratio for the peaks at 1091 cm^{-1} and 1064 cm^{-1} differs for C-100 and H-100.

C-100 spectrum was not taken into consideration for atomic ratio calculation. The ratio for the C-100 sample is approximately 16:3:1 (C:O:Si) which differs clearly from the 3:1:1 (C:O:Si) ratio for the H-100 sample. The results suggest a different surface chemistry for both samples.

References from different standard polymers were taken into consideration as a comparison. Figure 3.9 shows the reference spectrum for PDMS. Polydimethylsiloxane (PDMS) has an atomic ratio of 2:1:1 (C:O:Si) and poly(phenyl methyl)siloxane (PPMS) has an atomic ratio of 7:1:1 (C:O:Si).(111) These are the single polymers which are closest to the atomic ratio of the C-100 and H-100 fibers. More likely than a single polymer is that the measured XPS spectra show a combination of different polymers and copolymers present on the fiber surfaces. The recorded high resolution spectra from the valence band of the two fibers, not shown here, are supporting this assumption. They also show similarities to PPMS and PDMS but are not identical to either of them.

Figure 3.10 shows a reference spectrum for polyurethane, which is considered the bulk material of the fiber. No silicon peaks are visible for polyurethane, but a peak for nitrogen.

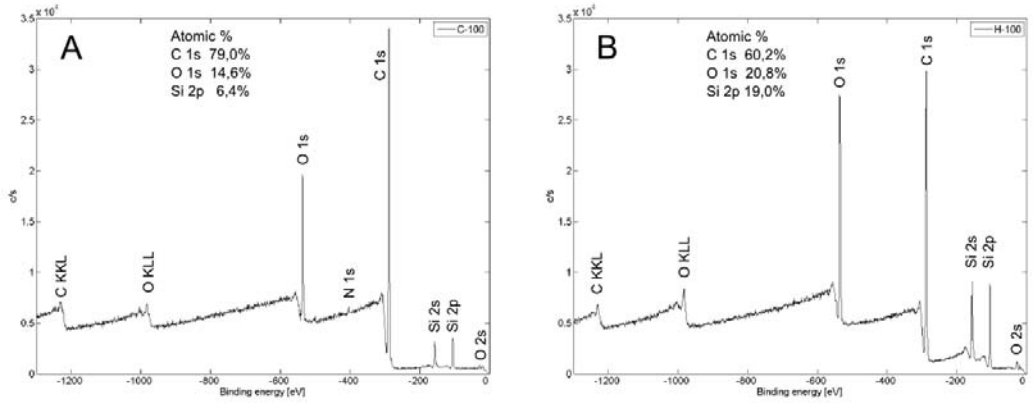

Figure 3.8: Comparison of XPS spectra from the two different fiber types. A) Shows the acquired spectrum for the C-100 fiber with indicated atomic percentages considering only elements C, O and Si. There is a small nitrogen peak visible for the C-100 fibers. B) The H-100 spectrum does not show a nitrogen peak and the atomic ratio differs from the C-100 sample.

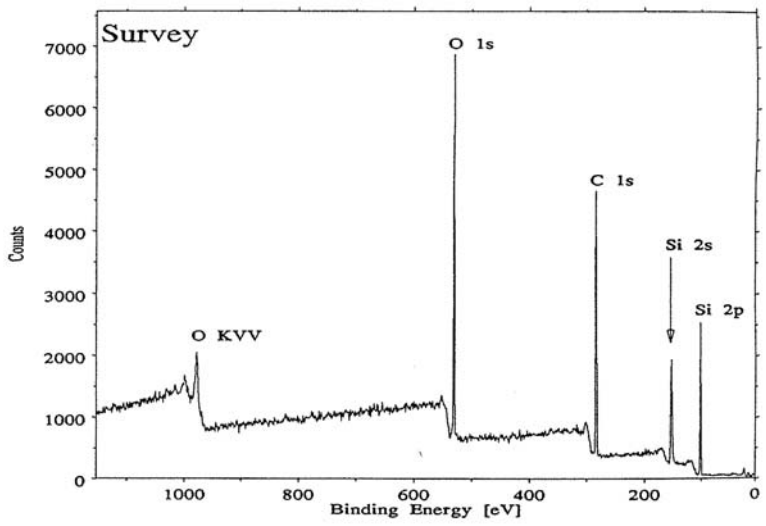

Figure 3.9: PDMS XPS reference spectrum.(111)

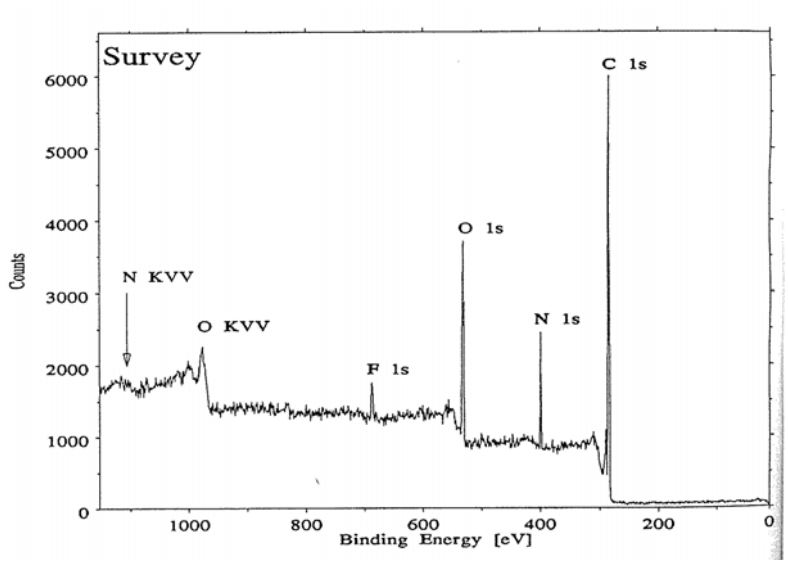

Figure 3.10: Polyurethane XPS reference spectrum.(111)

3.3 Cell experiments

3.3.1 Myoblast growth and differentiation on flat surfaces

The first cell experiment on flat untreated glass surfaces and culture polystyrene dishes was performed to study the three stages of myoblast growth and differentiation and identify markers for final cell differentiation, compare section 1.3.3. FIGURE 3.11 shows these three stages at different magnifications. A+D+B+E are images of cells cultured on plain glass surfaces, whereas images C+F are cells cultured on polystyrene. It was not possible to observe teminal differentiation of cells into muscle fibers on glass surfaces, because the cells detached from the surface before reaching the state of muscle fibers.

FIGURE 3.11 A+D show cell attachment and spreading after 48 hours. The cells are dividing and migrating on the surface, the orientation of cells is random. In section D different stages of cell division can be seen with dividing nuclei and large cell bodies. Directly in the mitotic phase the cells detach from the surface and are visible as round cells, FIGURE 3.11 A on the left side. These round cells have small dense nuclei and highly packed actin filaments resulting in a much stronger signal for the Rhodamin/Phalloidin and DAPI stain.

FIGURE 3.11 B+E show cell fusion and myotube formation after 7 days. The surface is covered with cells, it is not possible to distinguish individual cells any longer, at least not with the used microscope technique. Furthermore it is impossible to estimate the number of stacked cell layers. For samples at higher density, images not shown here, it is even more difficult since the Rhodamin/Phalloidin signal from the actin is overlaying each other resulting in a blurry signal. Nevertheless a clear orientation of cells and actin filaments can be seen in the images presented here. The cells are elongated and align parallel to each each other, this process results also

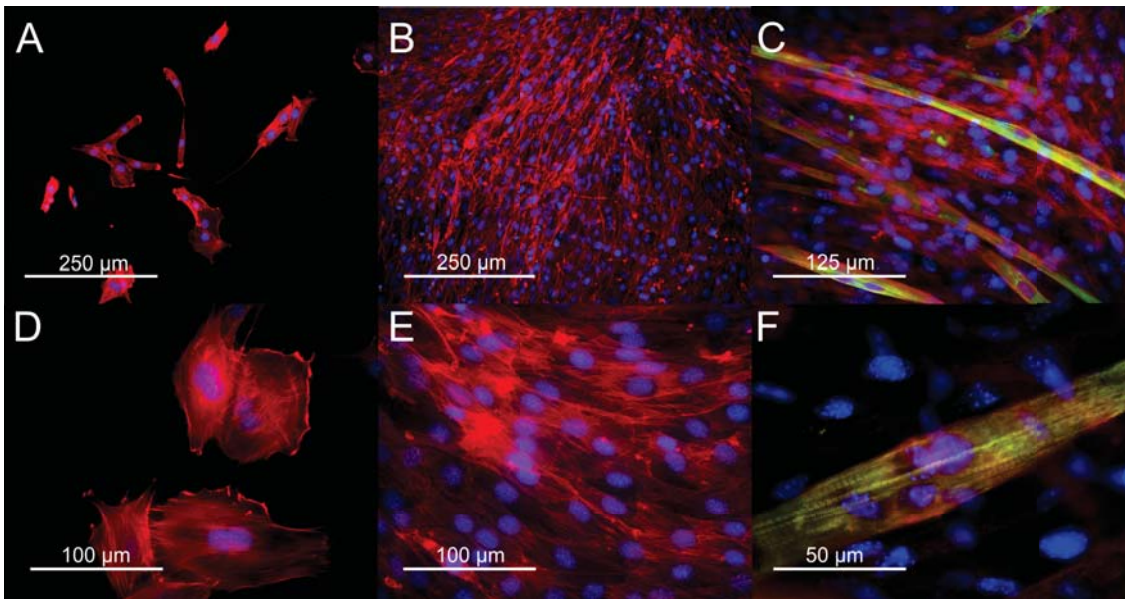

Figure 3.11: The three different stages of C2C12 growth and differentiation. False colored fluorescent images, red = Rhodamin/Phalloidin actin filaments, blue = DAPI DNA and green = Myosin heavy chains, scalings as depicted in the images. A)+D) show cell spreading and proliferation 48h after seeding. B)+E) show complete coverage of the surface, the alignment of neighboring cells and the fusion of cells after 7 days. C)+F) show differentiated muscle fibers which express the myogeneic marker MHC in green after 14 days. In F) the striation pattern originating from sarcomeric structures in the myofibers is visible for the green MHC staining.

in end-to-end fusion and even longer myotubes. In images at lower magnifications, not shown, it can be observed that cells are locally aligned but are slightly bending resulting in whirls at the millimeter scale and show no global alignment.

Figure 3.11 C+F show cell differentiation of myotubes into functional muscle fibers after 14 days. Cells were stained for the skeletal muscle protein myosin heavy chains coupled to a green fluorophor. In section C the specificity of the staining can be seen, the surface is completely covered with cells but only larger elongated muscle fibers are stained positive for MHC. Furthermore in section F the organization of MHC into myofibrils can be observed, showing the skeletal muscle typical striation pattern of sarcomeres. There are several microfibrils parallel to each other extending over the whole length of the cell. One of the problems with these small delicate structures is again the blurring effect of the microscope technique utilized. It is often difficult to resolve this fine structures in the images.

The specificity of the MHC staining is evidenced again in Figure 3.12. It shows a combined false color image as well as the individual channels separately. From the visualization of the MHC and actin filaments it is clearly visible that only a few long cells are stained positive for MHC. It also demonstrates the highly specific binding of primary and secondary antibodies resulting in an extremely low background in the MHC image. Negative controls which were incubated only with secondary antibodies did not show any signal, not shown.

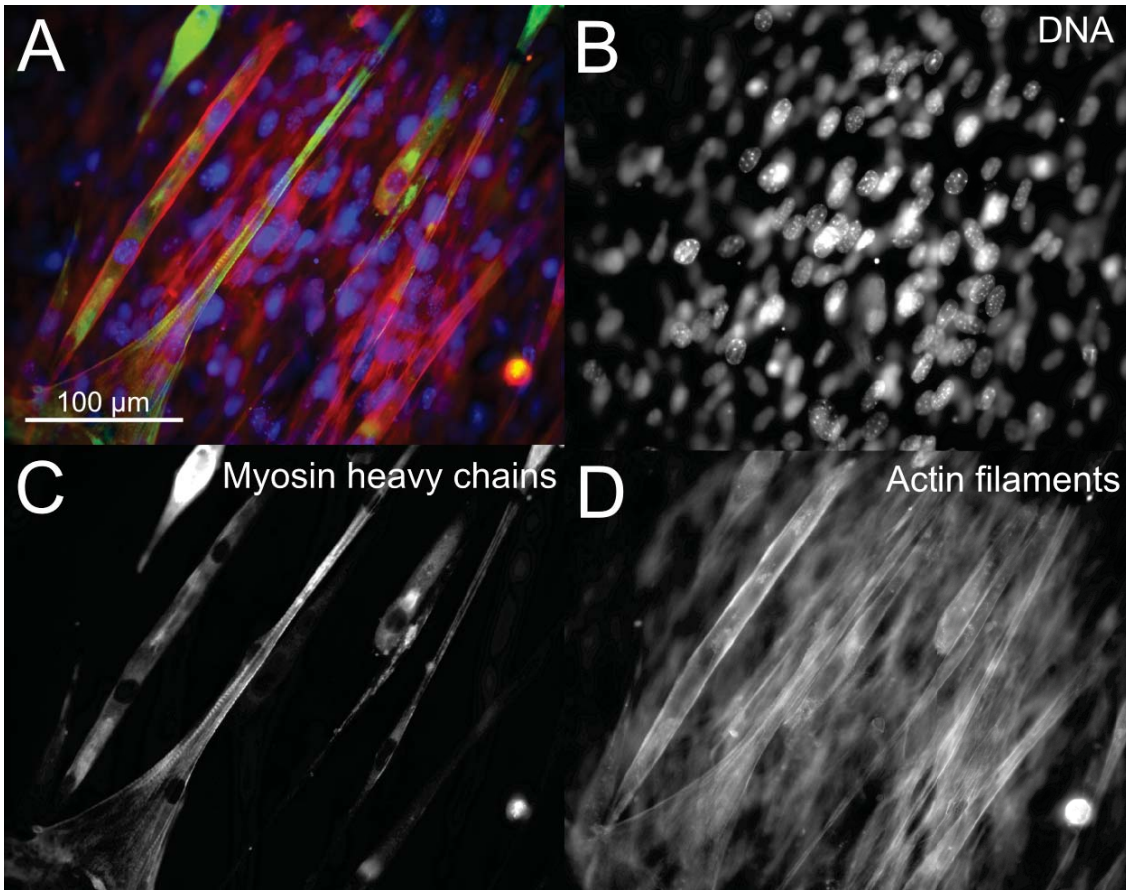

Figure 3.12: Specific binding of primary antibodies against myosin heavy chains, only larger elongated muscle fibers express myosin heavy chain proteins after 14 days in culture. The antibody can be used to monitor myogenesis. A) Combined false color image. B) DAPI DNA C) MHC visualized with Alexa Fluor 488 secondary antibody. There is nearly no background visible and the binding of the primary antibody against MHC is highly specific. D) Rhodamin/Phalloidin actin filament staining to visualize the cytoskeleton and show the specificity of the MHC staining. There are many cells present which are not fully mature and thus do not express MHC.

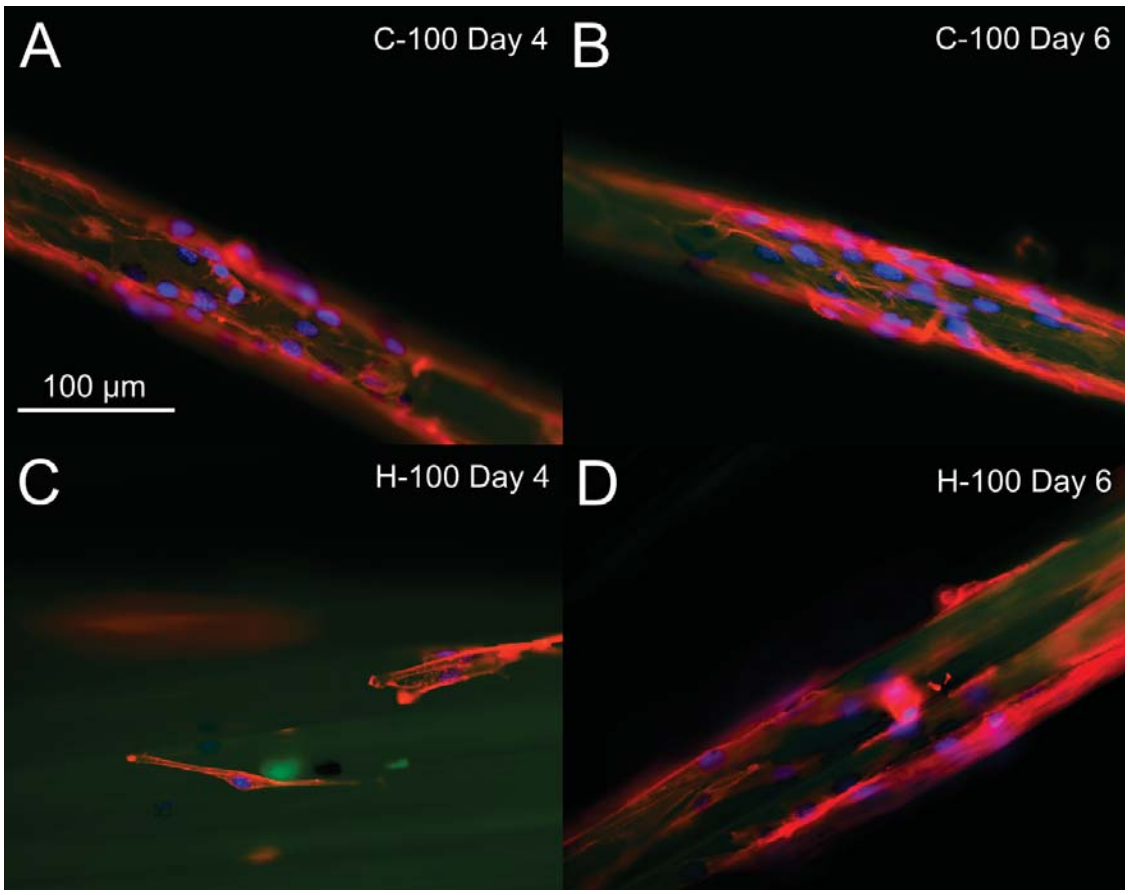

Figure 3.13: Comparison of C2C12 cell growth on H-100 and C-100 fibers. False color images red = Rhodamin/Phalloidin actin filaments, blue = DAPI DNA, green = Autofluorescence of the fibers. A+B) Show a high number of cells that are attached and spread out on C-100 fibers for both day 4 and 6. C+D) On H-100 less cells are present on the fibers. The number of cells increases at day 6 but is still less than on C-100 fibers.

3.3.2 Myoblast growth on fibers under static conditions

At the beginning the effects of the two different fibers on cell behavior were investigated under static conditions in cell culture dishes with special stainless steel frames for the fibers. Figure 3.13 shows a comparison of cell growth on C-100 and H-100 fibers. After 4 days in growth media (GM) it is clearly visible that more cells are present on C-100 fibers than on H-100 fibers. On C-100 fibers a fairly dense layer of cells has already formed. On H-100 fibers, on the other hand, mainly individual cells are present but these cells seem to be well attached and in good condition. After 6 days (media was switched to differentiation media (DM2%) after 4 days) the coverage on C-100 fibers is only slightly increased but the cells are more aligned and under go reorganization (compare Figure 3.14). On H-100 fibers the number of cells increases but does not reach the same density as on C-100 fibers. For later timepoints, images not shown, this trend continues and the cell density of H-100 is lower on all samples and the cells are less organized compared to cells on C-100 fibers.

FIGURE 3.14 shows a more detailed comparison of different time points for cells on C-100 fibers. At day 4 initial cell attachment and spreading can be seen, but the cells are randomly orientated and do not exhibit organized actin filaments. After 8 days (4 days in DM2%) the cell number is only slightly increased as seen before but the organization is changed considerably. The cells are aligned along the fiber axis and have a highly ordered actin skeleton. Using the observation from flat surfaces it can be said that it is likely that myotubes are formed or starting to form at this time point. After 11 days the cell number is increased resulting in multiple layers of cells. The cells are aligned and there are strong indications toward myotube formation. At day 14 no strong changes are visible in the images since the fibers are already covered with cells and cell number can only increase by forming new layers. One of the limitations with the used microscope technique is again that it is difficult to image multiple layers of cells and investigate changes at this time point.

The last step in muscle cell differentiation is the formation of muscle fibers and the expression of specific proteins. FIGURE 3.15 shows a fully differentiated muscle fiber after 14 days in culture which is stained positive for MHC expression. In section A) the combined false colored image can be seen and B-D) show the individual channels. The muscle fiber expressing MHC protein is formed in the area between two fibers. Unfortunately it was difficult to image fully differentiated cells directly on the fibers. This is again one of the limitations of the technique due to strong overlaying signals directly on the fibers. Even though it was difficult to image those muscle fibers, there are strong indications for their presents and the possibility of muscle fiber formation directly on C-100 fibers. The fact that muscle fibers are formed in the bridging area between fibers is one of the main indications. Furthermore it shows that the cells in the area between fibers are vital and are able to organize themselves. The high specificity observed for the flat surfaces is confirmed for the fiber samples, the only drawback is the autofluorescence of the fibers which are then visible in the image and complicates the identification of MHC positive cells.

One interesting question is how cells bridge the space between fibers and how this process occurs over time. FIGURE 3.16 shows this process at different time points. At day 4 it can be observed that some cells start spreading between two nearby fibers. The surface of the fibers is nearly covered, the top surface of the fiber is not in focus so no cells can be seen there. At day 6 and 8 the space between near fibers is filled and it seems that the cells in the center are no longer attached to a fiber but embedded in other cells. The cells can bridge large distances as indicated in section C, up to 125 μm at the front and even up to 150 μm for cells at the fibers that participate in the bridging. From a cell morphological point of view this is also very interesting. Cells that are at the upper front where the fibers are farthest apart from each other have less organized and aligned actin filaments. Whereas cells closer to the intersection of the two fibers are more aligned and organized.

Another interesting morphological aspect for cells growing on fibers is shown in FIGURE 3.17. The phenomenon of cells twisting around fibers instead of aligning completely parallel is observed for several fibers but not all. No data of the frequency of this occurrence was collected. The twisting of the actin filaments is obvious but in order to gain more quantitative information the FFT spectrum from the actin

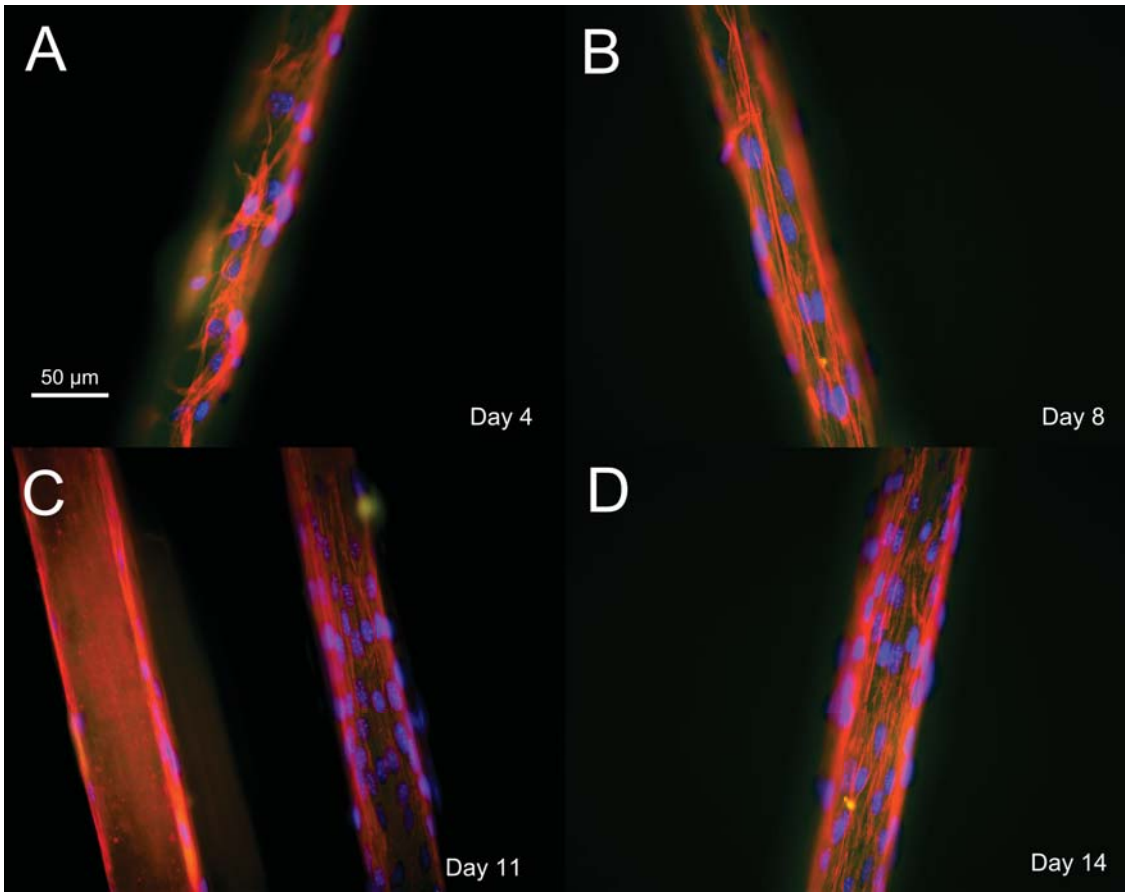

Figure 3.14: C2C12 growth and differentiation on C-100 fibers under static conditions. Cells were cultured in growth media for 4 days and then switched to differentiation media with 2% horse serum. The culture was maintained for 14 days, the duration of culture is indicated in the images. False color images red = Rhodamin/Phalloidin actin filaments, blue = DAPI DNA, green = Autofluorescens of the fibers A) Day 4: The cells are adhered and randomly spread on the fiber. B) Day 8: The cells are elongated along the fiber axis with actin filaments oriented parallel to the fibers. C) Day 11: The fibers are completely covered with cells which are oriented parallel to the fiber and the cells start to fuse. D) Day 14: No major differences between day 11 and day 14 are visible for individual fibers, there is no space for further cell proliferation.

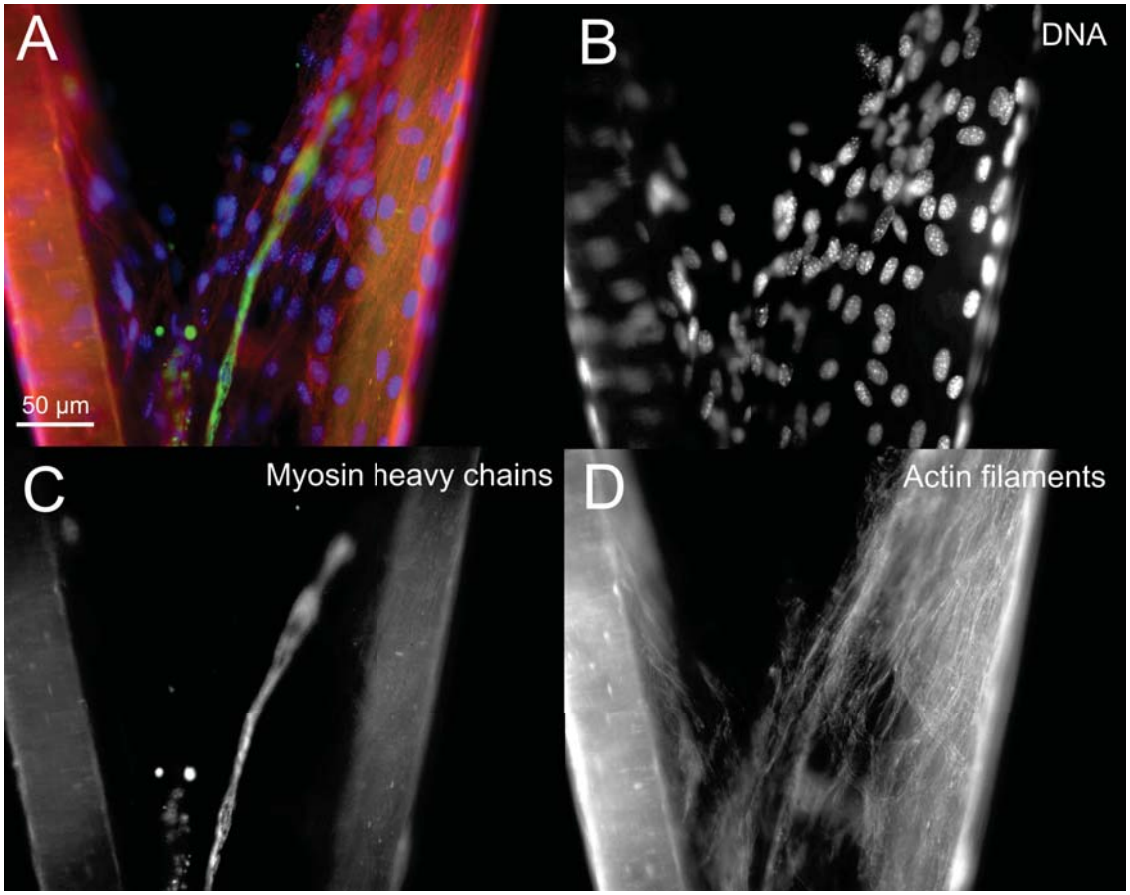

Figure 3.15: Muscle fiber formation on C-100 fibers positively stained for myosin heavy chains after 14 days in culture. The muscle fiber is formed in the area between two fibers. A) Combined false color image. B) DAPI DNA C) Myosin heavy chains visualization with Alexa Fluor 488 secondary antibody. The C-100 fibers are auto fluorescent for this excitation channel. Since the muscle fiber is between the scaffold it can be clearly distinguished. The form of the muscle fiber is similar to the owns observed on flat surfaces. D) Rhodamin/Phalloidin staining for actin filament visualization. There are many cells present in the area but only one is fully differentiated into a muscle fiber.

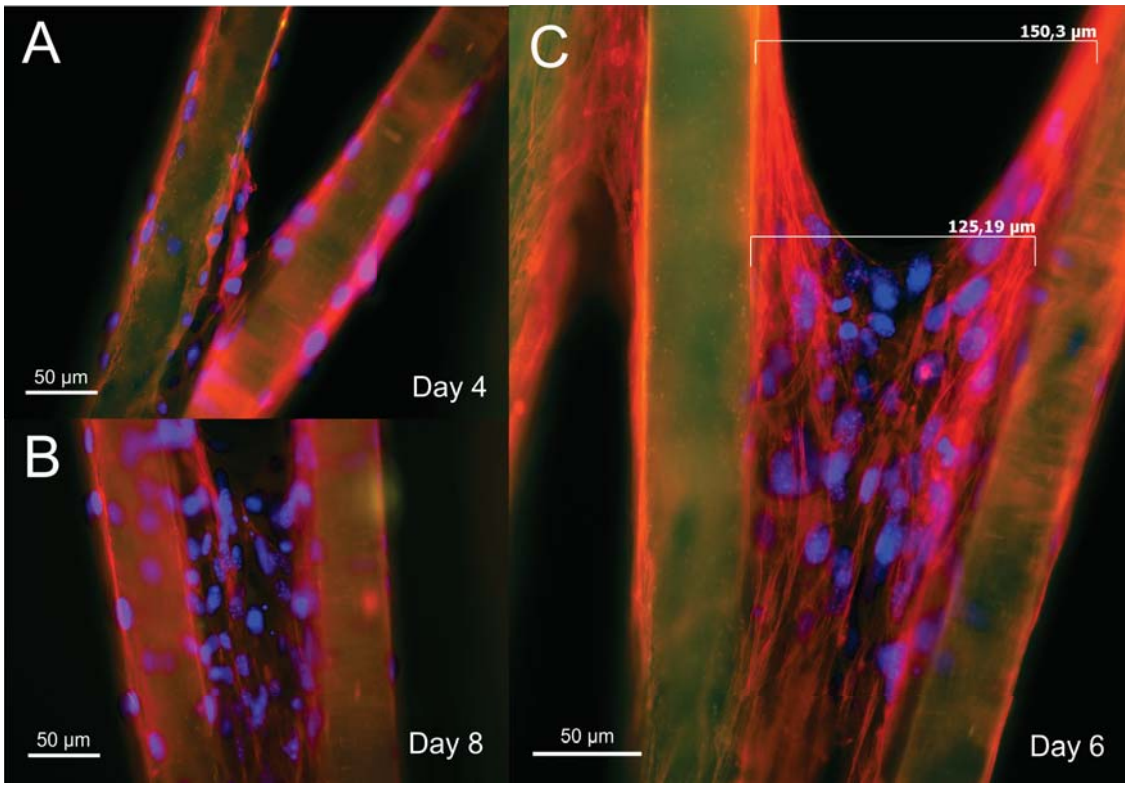

Figure 3.16: Bridging of cells between two spatially close fibers. Cells are able to span between fibers and this mostly occurs at fiber intersections. False color images red = Rhodamin/Phalloidin actin filaments, blue = DAPI DNA, green = Autofluorescence of the fibers. A) Day 4: Some cells are spreading between the two fibers closely to the intersection. B) Day 8: The area between the two fibers is covered with cells. C) Day 6: The images shows the large distance which can be bridged by the cells. The cells in the center seem not to be attached to the fibers anymore but are only attached to other cells. Near the intersection the cells are aligned parallel to the fibers whereas they are more randomly orientated at the front.

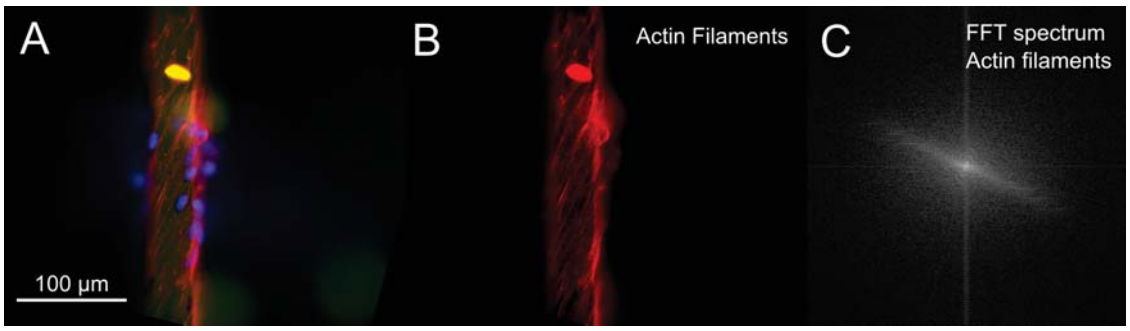

Figure 3.17: Twisting of cells around C-100 fibers. A) Combined false color image red = Rhodamin/Phalloidin actin filaments, blue = DAPI DNA, green = Autofluorescens of the fibers. B) The actin filaments show high degree of orientation and alignment. The cells are twisting in a right handed helix on the fiber. C) Calculated FFT spectrum from the actin filaments. A line around 20 degree from the horizontal line represents the right handed helix, the orientation of the line is perpendicular to the cell orientation.

channel was calculated. The FFT spectrum displayed in section C shows a blurry line at an angle of approximately 20 degree to the horizontal line. This line represents the pattern created by the twisting actin filaments and is therefore perpendicular to cell alignment. Even more interesting than the pure fact of cells twisting around fibers is that every time this phenomenon was observed the direction of twisting is similar. The cells are always twisting around the fiber in a right handed helix.

3.3.3 Preliminary bioreactor cell experiments

The first bioreactor experiment was designed to test the system for problems and help to modify it for future experiments. The test revealed some problems and some promising aspects.

The temperature in the system is stable, there are no signs for overheating killing the cells. Furthermore there are no indications for infections, but since the cells were cultured with antibiotics a possible infection may be suppressed. However no final examination of these two aspects can be conducted because of a different problem occurring during the experiment, limiting the intended culture duration. At least there are strong indications that temperature stability and sterility are given for the bioreactor.

The major problem remaining is massive evaporation of liquid from the system. Even filling the wells that are not used for cell culture with water is not suitable to counter the issue. The problem is that the culture chamber cannot be sealed in order to create a high humidity atmosphere because such sealing of the chamber will result in an altered gas composition over time. Thus the cells would die due to a lack of oxygen after some time. A resulting problem of evaporation is a change in the osmolarity of the media. The attempt to solve this problem by making up lost volume with pure sterile water was not successful.

Figure 3.18 shows the results from the cell cultures carried out in the bioreactor on glass coverslips. After 24 hours the cells look normal, are well adhered and spread

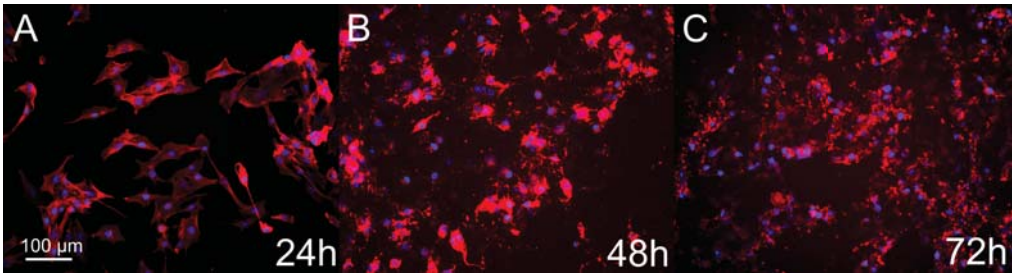

Figure 3.18: Time series of cells cultured on glass coverslips in the bioreactor. Cells were cultured for 72h and evaporated liquid from the culture well was replaced daily with sterile water. False color images red = Rhodamin/Phalloidin actin filaments, blue = DAPI DNA. A) After 24h cells are attached and spread out on the surface, cell behavior is normal and comparable to standard culture conditions. B) After 48h most of the cells are deformed and a large amount of dead cell substance is visible. There are only a few intact cells. C) After 72h the experiment was stopped. Cells have completely lost their normal morphology and most of the cells seem to be dead.

on the surface and proliferate. The change in osmolarity results in severe cell death, after 48 hours many cells are dead and there are only a few remaining cells. After 72 hours all the cells are dead. In the images it can be observed that the cells are disintegrating and shrinking, actin filaments are randomly distributed on the surface and cells can no longer be located individually. Furthermore it is obvious from the samples that cells and cell remains are no longer well attached to the glass. Most of the area on the glass coverslip is clear without indications of cells, images no shown here.

The fiber samples, cultured in the bioreactor simultaneously, were not analyzed further. It can be assumed that similar problems occurred for those samples. Furthermore another problem with the fiber samples was encountered. It was difficult to image the mounted fibers and cells with the scaffold holder and retainer in place. At the moment there is no suitable way to solve the problem, probably it is necessary to dismount the scaffold from the holder or redesign the scaffold holder.

Chapter 4

Discussion

4.1 Bioreactor system

A whole bioreactor system was developed from scratch and the system was preliminarily evaluated in this thesis. The system consist of four individual modules that were tested separately and in combination. The four modules are the electronics control unit, the mechanical unit which generates the movement, the heating system and the culture chamber. The modular design has proven to be of great value and allows modification to meet needs in the future.

The mechanical system generates movement via a stepper motor and a ball screw spindle which translates the rotational movement of the motor into a translational movement of the carriage. The aim was to realize frequencies up to 2 Hz for cyclic stimulation which is the maximum value used for elongation found in literature.(36) On the other hand several other studies suggest much lower stimulation rates.(28; 112; 48; 12) In the current systems frequencies up to 1 Hz are possible. However it is important to note that frequency is not an appropriate parameter for the developed system since the frequency is depending on the elongation distance. A more appropriate parameter is to talk about the velocity that the system can generate. Here the system is well in the range of other studies that used velocities around 0,5 mm/s, the maximum we can achieve at the moment is around 5mm/s.(28) Furthermore the system is also suitable to realize extremely slow continuous elongation to mimic bone elongation. The minimum distance is one motor step which correspondents to approximately 5 μm. Collinsworth et al. successfully used 0,05 mm/h to mimic bone elongation which would accord to 10 steps per hour in our system.(11)

The elongation range of the system is currently limited by the length of the culture wells. The mechanical system is able to generate elogation of up to 180mm. Taking into account that 26% is the reported physiological maximum for muscle elongation (104) that would corresponded to a scaffold length around 700mm which is far beyond suitable length. With the current culture chamber scaffold lengths of up to 40mm are suitable and allow elongation rates up to 50% if necessary. This resembles the typical maximal length of the largest BAMs used for mechanical stimulation.(42; 28; 12)

The scaffold holders currently used in the system are designed to allow simple

experiments on fiber samples. The scaffold holders are removable and specialized holders can be designed and built to meet the requirements of a wide variety of different scaffold materials. In general the system is suitable for the elongation of fibers, foams, sheets and so on, allowing to test the influence of mechanical stimulation in many systems.

The accuracy with which the described elongation rates can be achieved was evaluated, and additionally some information is available about the force the bioreactor can create. The error for repeated positioning of the carriage is between 13 and 40 μm depending on the parameters, and there are several possible reasons for this error. One is due to the acceleration ramps that are used to accelerate the motor from standstill to the desired speed. It was observed that the parameters for this acceleration influence the precision of the positioning precision of the system. This effect is due to the fact that no external measurement system is used and the assumption that each step signal results in a similar displacement. During acceleration it can happen that the motor does not executes a step because the torque is not high enough. The torque for a stepper motor is decreasing for higher step frequencies. Therefore it is necessary to accelerate the system slowly to avoid losing steps.(113) Another factor that should increase the torque is the current control circuit in the stepper driver. Unfortunately this part is not working properly and can thus not enhance the precision. The reason for this malfunction is ambiguous at the moment and analysis with an oscilloscope could not unveil it. Most likely it is due to interference between the high current part that drive the motor and the logic signal part. Even though the parts were separated on the circuit board as much as possible, it might still come to cross talk and induction. This interference can potentially alter the logic signals, and thus cause the malfunction of the current control circuit.

When talking about accuracy and precision it is important to take the whole system into account including the measurement system which is used to validate those parameters. The method used in this thesis is not optimal and may influence the measurement. The bioreactor was not fixated and only loosely coupled to the microscope during the measurement which might result in a displacement of the whole system during measurements. Additionally, the analysis was carried out by hand and it was sometimes difficult to define the edge of the metal shaft that was used to measure the displacement. It should be mentioned that one pixel in the image correspondents to 0.58 μm and a standard error of four or five pixel is clearly possible when selecting the edge. Furthermore the measurement in the current configuration can only give information about the relative error between repositioning steps and not about the absolute error in position.

The experiment that was performed to measure the step width did not use acceleration ramps and hence should not be used to conclude anything about the absolute error during high speed repositioning. The step width was measured to be 4,89 μm/step which is 0,11 μm less than the theoretical value. It is most likely that this is not a constant error for individual steps but is also the result of losing steps. The error is accumulated over the distance of 100 steps. To test this hypothesis different distances could be used and compared. The other explanation would be that the ball screw spindle has a different pitch which is not likely regarding the precision

information for the product provided by SKF.

This first evaluation gives some basic informations about the system but to gain a complete picture about the precision and limitations additional experiments are needed. The force that the bioreactor can create was not measured with a specialized system but from observations it is evident that the system can generate high enough forces for the designed purpose. It was possible to deflect fiber scaffolds attached to the bioreactor under dry conditions without any problems. The cultivation of cells and presence of media are not suspected to increase the fiber stiffness significantly to limit deflection of the fibers.

The first cell experiment carried out with the bioreactor was designed to reveal problems of the system and to test the suitability for cell culture. During the preparation it became obvious that the sterilization of the system is possible but that the assembly of the system under sterile conditions is complicated. Especially the placement of the scaffold with the holder into the well and the detachment of the retainer is difficult. One drawback is that the plastic parts of the culture chamber cannot be autoclaved at the moment since it most likely that it will result in a deformation of the parts according to information from Nordbergs Tekniska AB (Supplier of polymer materials). A different material like PSU or PMP would simplify the process and would allow steam sterilization of the whole pre-assembled culture chamber. The main limitation is the high price for those plastics. No contamination was observed during the preliminary experiment, and this could be due to the short duration of the experiment, antibiotics present in the culture media or the changed osmolarity. It is difficult to conclude anything about the sterility of the system from this first experiment.

The major problem for the first cell experiment was water loss in the culture wells due to evaporation. Evaporation of water from the cell culture media changes the osmolarity of the media and thus results in osmotic stress for the cells.(63; 16) The images from the cells and observation of the liquid during the experiment are clear evidence that cell death was caused by altered osmolarity in the media. No system to control the humidity in the culture chamber was available during the experiments. Before new experiments can be carried out such a system definitely must be constructed and installed. In section 6.1 some possible ideas for such a system are mentioned.

Mechanical stimulation of one fiber scaffold after 24 hours revealed another problem which was already observed during the precision measurements, the cyclic change of direction is not reliable at the moment. It was observed that after a random number of cycles direction was not changed and the scaffold was thus overstretched or the two holders collided. This can either be due to some electronic problems or more likely to a programming error. Since the problem occurs randomly and is not reproducible the reason is most likely the programmed interrupt routine. Such an error is difficult to eliminate with normal program debugging because it occurs only under specific conditions. To solve the problem the code most be thoroughly checked and possible parameter combinations must be tested by hand.(29) For this reasons and mainly due to the evaporation problem mechanical stimulation of cells seeded on fibers were not further investigated in this first experiment.

During the cell experiment as well as in the previously carried out measurement temperature stability does not appear to be a problem. The system needs a certain time to reach a steady state but is afterwards stable. No measurements of the temperature gradient in the wells was performed but it can be assumed that the media is heated sufficiently homogeneously. The sides of the culture wells are nearly completely enclosed by the heating spiral and the volume inside each well is relatively small.(20)

4.2 Scaffold material choice and characterization

The chosen scaffold material fulfills most of the requirements defined at the beginning of the project. It is highly elastic and even though no data was obtained for the mechanical properties, it can be assumed that it is suitable for the mechanical stimulation of cells. Since it is a product designed for textile industry it should have a sufficient stability and material failure due to repeated stretching should not be an issue. Since those fibers are often used in swimsuits the presence of liquid should not effect them either. Additionally the large amounts required in textile industry make the material inexpensive. Unfortunately the origin of the material results also in a major problem because no scientific information about the material is available. More information about the fiber was requested from the company and the associated research and development division without success. Even basic information about the production process and materials cannot be provided due to company policy.

Our own studies offer a starting point to investigate the properties of the material. It is important to note that all analysis methods were used on fibers that were not autoclaved prior to the measurement. At the moment it is unknown if this process might influence the shape, composition and especially the surface chemistry. We showed that both fibers have a distinct surface topography but it was difficult to define the exact topography of the H-100 fibers. It is not clear at the moment if the fiber topography is the result of fuse individual fibers or defined by a special extrusion process. In literature both methods are mentioned to be commonly used in textile industry.(52)

Information about the chemical composition is even more difficult to interpret. From the obtained FT-IR spectra it is difficult to conclude the exact composition of the fibers. Comparison to FT-IR spectra obtained by other research groups helped to identify several groups but did not completely correlate to our spectra.(54) The major problem is that different chemical groups highly influence and overlay each other in FT-IR spectra which makes identification of blended polymers difficult. The differences observed between the two fibers are corresponding to differences in hydrocarbon, C-C, C-O and silicon oxides groups and indicate slightly different composition. It was not possible to couple the variations in the FTIR spectra to the presences of specific polymers. The assumption that both fiber types differ in their polymer composition is support by the XPS analysis which gave information about the surface chemistry of the fibers.

The high concentration for hydrocarbon groups (-CH_2-) indicates long back bone

structures expected for many polymers like polyurethane which shows that it should be possible to measure the fiber composition with the employed FT-IR setup. Information about the exact compositions of the backbone chains were not conducted and the determination is complicated.

The second-most abundant peak is characteristic for silicon oxides and was not expected at the beginning. XPS data support the FT-IR data and confirmed the presence of silicon atoms on the fiber surface. The most reasonable explanation is that different polymers such as PDMS or PPMS are used as finishing agents in the production of elastic polyurethane fibers to minimize the effect of fibers sticking together. From the data presented here it seems that different finishing agents were used for the two fiber types which result in a different surface chemistry. The exact composition of the finishing agent could not be determined and the spectra do not resemble pure PDMS nor PPMS.(52; 114)

Furthermore it is not clear at the moment if differences in composition are only limited to the finishing agent, which can be seen in FT-IR and XPS, or the whole bulk material. Another indication for the differences in material offers the marketing information for the fibers which mentions C-100 as “soft” and H-100 as “hard” modulus fibers.(115) This is normally associated with the differences in tensile modulus but do not give information about the exact composition.(115; 116)

The two fiber types used in this study should not be considered as an optimal scaffold material for later applications, especially for transplantation medicine and *in vitro* meat. But the fibers offer a scaffold material to study the mechanical stimulation of muscle cells in general with a focus on the influence of different stimulation patterns. For this reason and for the evaluation of the bioreactor they were selected in this study. In general polyurethane fibers are a promising scaffold material for tissue engineering and its properties could be tailored to specific needs. Special polyurethane compositions could be used to produce biodegradable fibers with customized elongation limits.(38) The manufacturing process could be adjusted to produce desired fiber diameters and cross-section shapes. C-100 and H-100 fibers offer a simple and inexpensive approach to test hypotheses on the effect of mechanical stimulation of muscle cells. Once those effects are understood the material should be adjusted towards materials for later applications.

4.3 Cell experiments

In the first cell experiment the different stages of myogenesis were investigated and protocols to identify differentiation markers in muscle fibers were developed. During the experiments it became apparent that it is not possible to finally differentiate muscle cells into muscle fibers on plain glass coverslips. Before the stage of muscle fibers was reached a large amount of cells detached and could no longer be stained in a sufficient way. Therefore final muscle fiber formation was investigated in cell cultures on TPCS which show a better support for cell attachment.(117; 50) Another approach would be to use different protein coatings on glass surfaces to enhance the attachment of cells on the substrate. Commonly used for this purpose are Matrigel®,

laminin or fibronectin which all result in ability to culture muscle cells for prolonged time periods on a substrate.(37)

Myosin heavy chain (MHC) and α-actinin were chosen as differentiation markers. According to literature those proteins are only expressed in finally differentiated muscle fibers and assemble the functional motor unit inside those cells. This was confirmed in our experiments which show no positive staining in myoblasts or myotubes. Skimmed milk powder was chosen over BSA as a blocking agent during the staining process because it is less expensive and shows comparable or lower background levels. Overall highly specific staining of the two markers was achieved at low antibody concentrations.

Co-staining with both markers showed that both proteins are located at similar positions which is consistent which observation in literature.(118) Furthermore it was observed that the MHC marker shows slightly clearer results and was therefore chosen as marker for later experiments.

Striation patterns in the cells which represent a functional contraction apparatus (microfibril) were observed for several cells. There are two main reasons why it might not be seen in all positively stained cells. First it might be the case that the proteins are expressed but not finally assembled into the apparatus at the time of the staining. The second reason is that it might be a problem of the imaging technique and striation patterns are presented but cannot be observed. Overlaying of several microfibrils result in a blurring effect which makes it difficult to image such small features.

Cell growth was investigated on plain fibers without surface modifications, the fibers were only autoclaved before usage. From the results it is apparent that cell growth differs on the two fiber types and the cells prefer thin smooth C-100 fibers. This difference could be due to either surface topography or surface chemistry or another factor. It has been shown that cells are sensitive to small features on surfaces in the nanometer regime as well as larger structures in the micrometer range.(37; 119) Since the topography is significantly different for the two fiber types it could explain the differences in cell numbers. From the FT-IR and XPS spectra it is evident that the surface chemistry varies between the two fiber types. Surface chemistry is known to play a key role for cell attachment and growth.(63; 6; 120; 5) Even the small differences observed in the spectra for the fibers might highly influence cell growth on the fibers. Other factors which might affect cell growth include mechanical properties such as tensile strength and elasticity of the fibers which can also be sensed by cells.(24) Most likely is that all factors play a role and result in the different cell growth for the two fiber types.

For both fiber types it was observed that cells are not equally distributed over the whole fiber. There are different possible explanations for this effect. First of all is the seeding method. Cell solution was dispensed over the scaffold by hand which can result in an initial unequal distribution. Second is the fact that small air bubbles were observed directly on the fibers. It was difficult to completely remove these air bubbles from the fibers directly after seeding, though it was possible after 24 hours. The air bubbles create a local environment where cell attachment is not expected.(63; 16) It could also be the case that the finishing agent is not consistent over the whole fiber

or the observed surface defects influence the initial cell attachment.

It was shown that it is possible to finally differentiate muscle cells into muscle fibers on the C-100 fibers. MHC positively stained cells were mainly observed in the area between fibers most likely represents not a significant difference in muscle fiber location but rather an imaging issue. The fibers are autofluorescenct which was a benefit to identify and image the fibers, but results in a problem for imaging fully differentiated cells on fibers. The high cell density which is required to see muscle fiber formation limits the ability to get clear images with the used microscope. A blurring effect makes it difficult to identify small structures and the effect is most pronounced directly on the fibers where the strongest overall signal is present. This is thought to be the main reason why MHC positive cells were difficult to see directly on the fibers. From the images presented in this thesis it is obvious that muscle fiber formation is possible on C-100 fiber and it can be assumed that final differentiation also occurs directly on the fibers. During the experiments it was not tested how long cells can be cultured on the fibers and if cell detachment occurs at later time points. The longest period of time in the cell experiments was 14 days and cell detachment was only observed on the edges where fibers are in contact with the stainless steel frame.

During the experiments it was observed that cells are able to bridge the space between fibers. This behavior is important when large skeletal muscle should be formed. It offers the possibility to form larger complex tissue constructs which would be difficult if cells would only grow directly on the fibers. Neumann et al. showed that muscle cells are able to bridge distances as large as 80 μm for parallel aligned fibers and form continuous cell sheets between fibers for fiber spacings up to 50 μm.(39) Our results suggest that even larger distances are possible when the cells have the possibility to start at in intersections. Measurements after 6 days showed distances of 120 μm for two fibers that are dispersing from an intersection. Such intersection could be integrated deliberately into scaffolds with parallel fibers to enhance the formation of muscle cell sheets. Since the fiber spacing was not controlled in our experiments no information about the formation of large cell sheets could be obtained. It was observed that cells are aligned inside the sheets and could be differentiated into muscle fibers. At the moment no information about 3-dimensional fiber spacing and its effect are available neither from our experiments nor from literature. In my opinion it should be possible to form muscle tissue in the whole area of a 3-dimensional fiber construct with the optimal spacing parameters.

Another phenomenon that was observed for cells cultured on C-100 fibers is related to cell alignment. Cell alignment and elongation was not always parallel to the fiber axis, but cells were sometimes describing a helix twisting around the fibers. Even more interesting is the fact that in such cases cells aligned at an angle of around 20 degree in a right handed helix, no spots were imaged were a left handed helix was observed. The effect was seen at several spots in different samples. This points towards a chirality effects that influences cell orientation and organization. Chirality effects and cell polarization are widely known in many biological systems.(63) However such an effect for muscle cell alignment has not been reported in literature yet. Our group observed similar effects on 2-dimensional surfaces with parallel micrometer features

were a similar offset in alignment orientation in the same direction was observed, data not published. The reason might be related to feature size or in case of the fibers, fiber curvature. The biological and molecular background for the offset in alignment are not clear at the moment and further experiments are needed to prove the significance of the effect and explain the reasons for this right-hand chirality and 20 degree offset.

Chapter 5

Conclusion

During the thesis a complete modular bioreactor system for the mechanical stimulation of cells was developed. Elongation rates and frequencies for stimulation can be varied over an extensive range to allow studies on the effect of versatile stimulation patterns on muscle cell growth, differentiation and tissue formation. The bioreactor allows simultaneous cultivation of 9 samples that can be individually coupled for mechanical stimulation to provide statistical significance and enhance throughput. It permits the utilization of many different scaffold materials and designs via customizable scaffold holders. The precision and reliability for elongation generation is currently compromised by minor problems on the electronic and programming level, these problems need to be solved before mechanical stimulation of scaffolds is feasible. It has been shown that the integrated water-based heating system for the bioreactor is sufficient to maintain a stable, physiological temperature in the culture wells. Sterilization of the system is possible but it is not advisable to draw any further conclusions about the sterility maintenance on the basis of the limited data. It was necessary to stop the first cell experiment because of severe evaporation problems in the culture chamber and exhaustive cell death after 72 hours. Subsequently it was not possible to solve the problem but there are several suggestions mentioned in section 6.1. The aim to realize mechanical stimulation of cells on fibrous scaffolds was not achieved during this thesis due to the described problems.

In this thesis polyurethane elastic micro diameter fibers (Creora® C-100 and H-100) were used as a scaffold material. The fiber properties were characterized with light microscopy, SEM, XPS and FT-IR ATR. The two fibers differ in shape, diameter, topography, surface chemistry and bulk composition. The surface of the fibers is coated with different silicon containing finishing agents, as silicon is visible in both XPS and FT-IR ATR spectra. FT-IR ATR peaks additionally show indications for hydrocarbon polymer back bones and the presence of ester groups, both are expected to originate from the polyurethane fiber core. It was not possible to conclude exact chemical properties from the obtained FT-IR and XPS data and assign differences between the two fibers to specific polymers.

The C2C12 cell line weas used as a model system for skeletal muscle cells. The three stages of muscle cell differentiation were studied on flat surfaces and it was possible to terminally differentiate cells into muscle fibers. The two proteins myosin

heavy chains and α-actinin were identified as potential muscle fiber markers. Antibody concentrations and staining protocols were developed and optimized in this thesis, resulting in high specific stains with low background levels that provide the opportunity to identify mature muscle fibers.

In addition cells were successfully cultured on the described elastic polyurethane fibers in different static experiments up to 14 days. C-100 are more suitable for cell culture since they show a higher degree of initial cell attachment and growth over time than H-100. It is unclear which factors mediate these differences, most likely it is the combination of structural and chemical surface properties. Furthermore it was shown that it is possible to terminally differentiate muscle cells (MHC and α-actinin positive) on C-100 fibers. Cell bridging between fibers and twisting around fibers were two observed cytoskeleton related phenomena that cannot be explained in detail yet. The ability of cells to bridge small distances between nearby fibers was expected but the underlaying cellular processes are still obscure. This property is important to culture large muscle constructs in the future. The significance of the right handed helix with which cells are sometimes aligned on fibers is unclear. Additional experiments and evaluation are necessary to clarify this subject. C-100 fibers are proposed to be suitable to study effects of mechanical stimulation on muscle cells but do not represent an applicable scaffold material for later applications. The availability and low cost make them practical for fundamental research like our experiments.

All things considered a bioreactor system for the mechanical stimulation of cells on diverse scaffolds was developed, muscle differentiation markers were identified and tested and a suitable scaffold material was characterized during this thesis offering a wide variety of potential experimental setups for the future.

Chapter 6

Future

6.1 Improvements of the bioreactor

The design of the bioreactor and the modular structure offer a convenient way for future modifications and improvements. The very first step is to solve the evaporation problem of the system. This is absolutely necessary in order to use the system for its purpose and to perform successful cell culture experiments. There are different possible approaches that are currently under consideration. The first is to seal the culture chamber and continuously pump fresh humidified air into the system. The air could be humidified in the water bath for the heating system, passed through a filter for sterilization and pumped into the culture chamber. Such a solution could be integrated to the existing system at reasonable cost. Furthermore it would be a first step towards a system with full atmosphere composition control. The second approach would be to use a perfusion system and continuously pump media through the culture wells. In this case the media would be pumped from a reservoir into the wells and back into the reservoir, with a feedback loop controlling the liquid levels in the wells. The effect of changed osmolarity would be minimized through the large amount of media in the reservoir. The advantage of this implementation would be the possibility to easily use more complex perfusion system in the future to culture and maintain larger complex muscle tissue constructs which require active transportation of oxygen and nutrients. Eventually such a system is needed regardless to culture large tissues. However the drawbacks of this approach are the complexity and costs for the system, it is problematic to integrate for all 9 culture wells and the evaporation problem would still be not solved but only minimized.

A second issue that needs to be solved before the bioreactor is fully operational and can be used for the mechanical stimulation is the control program on the micro controller. At the moment there are still problems with the reliability of the program and some minor software modifications are needed.

Besides the two mentioned tasks which are essential for the bioreactor functionality and necessary to be solved to reach the goal for which the reactor was designed, there are other tasks to enhance and improve the system. Here the design of a specialized culture chamber, which allows the in situ application of a microscope immersion

objective, should be mentioned. This would allow time lapse microscopy during mechanical stimulation and would allow to study effects of stimulation on the cells in real-time. Other areas where bioreactor usability and performance could be improved are electronics and programming. The programming at the moment is rudimentary and no optimization of the code was carried out. Precision and accuracy of the system could be improved by solving the problems related to the current control circuit in the electronics and optimization of the acceleration ramps. Addition of a keyboard and display together with a more complex software in order to establish a real human machine interface would improve the usability and allow the application of the bioreactor as a completely autonomic system. Additionally the integration of more sensors for example to measure gas composition and temperature and the ability to record these parameters would help to closely monitor the system and might allow better interpretation of cell experiments.

6.2 Possible scaffold materials

There are two different considerations for the future. One option is to use the material presented here and further characterize it, second is to use different materials and compare their performance to the results observed for the two fibers tested here. My plan for the near future is to do both types of experiments.

C-100 and H-100 fibers will be coated with laminin and cell experiments will be repeated. This experiment hopefully helps to distinguish if the observed differences in cell growth are mediated by surface chemistry or surface topography. The idea is to achieve a similar surface chemistry on both fibers to study the surface topography independently. It has to be investigated if this can be achieved with laminin coating. It is possible that the laminin absorbance is affected by the topography or the original surface chemistry. Staining for functional bound laminin should be able to determine the quality of the coating.

A second experiment which is already planned is to test a different fiber which was supplied by W. Zimmermann Gmbh. It has an elastic core fiber (Lycra) and is coated with a cellulose/chitosan fiber. This two fiber system significantly differs from the fibers tested in this thesis, it is much thicker and exhibits a more complex organization. Chitosan is a known biomaterial and has been used in several other applications.(121; 30) The plan is to compare the materials with each other and describe their suitability for muscle cell culture and future application.

Looking even further into the future there are several ideas for different materials and organized structured scaffold production. The current scaffold design is fairly simple and quasi 2-dimensional without defined fiber spacings and complex organization. In a first step exact parallel fiber alignment with defined spacing in 2-dimensional fiber system and later in 3-dimensional fiber organization should be investigated to study the effects on cells. One possible way to simply realize large quantities of complex scaffolds might be to use textile industry techniques for the production like knitting or weaving. In the future biodegradable materials should be considered which is especially important for medical applications as well as *in vitro*

meat products. Here the currently used material is not suitable. But it is possible to tailor the properties of polyurethane to match our requirements and simultaneously being biodegradable. Furthermore it might be beneficial to use different fiber types combined in one scaffold to get optimal performance and use synergy effects of different materials. For example hollow permeable fibers could be used to supply oxygen and nutrients to large muscle tissue constructs. Eventually it might be possible to co-culture endothelial cells in those hollow fibers to achieve real *in vitro* vascularization of the tissue.

6.3 Methods to study cell behavior in detail

In the area of cell culture the focus in the future should lie first on the explanation and reproduction of the observed cell behavior, for this purpose it would be necessary to use different analysis methods. Methods that give quantitative data should be used in conjunction with microscopy imaging techniques in order to get a more reliable view and stronger data to support explanations of cell behavior.

The MTT cell viability assay could be used for cell quantification. The protocols were developed during this thesis but it was not used for quantification of cells on elastic fibers. It should clearly be possible and requires a limited amount of time. A technique that gives even more detailed quantitative information about cells is Western blotting. There was insufficient time to include this method in the thesis but the reagents and equipment are available for immediate use. Prepared samples from cells cultured on plain surfaces are stored in the freezer and total protein concentration was already determined. By using the same MHC marker it would be possible to conduct information about the amount of expressed protein and allow the study of factors that influence the amount without constrains that imaging can have especially for complex 3-dimensional structures.

Later on real time polymerase chain reaction (RT-PCR) might be useful to study RNA levels and determine the activation and quantify the activity of different genes. This technique is widely used in cell biology and is nowadays a standard tool and available in many places. Even though I do not have the ability to do it in our lab there are several groups at Chalmers University, Gothenburg University and Sahlgrenska Medical School which have the required equipment and expertise.

Besides the application of quantitative techniques it should be considered to improve the existing imaging modalities and additionally use laser scanning confocal microscopy (LSCM). LSCM has a much higher z resolution and less blurring effect of overlaying structures. This would allow imaging of multi cell layers and cells on fibers in a more efficient way, revealing more details of the cell structure in such situations. It would give more information about small structures like the microfibril composition and would help to determine the formation of striation patterns. Furthermore it would enable the recording of z-stacks which can be reconstructed into 3-dimensional models and allow investigation of cell organization in complex scaffold structures. The main limitations at the moment are the cost to use the LSCM which hopefully will be solved soon. Our own fluorescent microscope could be used to in-

vestigate cell behavior from another angle using time lapse microscopy. This can help to understand the process of cell attachment and growth on fibers in general and find the mechanism underlaying the two observed phenomena (fiber bridging and twisting of cells). The idea is to genetically modify the cells to expressed fluorescently labeled actin or other cytoskeleton proteins. With time lapse microscopy it would be possible to follow those cells and study the organization and reorganization of the cytoskeleton in real time. Eventually it might be even possible to study the effects of mechanical stimulation of cells on fibers in real time with this technique.

Concerning the cell line it is suggested to keep on working with the C2C12 cells because they have shown good performance and are suitable for the current type of fundamental experiments. However it is important to mention that for later applications other cells must be used eventually. But the source of cells and availability should not be considered at the current stage of the project as well as co-culture systems which might be beneficial but complex to design and maintain.

Appendix A

Bioreactor drafts

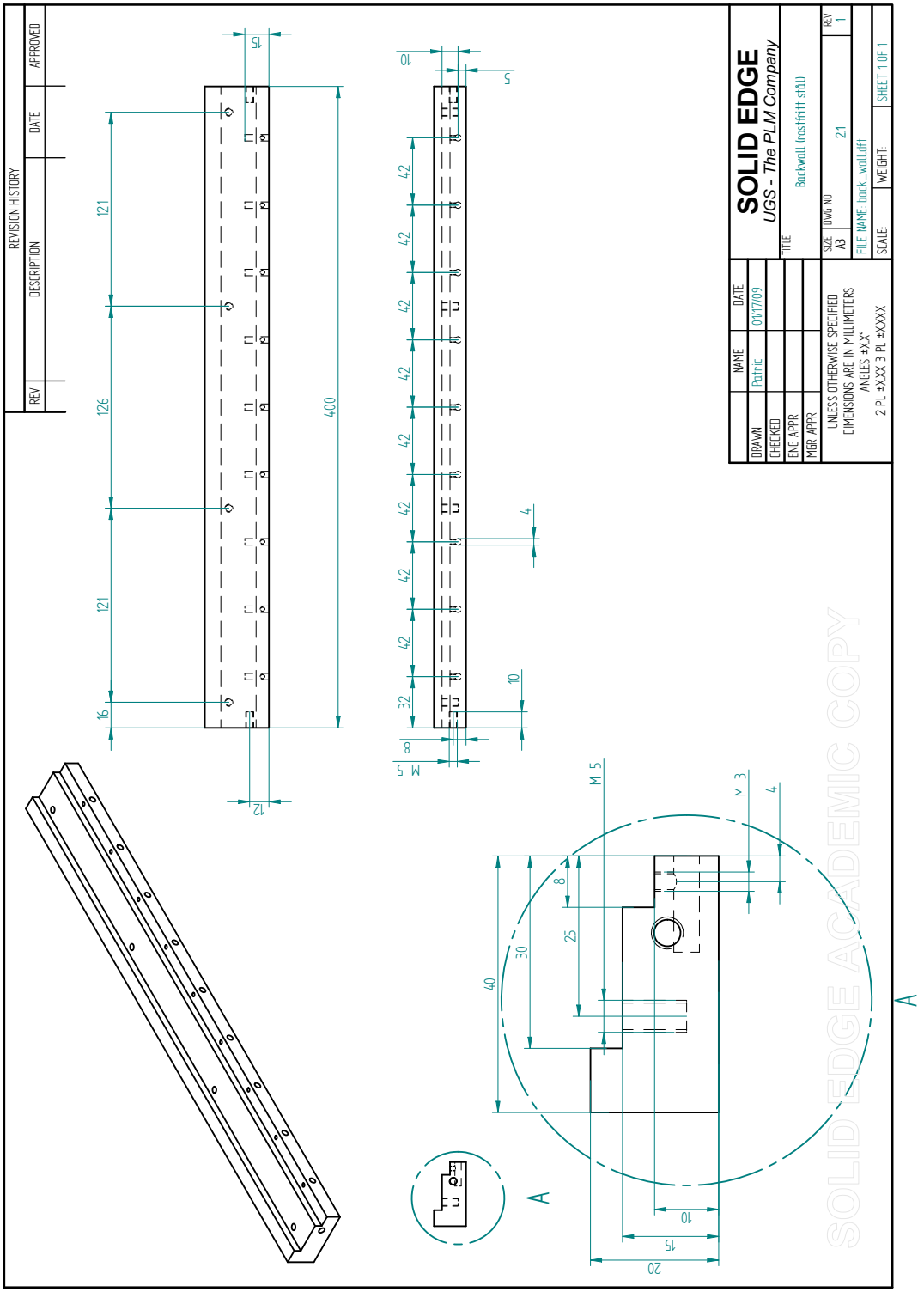

Figure A.1: Draft: Back wall of the culture chamber

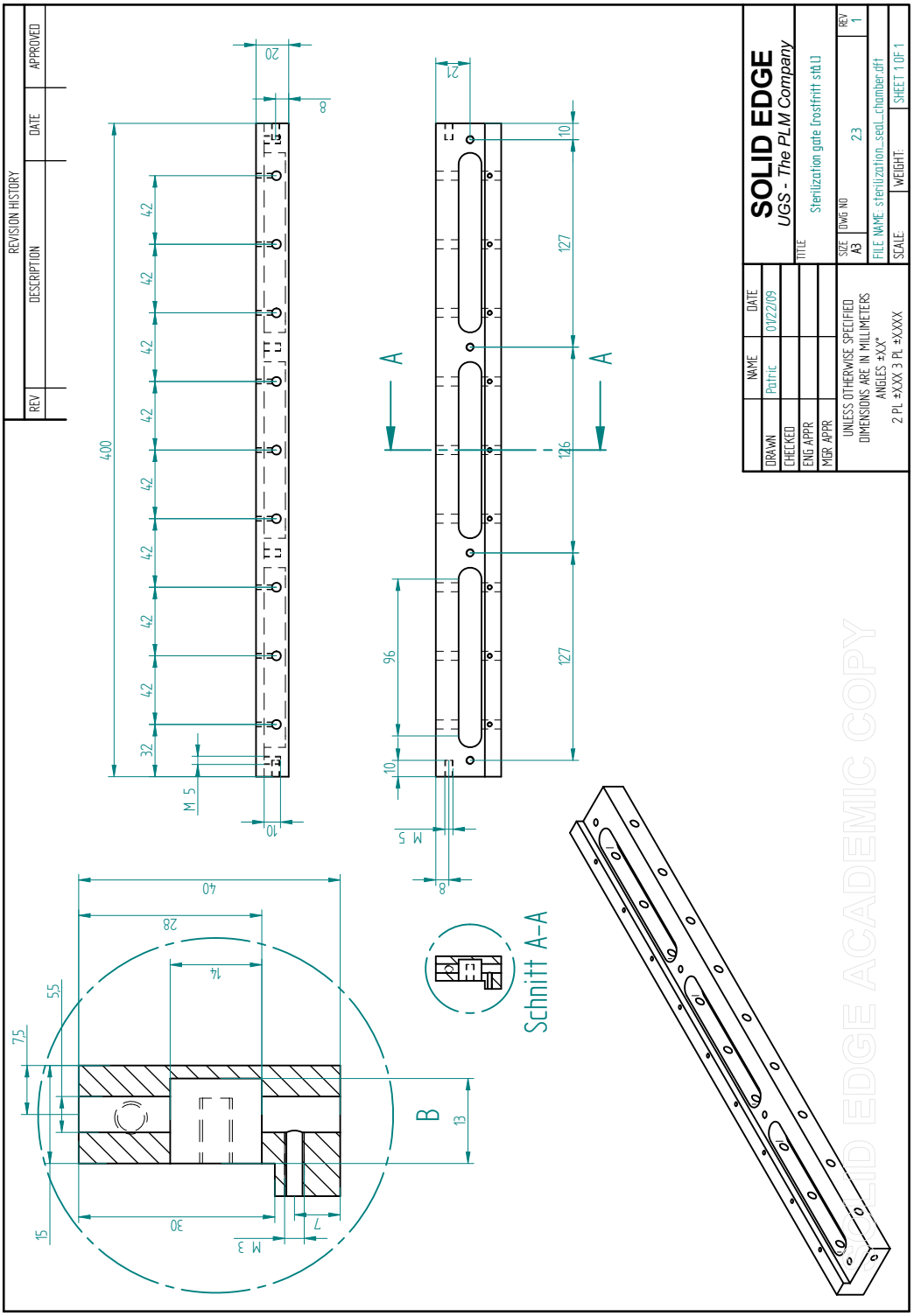

Figure A.2: Draft: Front wall of the culture chamber

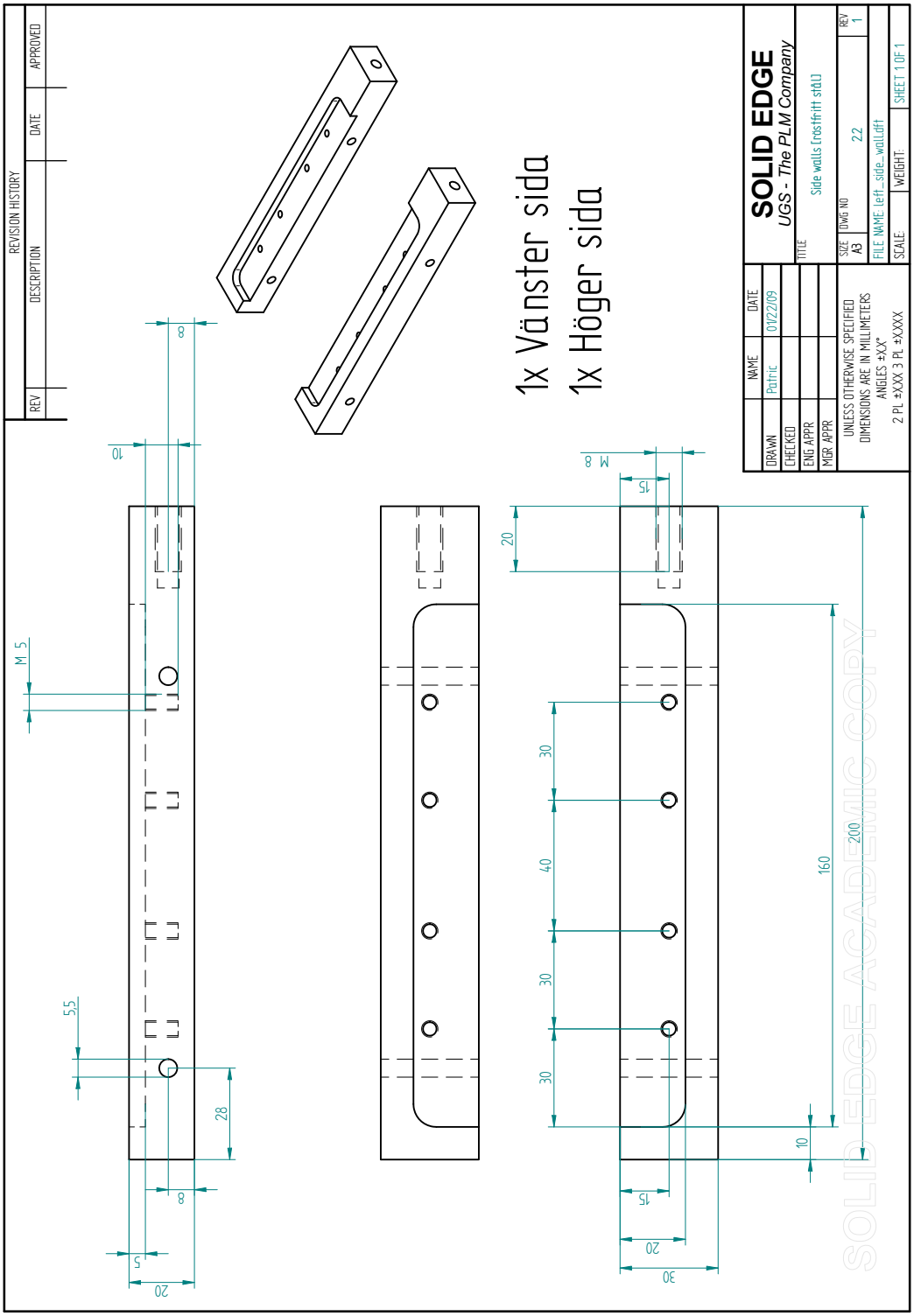

Figure A.3: Draft: Side wall of the culture chamber

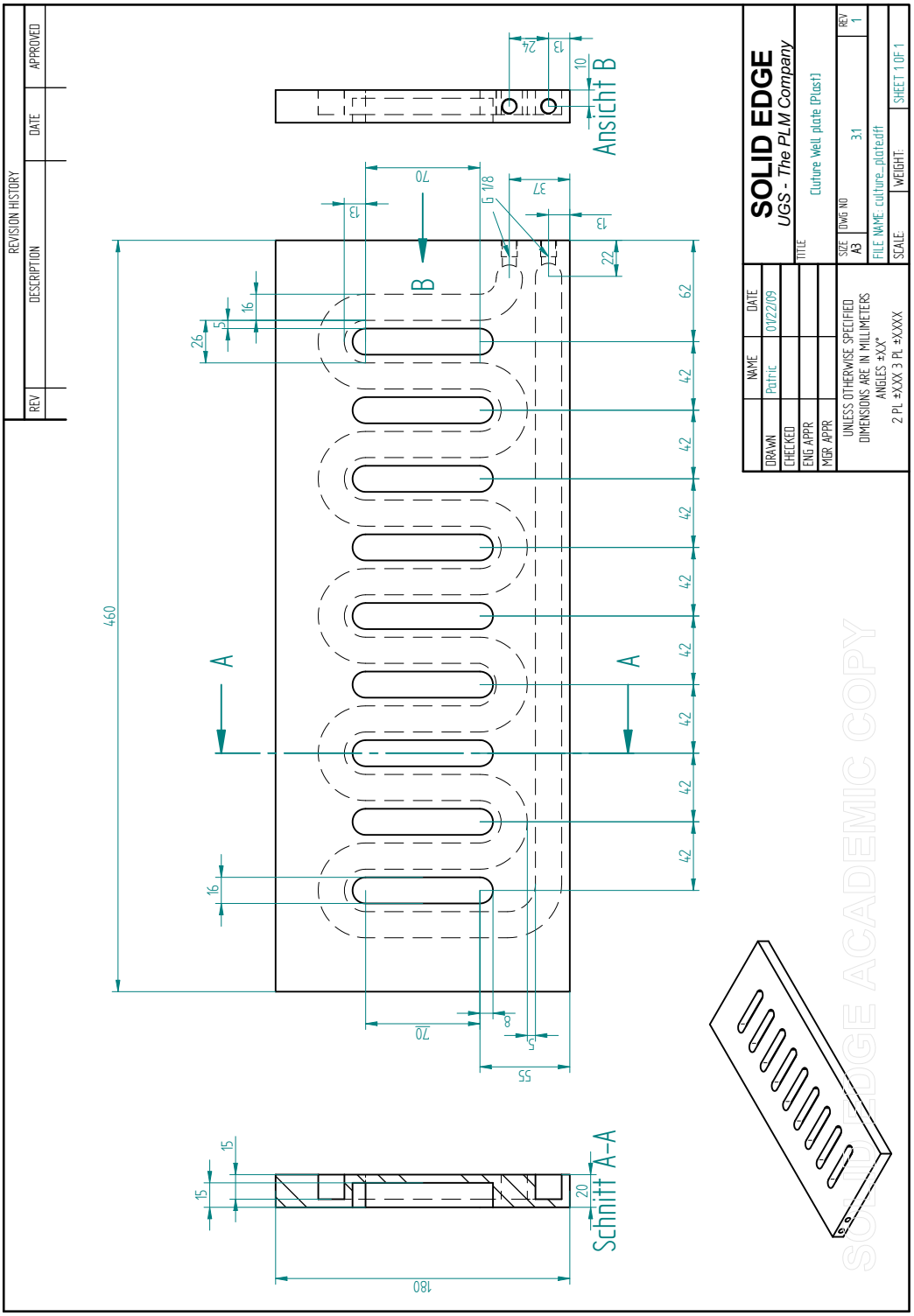

Figure A.4: Draft: Culture plate

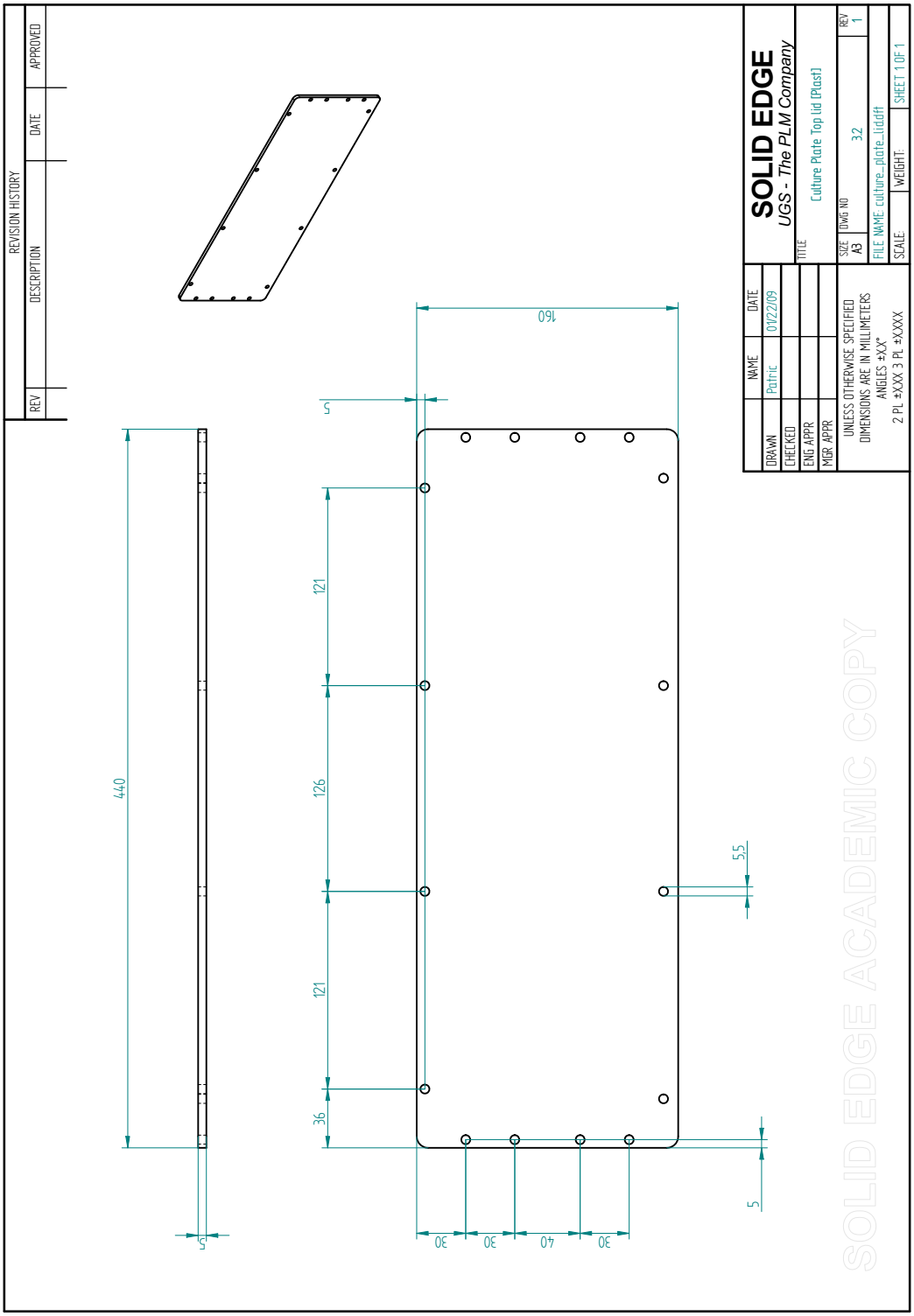

Figure A.5: Draft: Top lid of the culture chamber

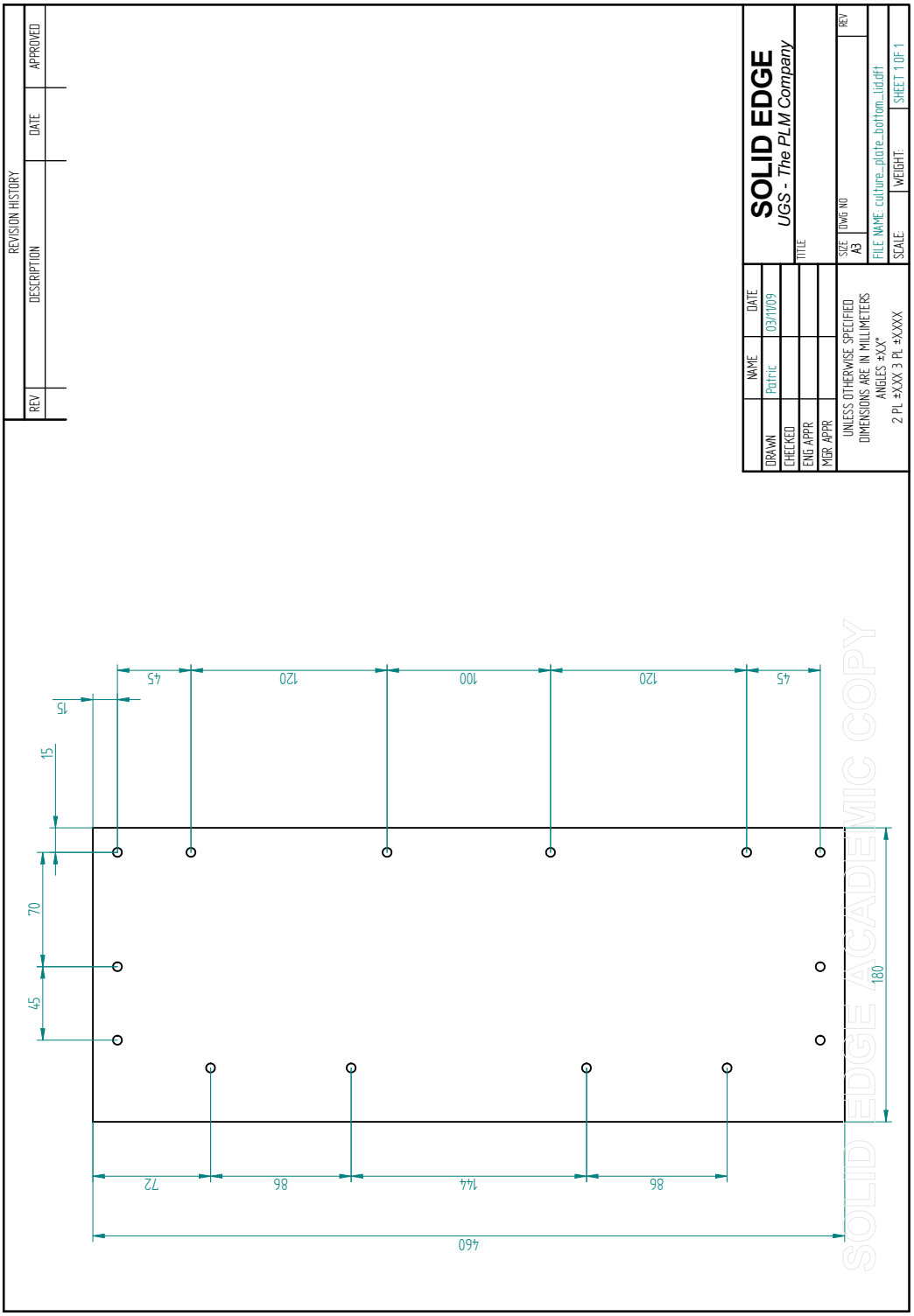

Figure A.6: Draft: Bottom lid of the culture chamber

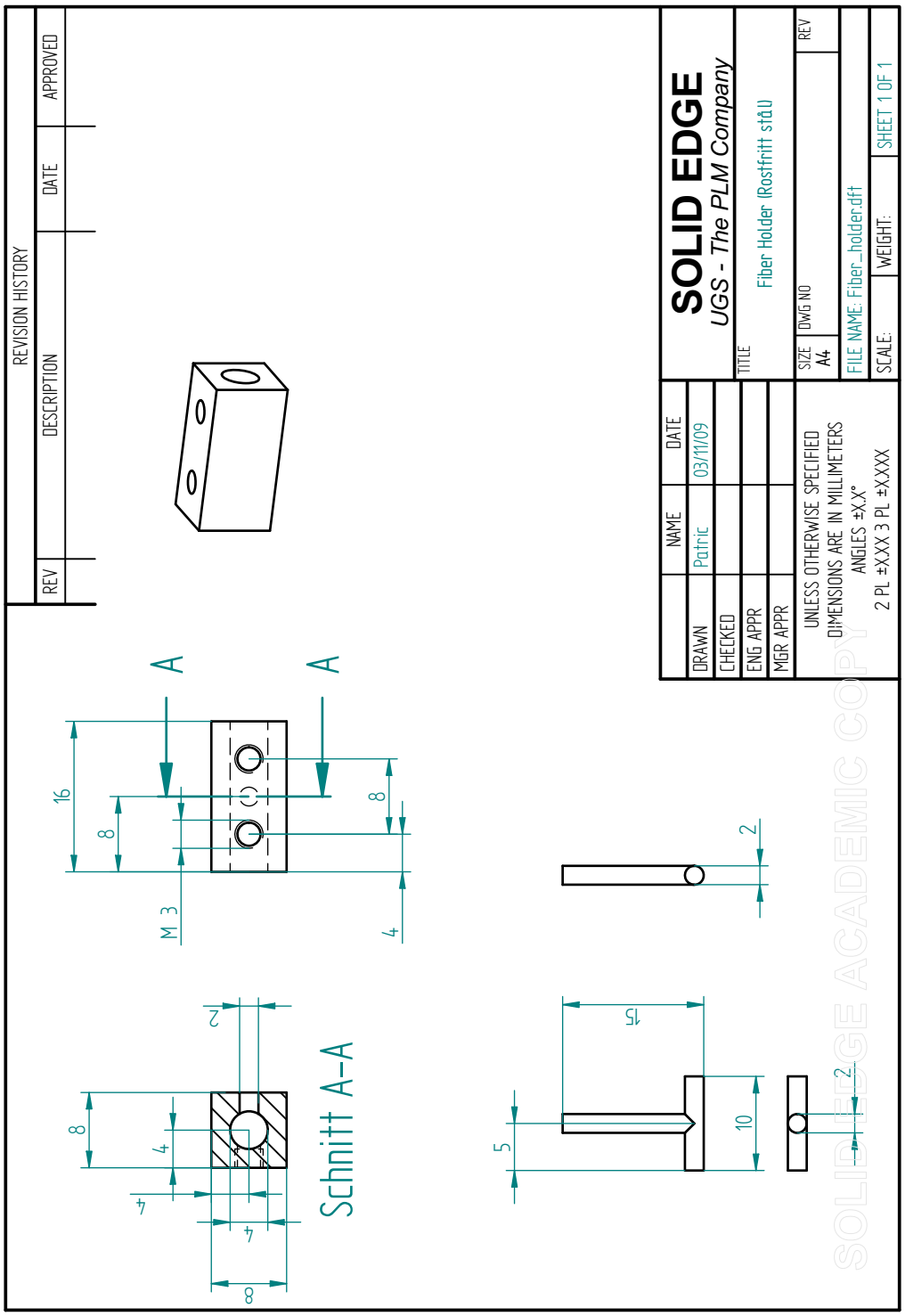

Figure A.7: Draft: Scaffold holder

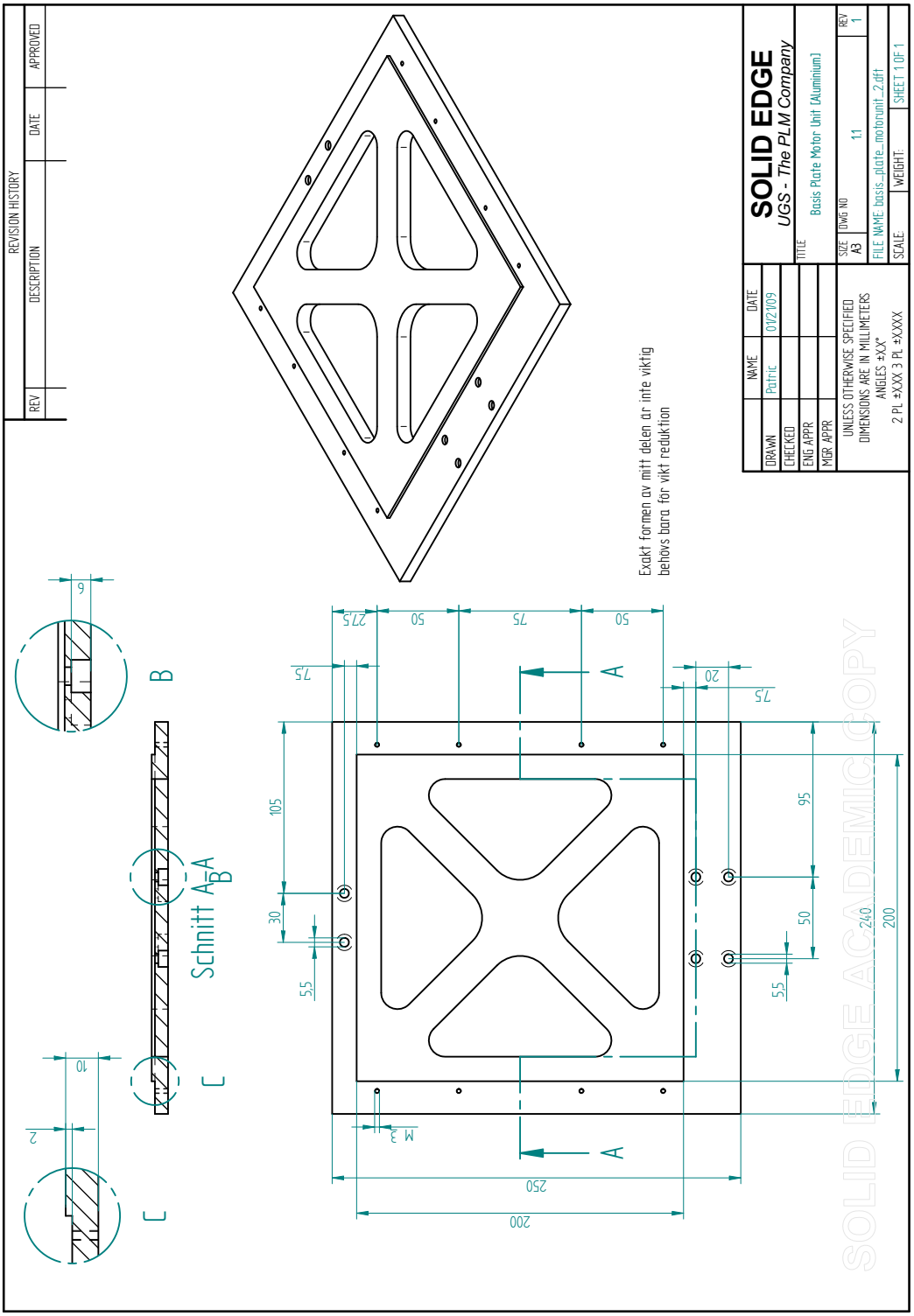

Figure A.8: Draft: Basis plate of the motor unit

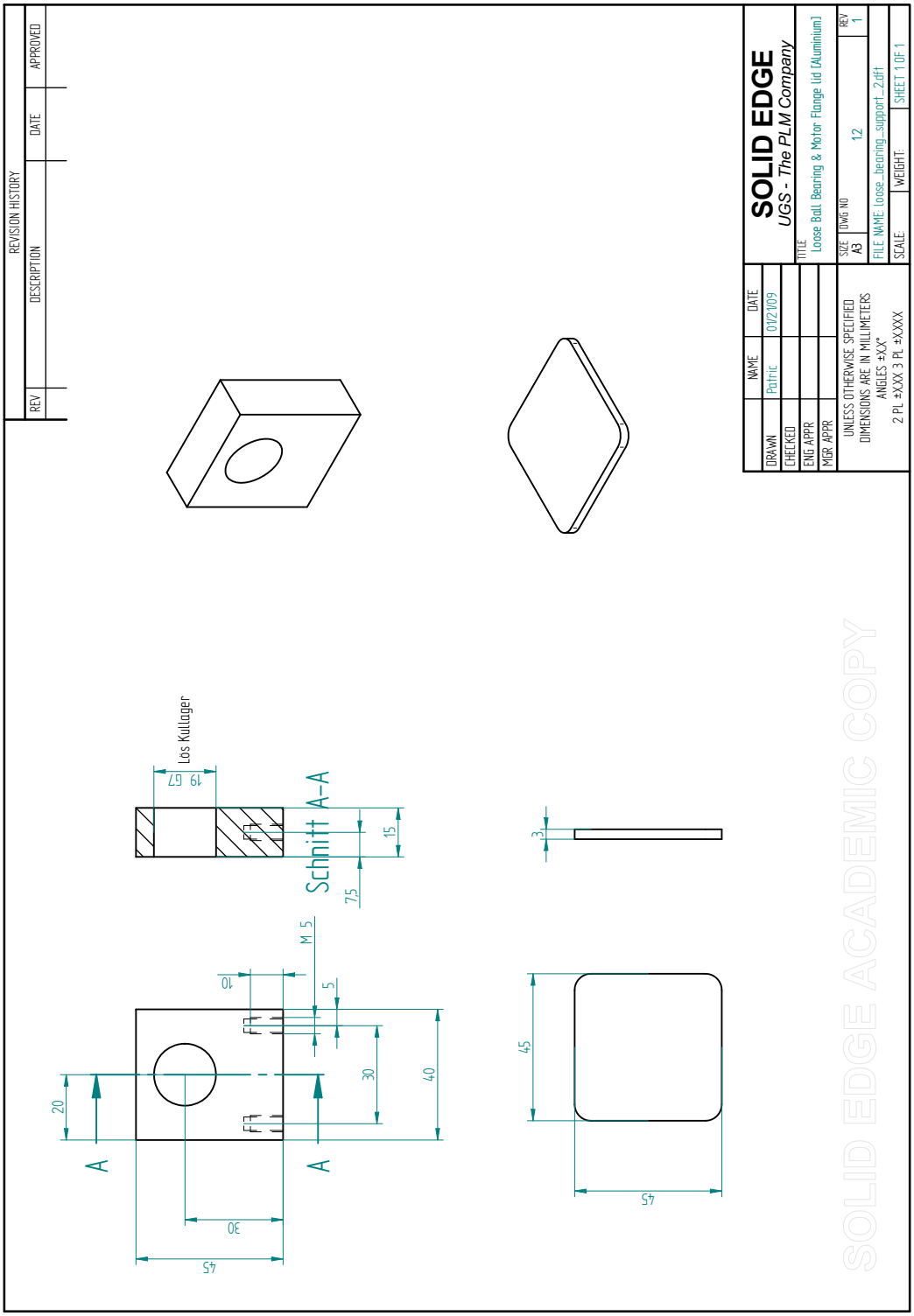

Figure A.9: Draft: Loose ball bearing support

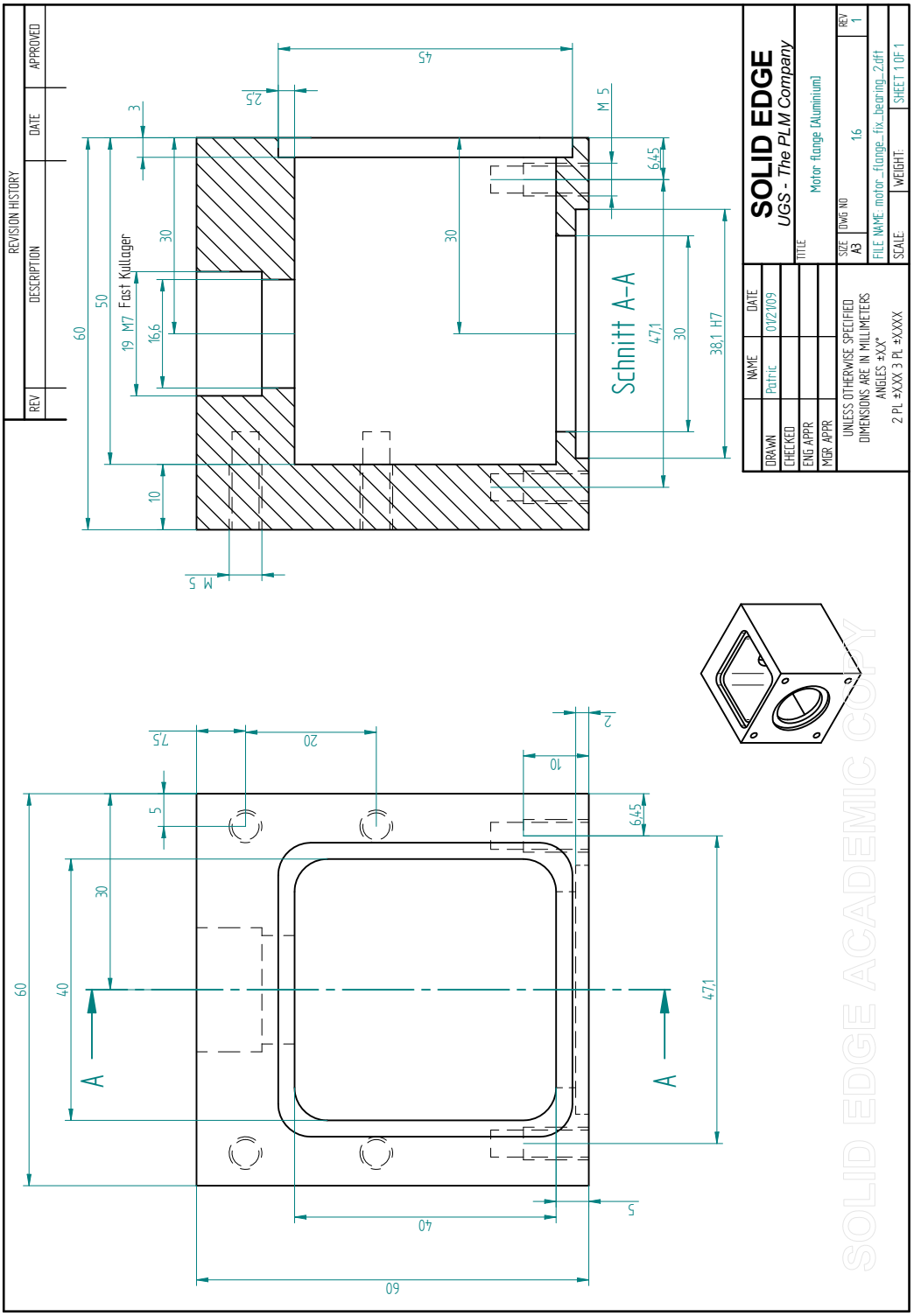

Figure A.10: Draft: Motor flange and fixed ball bearing support

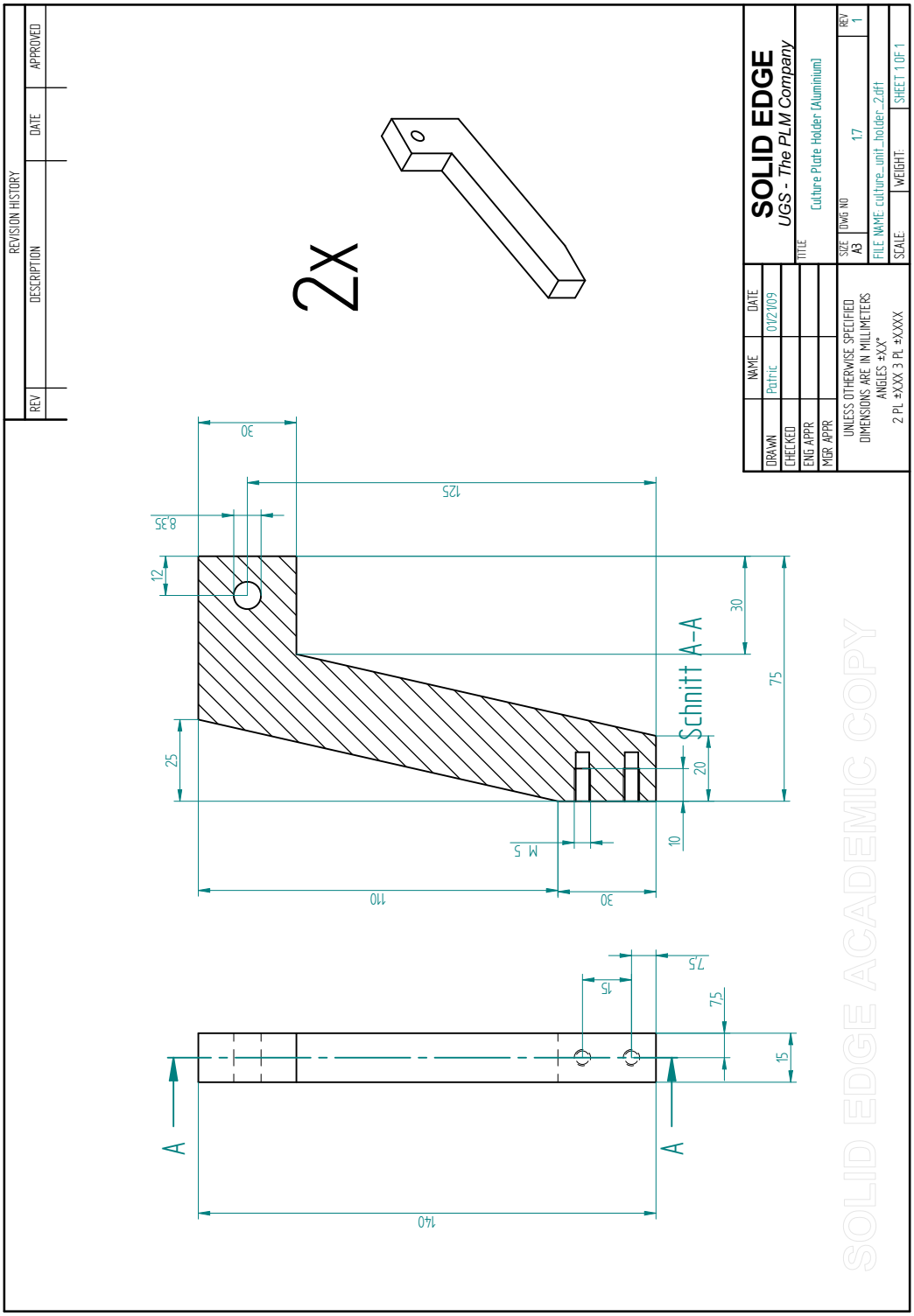

Figure A.11: Draft: Holder for the culture unit

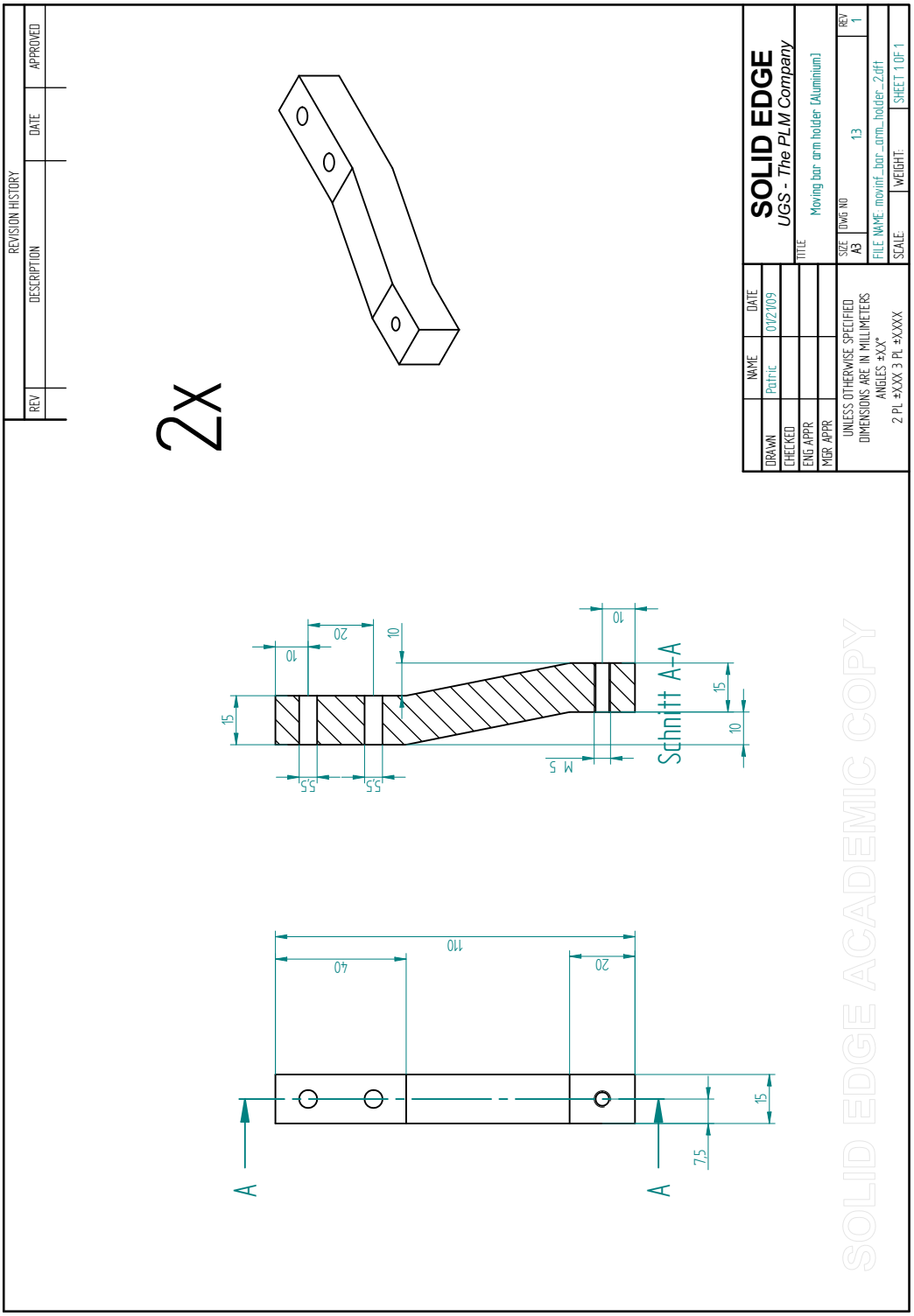

Figure A.12: Draft: Holder for the moving bar

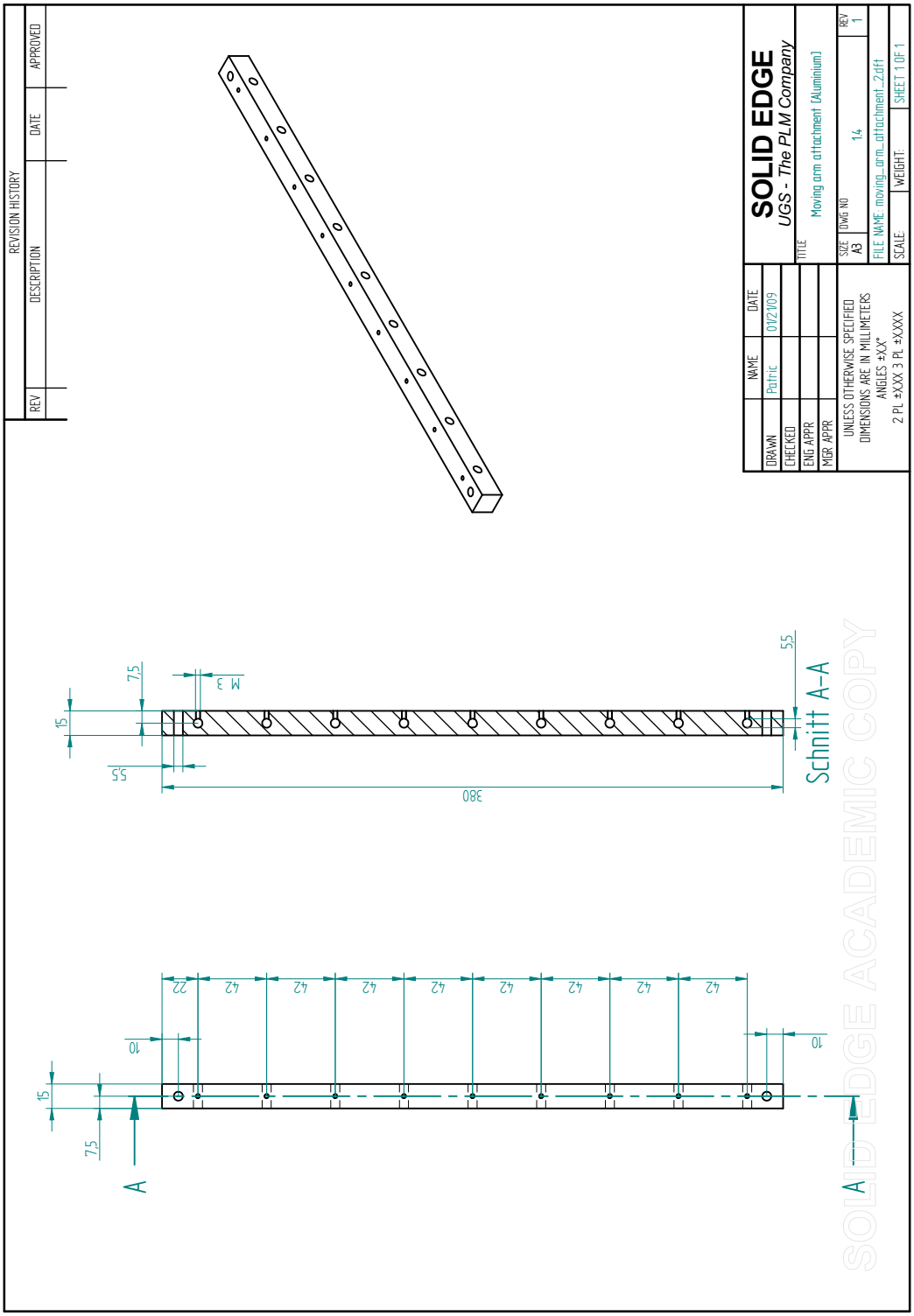

Figure A.13: Draft: Moving arm part for metal shaft attachment

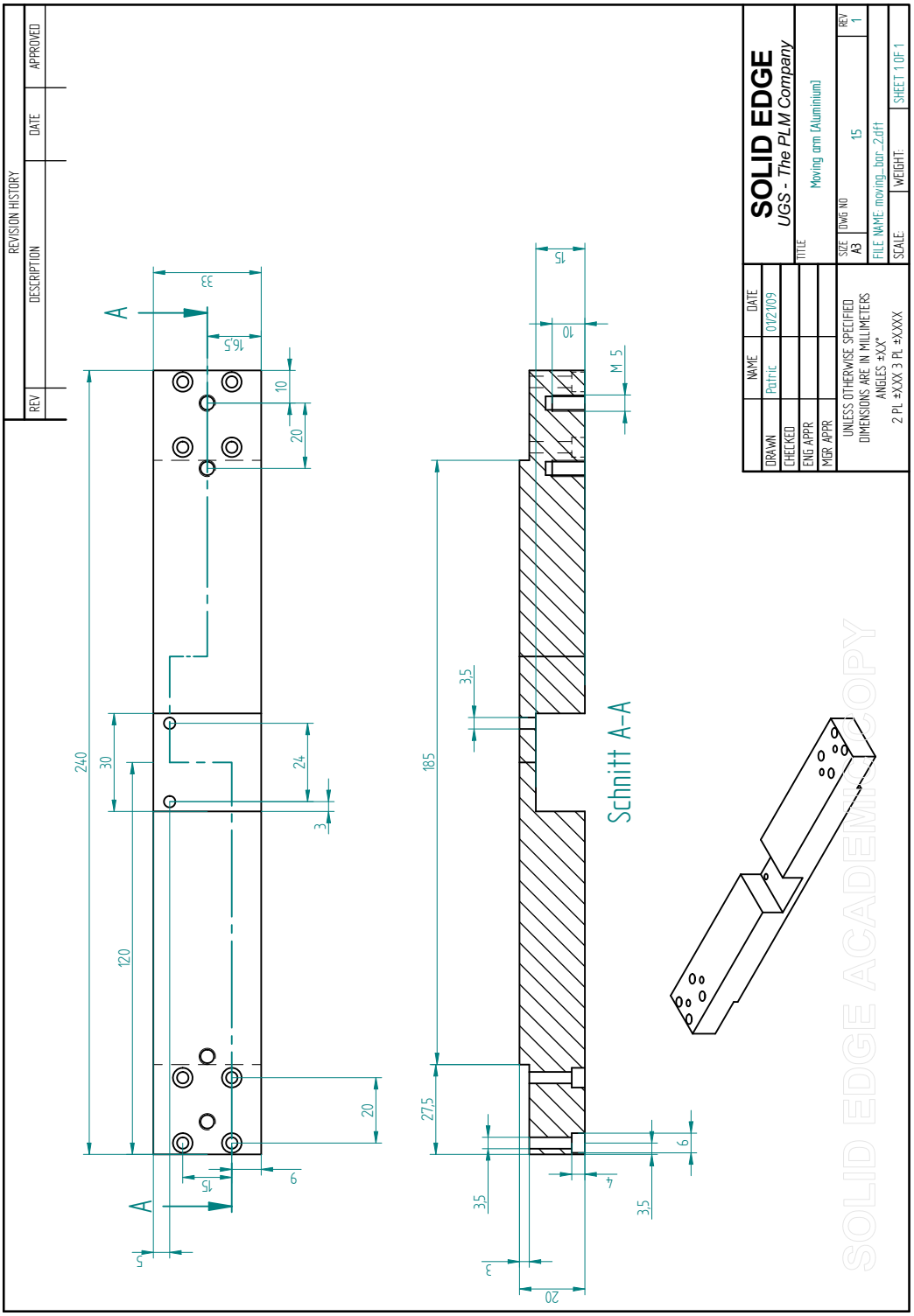

Figure A.14: Draft: Moving arm part for connection between both carriages

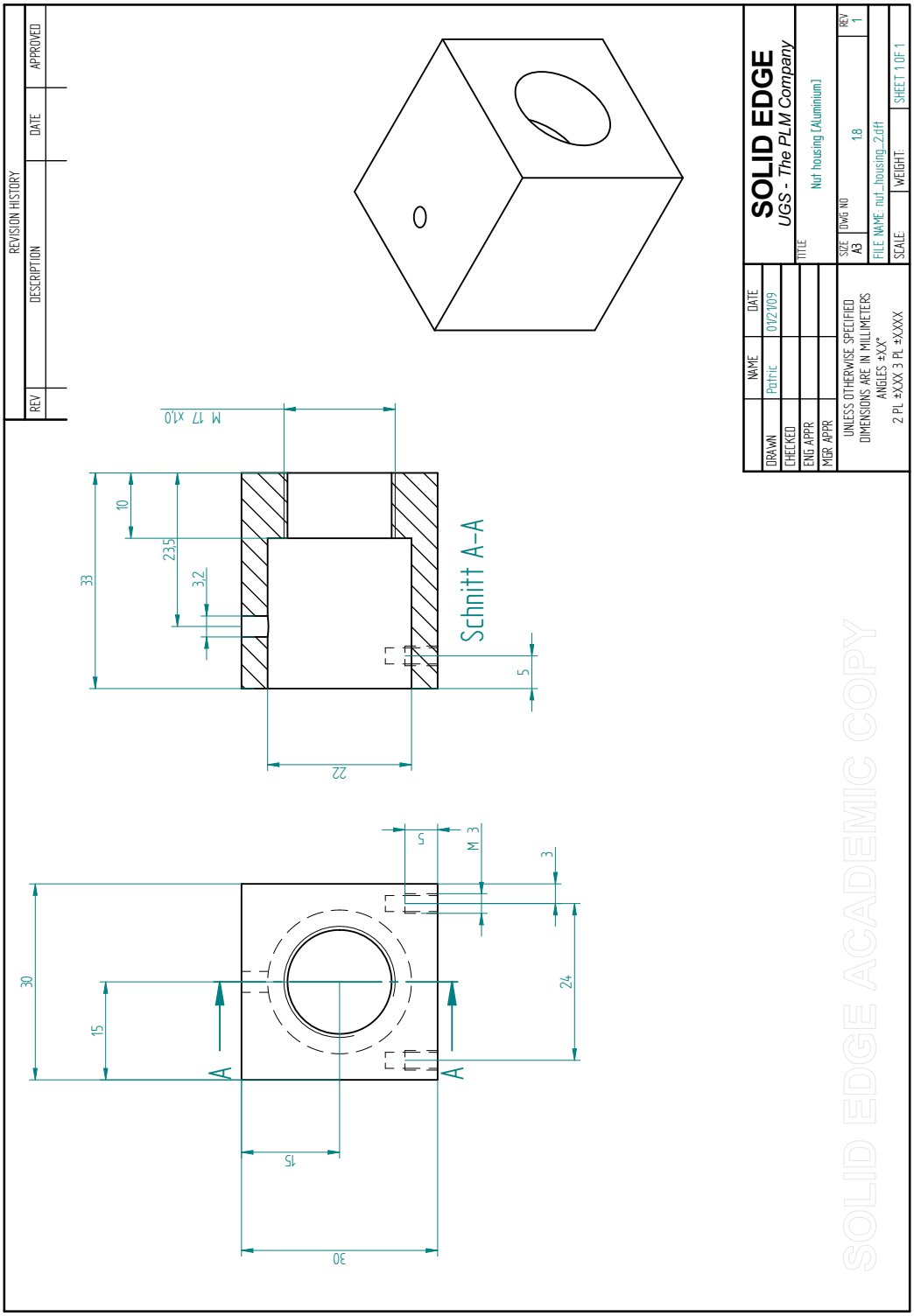

Figure A.15: Draft: Nut housing for the ball screw

Appendix B

Electronics

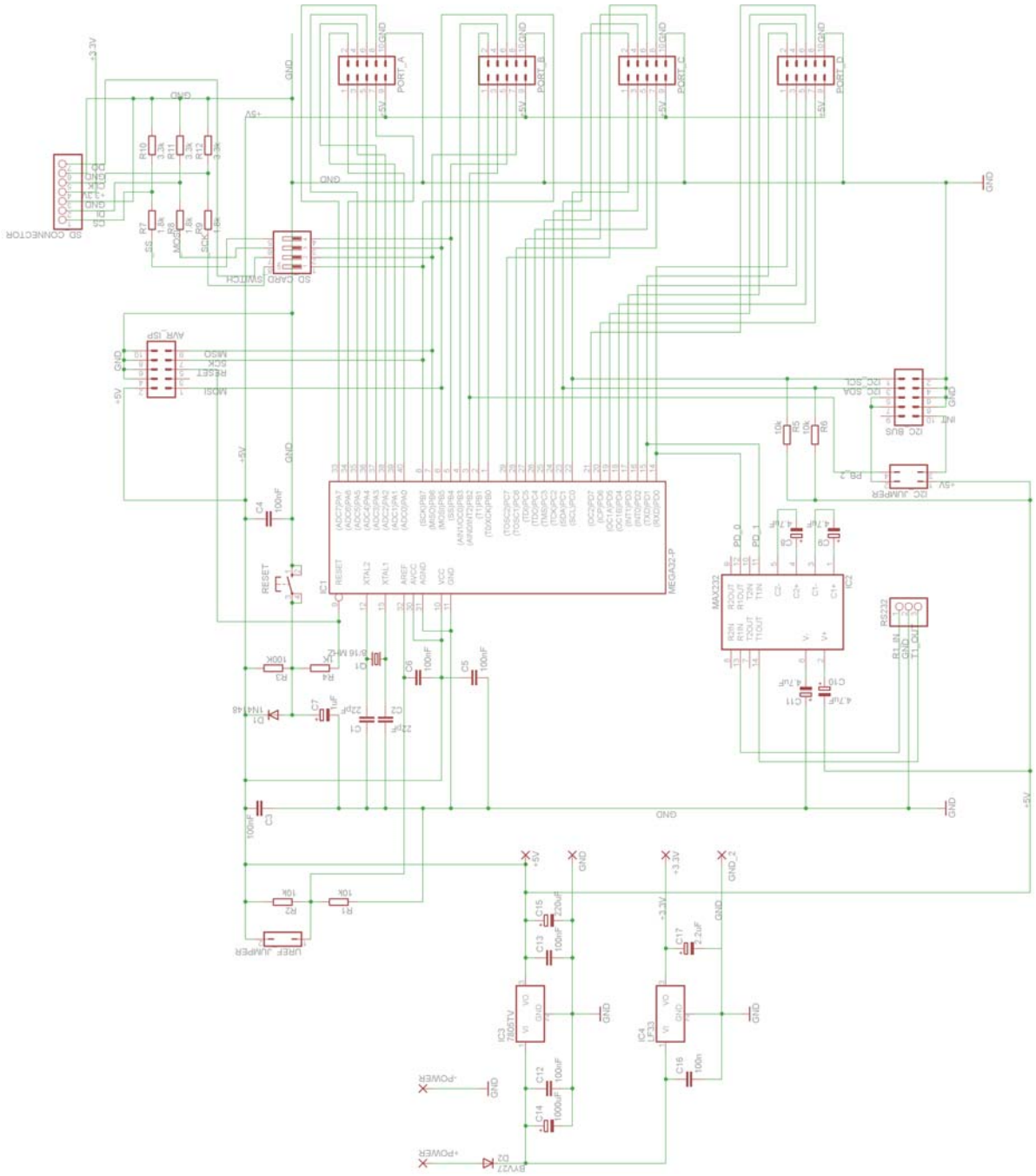

Figure B.1: Circuit diagram micro controller board

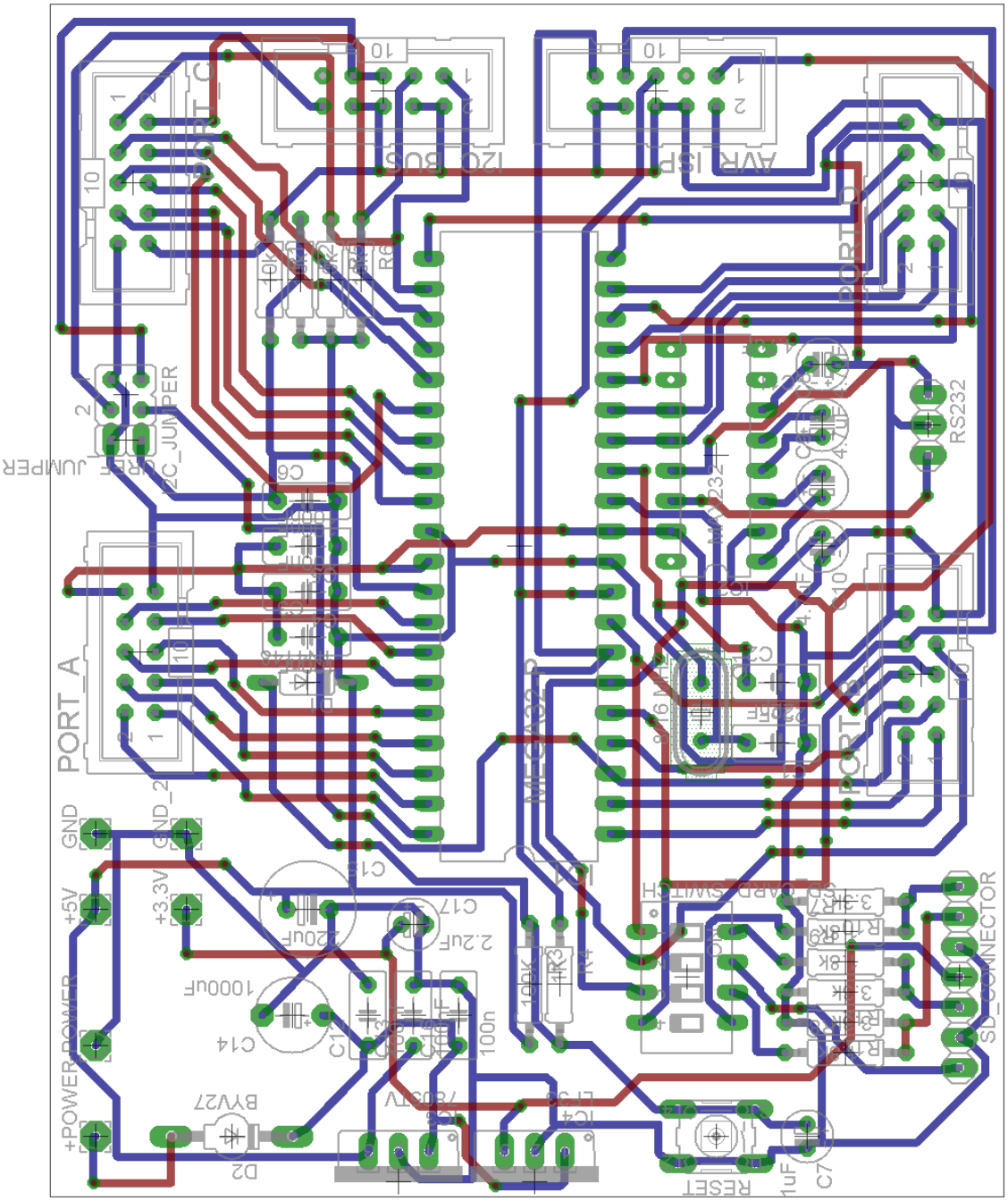

Figure B.2: PCB design micro controller board

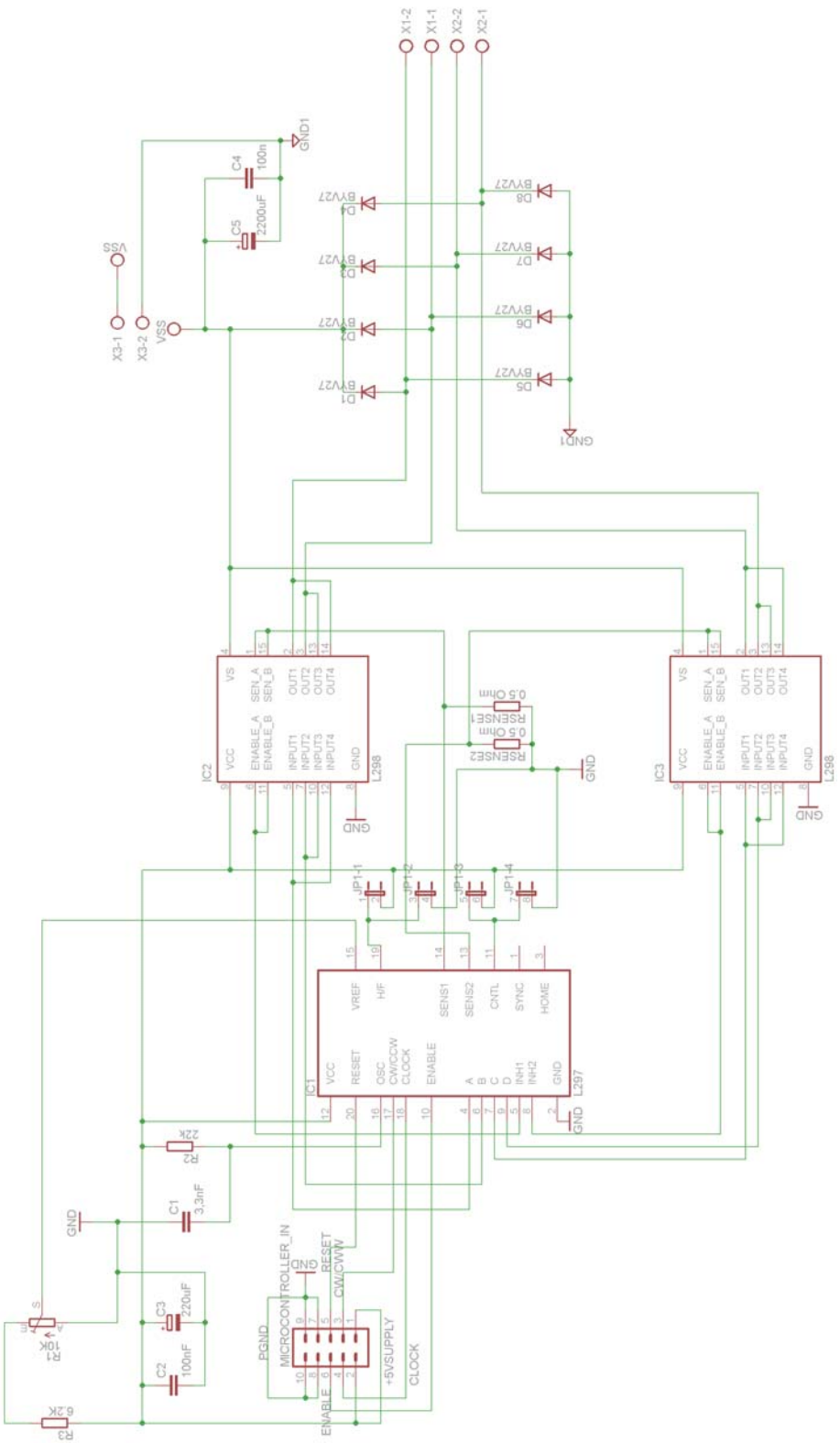

Figure B.3: Circuit diagram stepper driver board

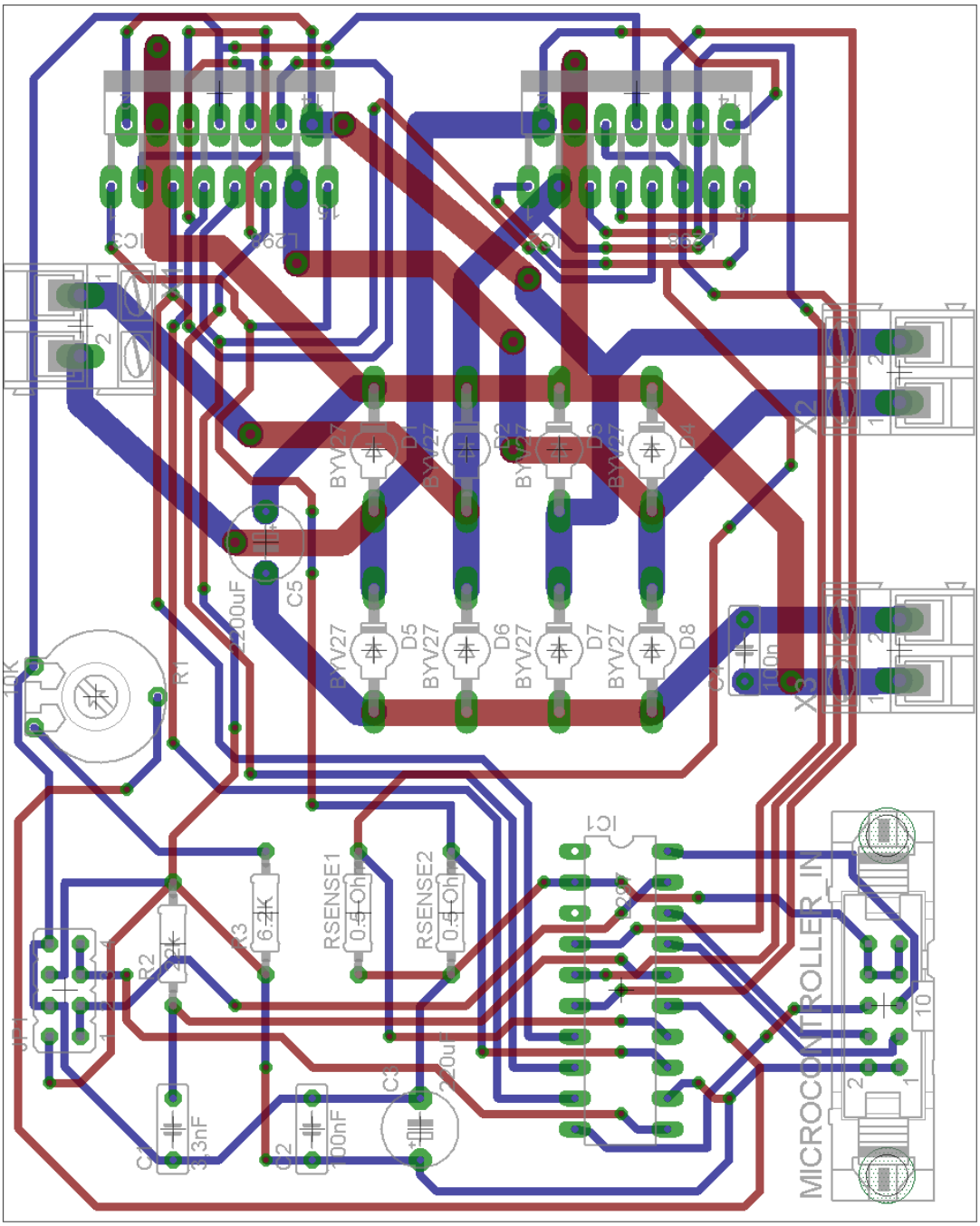

Figure B.4: PCB design stepper driver board

Appendix C

Micro controller source code

```
1  // Including the required libraries
2  #include <avr/io.h>      // I/O functionality
3  #include <stdint.h>      // Data type definition library
4  #include <avr/interrupt.h> // Interrupt library
5  #include <avr/wdt.h>
6
7  volatile uint8_t x=0;
8  volatile uint8_t z=0;
9
10
11
12 ISR(TIMER0_COMP_vect)
13 {
14          x++;
15          z++;
16          PORTD |= ( 1 << PD3 );
17 }
18
19 int main (void)
20 {
21
22 ////////////////////////////////////
23 // Definition of the variables
24 ////////////////////////////////////
25
26
27 DDRC |= (1 << PC2 ); //Status LED
28
29 DDRD |= (1 << PD2 ); //high=CCW low=CW
30 DDRD |= (1 << PD3 ); //Clock
31 DDRD |= (1 << PD4 ); //Reset
32 DDRD |= (1 << PD5 ); //Enable
```

```
33
34
35
36 /*
37 PORTD &= ~( 1 << PD2 );
38 PORTD &= ~( 1 << PD3 );
39 PORTD &= ~( 1 << PD4 );
40 PORTD &= ~( 1 << PD5 );
41 PORTD &= ~( 1 << PD6 );
42 */
43 PORTD |= ( 1 << PD2 ); //CCW
44
45 //PORTD |= ( 1 << PD3 );
46 PORTD |= ( 1 << PD4 ); //No reset
47 PORTD |= ( 1 << PD5 ); //Motor activation
48
49 TCCR0 |= (1<<WGM01); // CTC mode activation
50 //TCCR0 |= (1<<CS00); // Setting timer0 prescaler 8
51 TCCR0 |= (1<<CS01);
52 //TCCR0 |= (1<<CS02);
53 TIMSK |= (1<<OCIE0); // Enable the interrupt for a compare match
54 OCR0=200;
55
56 uint8_t wait=0;
57 uint8_t y=0;
58 uint8_t step=0;
59 uint8_t halfturn=0;
60 uint8_t direction=1;
61
62 sei(); // IR activation
63
64 while(1)
65 {
66 // Program activation / deactivation
67
68         // Real-time control
69         if (x==50)
70         {
71                 y++;
72                 x=0;
73         }
74
75         if (y==50)
76         {
77                 PORTC |= ( 1 << PC2 );
```

```
78          }
79
80          if (y==100)   //Second
81          {
82                  PORTC &= ~( 1 << PC2 );
83                  y=0;
84                  wait++;
85          }
86
87          //Precesion testing program
88
89          if ((z==7) && (wait>=2)) //5=1000Hz 10=500Hz 25=200Hz 50=100 Hz
90          {
91                  PORTD &= ~( 1 << PD3 );
92                  step++;
93                  z=0;
94          }
95
96          if (step==200) // Turn counter
97          {
98                  halfturn++;
99                  step=0;
100         }
101
102         if ((direction==1) && (halfturn==6))
103         {
104                 PORTD &= ~( 1 << PD2 );          //CW
105                 halfturn=0;
106                 direction=2;
107                 wait=0;
108         }
109
110         if ((direction==2) && (halfturn==6))
111         {
112                 PORTD |= ( 1 << PD2 );           //CCW
113                 halfturn=0;
114                 direction=1;
115                 wait=0;
116         }
117 }
118         return 0;
119 }
```

References

[1] N. I. o. B. I. NIH and Bioengineering, "Regenerative medicine," tech. rep., NIH, June 2004.

[2] R. Langer and J. P. Vacanti, "Tissue engineering," *Science*, vol. 260, no. 5110, pp. 920–926, 1993.

[3] K. George, A. Djordje, A. Douglas, B. G. Robert, G. Ronald, H. Paul, A. K. Penelope, S. Eric, S. Desmond, V. Michel, V. W. Gordon, A. Michael, D. Catherine, and G. W. Ronald, "Myoblast transfer in duchenne muscular dystrophy," *Annals of Neurology*, vol. 34, no. 1, pp. 8–17, 1993.

[4] J. T. Vilquin, "Myoblast transplantation: clinical trials and perspectives. minireview," *Acta Myol*, vol. 24, no. 2, pp. 119–27, 2005.

[5] W. N. Bian and N. Bursac, "Tissue engineering of functional skeletal muscle: challenges and recent advances," *Ieee Engineering in Medicine and Biology Magazine*, vol. 27, no. 5, pp. 109–113, 2008.

[6] A. D. Bach, J. P. Beier, J. Stern-Staeter, and R. E. Horch, "Skeletal muscle tissue engineering," *Journal of Cellular and Molecular Medicine*, vol. 8, no. 4, pp. 413–422, 2004.

[7] H. Vandenburgh, J. Shansky, F. Benesch-Lee, V. Barbata, J. Reid, L. Thorrez, R. Valentini, and G. Crawford, "Drug-screening platform based on the contractility of tissue-engineered muscle," in *Keystone Symposium on Tissue Engineering and Development Biology*, (Snowbird, UT), pp. 438–447, John Wiley & Sons Inc, 2007.

[8] P. D. Edelman, D. C. McFarland, V. A. Mironov, and J. G. Matheny, "In vitro-cultured meat production," *Tissue Engineering*, vol. 11, no. 5-6, pp. 659–662, 2005.

[9] P. Boudreault, "Scale-up of a myoblast culture process," *Journal of Biotechnology*, vol. 91, no. 1, pp. 63–74, 2001.

[10] C. Bardouille, J. Lehmann, P. Heimann, and H. Jockusch, "Growth and differentiation of permanent and secondary mouse myogenic cell lines on microcarriers," *Applied Microbiology and Biotechnology*, vol. 55, no. 5, pp. 556–562, 2001.

[11] A. M. Collinsworth, C. E. Torgan, S. N. Nagda, R. J. Rajalingam, W. E. Kraus, and G. A. Truskey, "Orientation and length of mammalian skeletal myocytes in response to a unidirectional stretch," *Cell and Tissue Research*, vol. 302, no. 2, pp. 243–251, 2000.

[12] D. G. Moon, G. Christ, J. D. Stitzel, A. Atala, and J. J. Yoo, "Cyclic mechanical preconditioning improves engineered muscle contraction," *Tissue Engineering Part A*, vol. 14, no. 4, pp. 473–482, 2008.

[13] IUPAC, *Compendium of Chemical Terminology*. Oxford: Blackwell Scientific Publications, 2 ed., 1997.

[14] I. Martin, D. Wendt, and M. Heberer, "The role of bioreactors in tissue engineering," *Trends in Biotechnology*, vol. 22, no. 2, pp. 80–86, 2004.

[15] G. C. Engelmayr, D. K. Hildebrand, F. W. H. Sutherland, J. E. Mayer, and M. S. Sacks, "A novel bioreactor for the dynamic flexural stimulation of tissue engineered heart valve biomaterials," *Biomaterials*, vol. 24, no. 14, pp. 2523–2532, 2003.

[16] R. I. Freshney, *Culture of animal cells : a manual of basic technique*. Hoboken, N.J. Chichester: Wiley ; John Wiley [distributor], 5. ed., 2005.

[17] Y. A. Engel, *Heat transfer : a practical approach*. Boston: WCB/McGraw-Hill, cop., 1998.

[18] H. Eagle, "Buffer combinations for mammalian cell culture," *Science*, vol. 174, no. 4008, pp. 500–503, 1971.

[19] M. V. Chakravarthy, E. E. Spangenburg, and F. W. Booth, "Culture in low levels of oxygen enhances in vitro proliferation potential of satellite cells from old skeletal muscles," *Cellular and Molecular Life Sciences*, vol. 58, no. 8, pp. 1150–1158, 2001.

[20] B. Palsson and S. Bhatia, *Tissue engineering*. Upper Saddle River, N.J.: Pearson Prentice Hall, 2004.

[21] T. J. Goodwin, T. L. Prewett, A. W. David, and G. F. Spaulding, "Reduced shear stress: A major component in the ability of mammalian tissues to form three-dimensional assemblies in simulated microgravity," *Journal of Cellular Biochemistry*, vol. 51, no. 3, pp. 301–311, 1993.

[22] J. A. Chromiak, J. Shansky, C. Perrone, and H. H. Vandenburgh, "Bioreactor perfusion system for the long-term maintenance of tissue-engineered skeletal muscle organoids," *In Vitro Cellular & Developmental Biology-Animal*, vol. 34, no. 9, pp. 694–703, 1998.

[23] B. D. Ratner, *Biomaterials science : an introduction to materials in medicine*. Amsterdam: Elsevier Academic Press, 2004. 2. ed.

[24] D. E. Ingber, "Mechanobiology and diseases of mechanotransduction," *Annals of Medicine*, vol. 35, no. 8, pp. 564–577, 2003.

[25] A. Kumar, R. Murphy, P. Robinson, L. Wei, and A. M. Boriek, "Cyclic mechanical strain inhibits skeletal myogenesis through activation of focal adhesion kinase, rac-1 gtpase, and nf-kappa b transcription factor," *Faseb Journal*, vol. 18, no. 13, pp. 1524–1535, 2004.

[26] I. C. Liao, J. B. Liu, N. Bursac, and K. W. Leong, "Effect of electromechanical stimulation on the maturation of myotubes on aligned electrospun fibers," *Cellular and Molecular Bioengineering*, vol. 1, no. 2-3, pp. 133–145, 2008.

[27] K. Webb, R. W. Hitchcock, R. M. Smeal, W. H. Li, S. D. Gray, and P. A. Tresco, "Cyclic strain increases fibroblast proliferation, matrix accumulation, and elastic modulus of fibroblast-seeded polyurethane constructs," *Journal of Biomechanics*, vol. 39, no. 6, pp. 1136–1144, 2006.

[28] C. A. Powell, B. L. Smiley, J. Mills, and H. H. Vandenburgh, "Mechanical stimulation improves tissue-engineered human skeletal muscle," *American Journal of Physiology-Cell Physiology*, vol. 283, no. 5, pp. C1557–C1565, 2002.

[29] D. Gadre, *Programming and customizing the AVR microcontroller*. Boston: McGraw-Hill Professiona, 2000.

[30] F. Couet, N. Rajan, and D. Mantovani, "Macromolecular biomaterials for scaffold-based vascular tissue engineering," *Macromolecular bioscience*, vol. 7, no. 5, pp. 701–18, 2007.

[31] L. J. Bonassar and C. A. Vacanti, "Tissue engineering: the first decade and beyond," *J Cell Biochem Suppl*, vol. 30-31, pp. 297–303, 1998.

[32] D. Williams, "Revisiting the definition of biocompatibility," *Med Device Technol*, vol. 14, no. 8, pp. 10–3, 2003.

[33] D. W. Hutmacher, "Scaffold design and fabrication technologies for engineering tissues - state of the art and future perspectives," *Journal of Biomaterials Science-Polymer Edition*, vol. 12, no. 1, pp. 107–124, 2001.

[34] A. J. Engler, M. A. Griffin, S. Sen, C. G. Bonnemann, H. L. Sweeney, and D. E. Discher, "Myotubes differentiate optimally on substrates with tissue-like stiffness: pathological implications for soft or stiff microenvironments," *J. Cell Biol.*, vol. 166, no. 6, pp. 877–887, 2004.

[35] M. P. Linnes, B. D. Ratner, and C. M. Giachelli, "A fibrinogen-based precision microporous scaffold for tissue engineering," *Biomaterials*, vol. 28, no. 35, pp. 5298–5306, 2007.

[36] S. C. Bryer and T. J. Koh, "Mechanical strain increases gene transfer to skeletal muscle cells," *Journal of Biomechanics*, vol. 40, no. 9, pp. 1995–2001, 2007.

[37] M. T. Lam, S. Sim, X. Y. Zhu, and S. Takayama, "The effect of continuous wavy micropatterns on silicone substrates on the alignment of skeletal muscle myoblasts and myotubes," *Biomaterials*, vol. 27, no. 24, pp. 4340–4347, 2006.

[38] S. A. Riboldi, M. Sampaolesi, P. Neuenschwander, G. Cossu, and S. Mantero, "Electrospun degradable polyesterurethane membranes: potential scaffolds for skeletal muscle tissue engineering," *Biomaterials*, vol. 26, no. 22, pp. 4606–4615, 2005.

[39] T. Neumann, S. D. Hauschka, and J. E. Sanders, "Tissue engineering of skeletal muscle using polymer fiber arrays," *Tissue Engineering*, vol. 9, no. 5, pp. 995–1003, 2003.

[40] L. Thorrez, J. Shansky, L. Wang, L. Fast, T. V. Driessche, M. Chuah, D. Mooney, and H. Vandenburgh, "Growth, differentiation, transplantation and survival of human skeletal myofibers on biodegradable scaffolds," *Biomaterials*, vol. 29, no. 1, pp. 75–84, 2008.

[41] F. S. Kamelger, R. Marksteiner, E. Margreiter, G. Klima, G. Wechselberger, S. Hering, and H. Piza, "A comparative study of three different biomaterials in the engineering of skeletal muscle using a rat animal model," *Biomaterials*, vol. 25, no. 9, pp. 1649–1655, 2004.

[42] H. H. Vandenburgh, S. Hatfaludy, P. Karlisch, and J. Shansky, "Skeletal-muscle growth is stimulated by intermittent stretch-relaxation in tissue-culture," *American Journal of Physiology*, vol. 256, no. 3, pp. C674–C682, 1989.

[43] H. H. Vandenburgh and P. Karlisch, "Longitudinal growth of skeletal myotubes invitro in a new horizontal mechanical cell stimulator," *In Vitro Cellular & Developmental Biology*, vol. 25, no. 7, pp. 607–616, 1989.

[44] D. W. Hutmacher and S. Cool, "Concepts of scaffold-based tissue engineering-the rationale to use solid free-form fabrication techniques," *Journal of Cellular and Molecular Medicine*, vol. 11, no. 4, pp. 654–669, 2007.

[45] S. A. Riboldi, N. Sadr, L. Pigini, P. Neuenschwander, M. Simonet, P. Mognol, M. Sarnpaolesi, G. Cossu, and S. Mantero, "Skeletal myogenesis on highly orientated microfibrous polyesterurethane scaffolds," *Journal of Biomedical Materials Research Part A*, vol. 84A, no. 4, pp. 1094–1101, 2008.

[46] R. Shah, A. C. M. Sinanan, J. C. Knowles, N. P. Hunt, and M. P. Lewis, "Craniofacial muscle engineering using a 3-dimensional phosphate glass fibre construct," *Biomaterials*, vol. 26, no. 13, pp. 1497–1505, 2005.

[47] T. J. Burkholder, "Permeability of c2c12 myotube membranes is influenced by stretch velocity," *Biochemical and Biophysical Research Communications*, vol. 305, no. 2, pp. 266–270, 2003.

[48] R. Tatsumi, S. M. Sheehan, H. Iwasaki, A. Hattori, and R. E. Allen, "Mechanical stretch induces activation of skeletal muscle satellite cells in vitro," *Experimental Cell Research*, vol. 267, no. 1, pp. 107–114, 2001.

[49] J. S. Otis, T. J. Burkholder, and G. K. Pavlath, "Stretch-induced myoblast proliferation is dependent on the cox2 pathway," *Experimental Cell Research*, vol. 310, no. 2, pp. 417–425, 2005.

[50] R. G. Dennis, P. E. Kosnik, M. E. Gilbert, and J. A. Faulkner, "Excitability and contractility of skeletal muscle engineered from primary cultures and cell lines," *American Journal of Physiology-Cell Physiology*, vol. 280, no. 2, pp. C288–C295, 2001.

[51] H. H. Vandenburgh, J. Shansky, R. Solerssi, and J. Chromiak, "Mechanical stimulation of skeletal-muscle increases prostaglandin-f2-alpha production, cyclooxygenase activity, and cell-growth by a pertussis-toxin-sensitive mechanism," *Journal of Cellular Physiology*, vol. 163, no. 2, pp. 285–294, 1995.

[52] Y. Z. Jinlian Hu, Jing Lu, "New development in elastic fibers," *Polymer Reviews*, vol. 48, no. 2, pp. 275–301, 2008.

[53] E. M. Hicks, A. J. Ultee, and J. Drougas, "Spandex elastic fibers - development of a new type of elastic fiber stimulates further work in growing field of stretch fabrics," *Science*, vol. 147, no. 3656, pp. 373–&, 1965.

[54] H. S. Lee, J. H. Ko, K. S. Song, and K. H. Choi, "Segmental and chain orientational behavior of spandex fibers," *Journal of Polymer Science Part B-Polymer Physics*, vol. 35, no. 11, pp. 1821–1832, 1997.

[55] B. MaterialScience, "Polyurethanes."

[56] K. H. Wong, M. Zinke-Allmang, W. K. Wan, J. Z. Zhang, and P. Hu, "Low energy oxygen ion beam modification of the surface morphology and chemical structure of polyurethane fibers," *Nuclear Instruments & Methods in Physics Research Section B-Beam Interactions with Materials and Atoms*, vol. 243, no. 1, pp. 63–74, 2006.

[57] P. R. Griffiths and J. A. De Haseth, *Fourier transform infrared spectrometry.* New York: Wiley, 2nd ed., 2006.

[58] Various, "http://commons.wikimedia.org," 2009.

[59] D. Briggs, *Surface analysis of polymers by XPS and static SIMS.* Cambridge solid state science series,, Cambridge: Cambridge University Press, 1998.

[60] L. Sabbatini, "Xps and sims surface chemical analysis of some important classes of polymeric biomaterials," *Journal of Electron Spectroscopy and Related Phenomena*, vol. 81, no. 3, pp. 285–301, 1996.

[61] J. I. Goldstein, *Scanning electron microscopy and x-ray microanalysis*. New York: Kluwer Academic / Plenum, 3. ed., 2003.

[62] G. J. Tortora, *Introduction to the human body*. New York: John Wiley & Sons Inc., 7 ed., 2007.

[63] B. Alberts, *Molecular biology of the cell*. New York: Taylor & Francis, 5. ed., 2008.

[64] A. Mauro, "Satellite cell of skeletal muscle fibers," *Journal of Biophysical and Biochemical Cytology*, vol. 9, no. 2, pp. 493–501, 1961.

[65] M. D. Grounds, "Age-associated changes in the response of skeletal muscle cells to exercise and regeneration," *Ann N Y Acad Sci*, vol. 854, pp. 78–91, 1998.

[66] M. Hill, A. Wernig, and G. Goldspink, "Muscle satellite (stem) cell activation during local tissue injury and repair," *J Anat*, vol. 203, no. 1, pp. 89–99, 2003.

[67] J. W. Sanger, P. Chowrashi, N. C. Shaner, S. Spalthoff, H. Wang, N. L. Freeman, and J. M. Sanger, "Myofibrillogenesis in skeletal muscle cells," *Clinical Orthopaedics and Related Research*, vol. 1, no. 403, pp. S153–S162, 2002.

[68] S. Begum, M. Komiyama, N. Toyota, T. Obinata, K. Maruyama, and Y. Shimada, "Differentiation of muscle-specific proteins in chicken somites as studied by immunofluorescence microscopy," *Cell and Tissue Research*, vol. 293, no. 2, pp. 305–311, 1998.

[69] Z. X. Lin, M. H. Lu, T. Schultheiss, J. Choi, S. Holtzer, C. Dilullo, D. A. Fischman, and H. Holtzer, "Sequential appearance of muscle-specific proteins in myoblasts as a function of time after cell-division - evidence for a conserved myoblast differentiation program in skeletal-muscle," *Cell Motility and the Cytoskeleton*, vol. 29, no. 1, pp. 1–19, 1994.

[70] R. A. Corriveau, S. J. Romano, W. G. Conroy, L. Oliva, and D. K. Berg, "Expression of neuronal acetylcholine receptor genes in vertebrate skeletal muscle during development," *J. Neurosci.*, vol. 15, no. 2, pp. 1372–1383, 1995.

[71] T. Hodge and M. J. Cope, "A myosin family tree," *J Cell Sci*, vol. 113, no. 19, pp. 3353–3354, 2000.

[72] B. M. Jockusch and G. Isenberg, "Interaction of alpha-actinin and vinculin with actin: opposite effects on filament network formation," *Proceedings of the National Academy of Sciences of the United States of America*, vol. 78, no. 5, pp. 3005–3009, 1981.

[73] H. P. Kubis, N. Hanke, R. J. Scheibe, J. D. Meissner, and G. Gros, "Ca2+ transients activate calcineurin/nfatc1 and initiate fast-to-slow transformation in a primary skeletal muscle culture," *American Journal of Physiology-Cell Physiology*, vol. 285, no. 1, pp. C56–C63, 2003.

[74] A. Andersson, A. Sjodin, A. Hedman, R. Olsson, and B. Vessby, "Fatty acid profile of skeletal muscle phospholipids in trained and untrained young men," *American Journal of Physiology-Endocrinology and Metabolism*, vol. 279, no. 4, pp. E744–E751, 2000.

[75] P. D. Gollnick, R. B. Armstrong, B. Saltin, C. W. t. Saubert, W. L. Sembrowich, and R. E. Shepherd, "Effect of training on enzyme activity and fiber composition of human skeletal muscle," *J Appl Physiol*, vol. 34, no. 1, pp. 107–111, 1973.

[76] G. N. C. Crawford, "An experimental study of muscle growth in the rabbit," *Journal of Bone and Joint Surgery-British Volume*, vol. 36, no. 2, pp. 294–303, 1954.

[77] H. Holtzer, J. Abbott, and J. Lash, "On the formation of multinucleated myotubes," *Anatomical Record*, vol. 131, no. 3, pp. 567–567, 1958.

[78] C. Neville, N. Rosenthal, M. McGrew, N. Bogdanova, and S. Hauschka, "Skeletal muscle cultures," *Methods in Cell Biology, Vol 52*, vol. 52, pp. 85–116, 1997.

[79] D. F. Pinney, S. H. Pearsonwhite, S. F. Konieczny, K. E. Latham, and C. P. Emerson, "Myogenic lineage determination and differentiation - evidence for a regulatory gene pathway," *Cell*, vol. 53, no. 5, pp. 781–793, 1988.

[80] C. A. Berkes and S. J. Tapscott, "Myod and the transcriptional control of myogenesis," *Seminars in Cell & Developmental Biology*, vol. 16, no. 4-5, pp. 585–595, 2005.

[81] T. Braun, G. Buschhausendenker, E. Bober, E. Tannich, and H. H. Arnold, "A novel human-muscle factor related to but distinct from myod1 induces myogenic conversion in 10t1/2 fibroblasts," *Embo Journal*, vol. 8, no. 3, pp. 701–709, 1989.

[82] D. G. Edmondson and E. N. Olson, "A gene with homology to the myc similarity region of myod1 is expressed during myogenesis and is sufficient to activate the muscle differentiation program," *Genes & Development*, vol. 3, no. 5, pp. 628–640, 1989.

[83] T. Braun, E. Bober, B. Winter, N. Rosenthal, and H. H. Arnold, "Myf-6, a new member of the human gene family of myogenic determination factors - evidence for a gene-cluster on chromosome-12," *Embo Journal*, vol. 9, no. 3, pp. 821–831, 1990.

[84] S. B. P. Charge and M. A. Rudnicki, "Cellular and molecular regulation of muscle regeneration," *Physiological Reviews*, vol. 84, no. 1, pp. 209–238, 2004.

[85] W. E. Wright, K. J. Farmer, M. Bouche, and T. Uestuki, "Multicomponent complexes involving myogenin, mrf4, myf5 and myod," *Journal of Cellular Biochemistry*, pp. 470–470, 1994.

[86] F. Aurade, C. Pinset, P. Chafey, F. Gros, and D. Montarras, "Myf5, myod, myogenin and mrf4 myogenic derivatives of the embryonic mesenchymal cell-line c3h10t1/2 exhibit the same adult muscle phenotype," *Differentiation*, vol. 55, no. 3, pp. 185–192, 1994.

[87] H. Li and Y. Capetanaki, "Regulation of the mouse desmin gene - transactivation by myod, myogenin, mrf4 and myf5," *Nucleic Acids Research*, vol. 21, no. 2, pp. 335–343, 1993.

[88] D. Montarras, J. Chelly, E. Bober, H. Arnold, M. O. Ott, F. Gros, and C. Pinset, "Developmental patterns in the expression of myf5, myod, myogenin, and mrf4 during myogenesis," *New Biologist*, vol. 3, no. 6, pp. 592–600, 1991.

[89] S. Dedieu, N. Dourdin, E. Dargelos, S. Poussard, P. Veschambre, P. Cottin, and J. J. Brustis, "Calpain and myogenesis: development of a convenient cell culture model," *Biology of the Cell*, vol. 94, no. 2, pp. 65–76, 2002.

[90] S. Yoon, M. J. Molloy, M. P. Wu, D. B. Cowan, and E. Gussoni, "C6orf32 is upregulated during muscle cell differentiation and induces the formation of cellular filopodia," *Dev Biol*, vol. 301, no. 1, pp. 70–81, 2007.

[91] D. Yaffe and O. Saxel, "Serial passaging and differentiation of myogenic cells isolated from dystrophic mouse muscle," *Nature*, vol. 270, no. 5639, pp. 725–7, 1977.

[92] T. W. Breese and W. Admassu, "Feasibility of culturing c2c12 mouse myoblasts on glass microcarriers in a continuous stirred tank bioreactor," *Bioprocess Engineering*, vol. 20, no. 5, pp. 463–468, 2006.

[93] Y. Kubo, "Comparison of initial-stages of muscle differentiation in rat and mouse myoblastic and mouse mesodermal stem-cell lines," *Journal of Physiology-London*, vol. 442, pp. 743–759, 1991.

[94] G. L. Portier, A. A. G. M. Benders, A. Oosterhof, J. H. Veerkamp, and T. H. van Kuppevelt, "Differentiation markers of mouse c2c12 and rat l-6 myogenic cell lines and the effect of the differentiation medium," *In Vitro Cellular & Developmental Biology-Animal*, vol. 35, no. 4, pp. 219–227, 1999.

[95] M. A. Lawson and P. P. Purslow, "Differentiation of myoblasts in serum-free media: Effects of modified media are cell line-specific," *Cells Tissues Organs*, vol. 167, no. 2-3, pp. 130–137, 2000.

[96] D. Gawlitta, K. J. M. Boonen, C. W. J. Oomens, F. P. T. Baaijens, and C. V. C. Bouten, "The influence of serum-free culture conditions on skeletal muscle differentiation in a tissue-engineered model," *Tissue Engineering Part A*, vol. 14, no. 1, pp. 161–171, 2008.

[97] A. R. Greenbaum, P. J. E. Etherington, S. Manek, D. Ohare, K. H. Parker, C. J. Green, J. R. Pepper, and C. P. Winlove, "Measurements of oxygenation and perfusion in skeletal muscle using multiple microelectrodes," *Journal of Muscle Research and Cell Motility*, vol. 18, no. 2, pp. 149–159, 1997.

[98] R. R. Miller, J. S. Rao, W. V. Burton, and B. W. Festoff, "Proteoglycan synthesis by clonal skeletal muscle cells during in vitro myogenesis: differences detected in the types and patterns from primary cultures," *Int J Dev Neurosci*, vol. 9, no. 3, pp. 259–67, 1991.

[99] A. Katsumi, A. W. Orr, E. Tzima, and M. A. Schwartz, "Integrins in mechanotransduction," *J. Biol. Chem.*, vol. 279, no. 13, pp. 12001–12004, 2004.

[100] C. J. Meyer, F. J. Alenghat, P. Rim, J. H.-J. Fong, B. Fabry, and D. E. Ingber, "Mechanical control of cyclic amp signalling and gene transcription through integrins," *Nat Cell Biol*, vol. 2, no. 9, pp. 666–668, 2000.

[101] F. Guharay and F. Sachs, "Stretch-activated single ion channel currents in tissue-cultured embryonic chick skeletal muscle," *The Journal of Physiology*, vol. 352, no. 1, pp. 685–701, 1984.

[102] I. M. Bernstein, K. Plociennik, S. Stahle, G. J. Badger, and R. Secker-Walker, "Impact of maternal cigarette smoking on fetal growth and body composition," *Am J Obstet Gynecol*, vol. 183, no. 4, pp. 883–6, 2000.

[103] D. M. Stewart, "The role of tension in muscle growth," in *Regulation of organ and tissue growth* (R. Goss, ed.), pp. 77–100, New York: Academic Press, 1972.

[104] T. J. Burkholder and R. L. Lieber, "Sarcomere length operating range of vertebrate muscles during movement," *J Exp Biol*, vol. 204, no. Pt 9, pp. 1529–36, 2001.

[105] G. Goldspink, A. Scutt, P. T. Loughna, D. J. Wells, T. Jaenicke, and G. F. Gerlach, "Gene-expression in skeletal-muscle in response to stretch and force generation," *American Journal of Physiology*, vol. 262, no. 3, pp. R356–R363, 1992.

[106] A. Maier, B. Gambke, and D. Pette, "Degeneration-regeneration as a mechanism contributing to the fast to slow conversion of chronically stimulated fast-twitch rabbit muscle," *Cell and Tissue Research*, vol. 244, no. 3, pp. 635–643, 1986.

[107] M. A. Febbraio and I. Koukoulas, "Hsp72 gene expression progressively increases in human skeletal muscle during prolonged, exhaustive exercise," *Journal of Applied Physiology*, vol. 89, no. 3, pp. 1055–1060, 2000.

[108] V. J. Allan, *Protein localization by fluorescence microscopy : a practical approach*. The practical approach series, Oxford: Oxford University Press, 2000.

[109] J. Slavik, *Fluorescence microscopy and fluorescent probes*. New York ; London: Plenum Press, 1996.

[110] Invitrogen, "Alexa fluor dyes spanning the visible and infrared spectrum," in *Molecular Probes: Handbook*, Invitrogen Corparation, 2009.

[111] G. Beamson and D. Briggs, *High resolution XPS of organic polymers : The Scienta ESCA300 database*. Chichester: Wiley, 1992. G. Beamson and D. Briggs.

[112] T. J. Burkholder, "Mechanotransduction in skeletal muscle," *Frontiers in Bioscience*, vol. 12, pp. 174–191, 2007.

[113] H. A. Toliyat and G. B. Kliman, *Handbook of electric motors*. New York: Dekker, 2 ed., 2004.

[114] Q. Dou, C. Wang, C. Cheng, W. Han, P. C. Thne, and W. Ming, "Pdms-modified polyurethane films with low water contact angle hysteresis," *Macromolecular Chemistry and Physics*, vol. 207, no. 23, pp. 2170–2179, 2006.

[115] Various, "http://www.creora.co.kr/," 2007.

[116] G. Bhat, S. Chand, and S. Yakopson, "Thermal properties of elastic fibers," in *27th North-American-Thermal-Analysis-Society Conference*, (Savannah, Georgia), pp. 161–164, Elsevier Science Bv, 1999.

[117] M. A. Griffin, S. Sen, H. L. Sweeney, and D. E. Discher, "Adhesion-contractile balance in myocyte differentiation," *J Cell Sci*, vol. 117, no. 24, pp. 5855–5863, 2004.

[118] C. Rhim, D. A. Lowell, M. C. Reedy, D. H. Slentz, S. J. Zhang, W. E. Kraus, and G. A. Truskey, "Morphology and ultrastructure of differentiating three-dimensional mammalian skeletal muscle in a collagen gel," *Muscle & Nerve*, vol. 36, no. 1, pp. 71–80, 2007.

[119] S. Arnesen, S. Mosler, N. B. Larsen, N. Gadegaard, P. P. Purslow, and M. A. Lawson, "The effects of collagen type i topography on myoblasts in vitro," *Connective Tissue Research*, vol. 45, no. 4-5, pp. 238–247, 2004.

[120] J. P. Beier, R. E. Horch, and A. D. Bach, "Tissue engineering of skeletal muscle," *Minerva Biotecnologica*, vol. 18, no. 2, pp. 89–96, 2006.

[121] W. Aijun, A. Qiang, C. Wenling, Z. Chang, G. Yandao, Z. Nanming, and Z. Xiufang, "Fiber-based chitosan tubular scaffolds for soft tissue engineering: Fabrication and in vitro evaluation," *Tsinghua Science and Technology*, vol. 10, no. 4, pp. 449–453, 2005.